100 1908 - 2008
UNIVERSITEIT VAN PRETORIA
UNIVERSITY OF PRETORIA
YUNIBESITHI YA PRETORIA

Towards determining the functional importance of African horse sickness virus NS2 protein phosphorylation

by

Ockert Bihl

Submitted in partial fulfilment of the requirements of the degree
Master of Science
in the Faculty of Natural and Agricultural Sciences
Department of Microbiology and Plant Pathology
University of Pretoria
Pretoria

October 2012

DECLARATION

I declare that the dissertation, which I hereby submit for the degree M.Sc (Microbiology) at the University of Pretoria, is my own work and has not previously been submitted by me for a degree at this or any other tertiary institution.

Signed: …….. Date: ……..

ACKNOWLEDGEMENTS

I would like to acknowledge and thank the following people:

My friends and colleagues in the Department of Microbiology and Plant Pathology for their academic and moral support.

Prof Theron for his patience and guidance throughout my study.

Flip Wege for his assistance with cell culture, and for providing the cells and virus used in this study.

Chris van der Merwe and Alan Hall for their assistance with microscopy.

My father and brother for their support and understanding during my studies.

Alan and Melaney for their support and encouragement.

And **Bronwyn** for all of her love, patience and encouragement during my studies.

The financial support of the NRF is also acknowledged.

Dedicated to my mother,

Wendy Bihl

1960-2012

SUMMARY

Towards determining the functional importance of African horse sickness virus NS2 protein phosphorylation

by

Ockert Johannes Bihl

Supervisor: Prof. J. Theron
Department of Microbiology and Plant Pathology
University of Pretoria

for the degree M.Sc

The aim of this investigation was to obtain more information regarding the phosphorylation of the non-structural protein NS2 of African horse sickness virus (AHSV), a member of the *Orbivirus* genus within the *Reoviridae* family. The NS2 protein is the only virus-specified phosphoprotein, it is capable of binding single-stranded RNA and it is also the main component of the characteristic virus inclusion bodies observed in the cytoplasm of orbivirus-infected cells. These properties of NS2 suggest that it may play an important role in viral replication and morphogenesis.

It has been reported that the NS2 protein of different orbiviruses is phosphorylated on serine residues within its carboxy (C) terminus, most likely by the ubiquitous cellular kinase casein kinase II (CK2). Bioinformatic analysis of the AHSV-9 NS2 amino acid sequence led to the identification of three C-terminal serine residues at positions 256, 258 and 262 that were predicted to be CK2 phosphorylation sites. The importance of these serine residues for phosphorylation of the AHSV-9 NS2 protein was subsequently investigated by analysis of recombinant baculovirus-expressed mutant versions of the NS2 protein. These comprised of single and dual mutant NS2 proteins in which the identified serine residues were respectively substituted either with alanine or with negatively charged aspartic acid residues to mimic phosphoserine residues.

Since it has been reported that phosphorylation of the NS2 protein of bluetongue virus, the prototype orbivirus, influences its ability to form virus inclusion bodies (VIBs), it was

investigated whether differences could be observed in the inclusion bodies formed by the respective mutant AHSV-9 NS2 proteins. Transmission electron microscope analysis of recombinant baculovirus-infected *Spodoptera frugiperda* insect cells indicated that a mutant NS2 protein in which the serine residues at both positions 256 and 258 were substituted with alanine was unable to form cytoplasmic inclusions. However, when both of these residues were substituted with aspartic acid residues, inclusion bodies could be observed and thus suggested that both of these serine residues may serve as phosphate-acceptor sites. To further investigate whether NS2 protein phosphorylation may be important for the formation of VIBs, *Culicoides variipennis* insect cells were treated with myricetin, an inhibitor of CK2 activity, prior to infection with AHSV-9. In contrast to the untreated virus-infected cells, immunofluorescent confocal laser microscopy using a monospecific anti-NS2 antibody revealed no distinctive NS2 aggregates in the treated cells. Furthermore, immunofluorescence analysis of bromouridine (BrU)-labelled RNA made in infected cells indicated that it localizes to the VIBs. Overall, the results obtained during the course of this investigation suggest that NS2 phosphorylation of serine residues is mediated by CK2 and that this post-translational modification of the NS2 protein is required for the formation of VIBs in AHSV-infected cells.

TABLE OF CONTENTS

LIST OF ABBREVIATIONS

Acc.	accession
AHS	African horse sickness
AHSV	African horse sickness virus
Ala	alanine
Asp	aspartic acid/aspartate
ATP	adenosine-5'-triphosphate
BLAST	Basic Local Alignment Search Tool
bp	base pair
BrdU	5'-bromo-uracil
BrUTP	5'-bromo-uridine triphosphate
BTV	bluetongue virus
C	carboxy
ca.	approximately
cDNA	complementary DNA
CK2	casein kinase 2
cm^3	cubic centimetre
CPE	cytopathic effect
Da	Dalton
dH_2O	distilled water
DNA	deoxyribonucleic acid
dNTP	deoxyribonucleoside-5'-triphosphate
ds	double-stranded
e.g.	*exempli gratia* (*Latin:* for example)
EDTA	ethylenediaminetetra-acetic acid
EHDV	epizootic haemorrhagic disease virus
et al.	*et alia* (*Latin:* and others)
FBS	foetal bovine serum
Fig.	figure
FITC	fluorescein isothiocyanate
GPS	Group-based prediction system
h	hour
H_2O_2	hydrogen peroxide
IB	inclusion body
i.e.	*id est* (*Latin*: that is)

IgG	immunoglobulin G
IFN	interferon
IPTG	isopropyl-β-D-thiogalactopyranoside
kb	kilobase pairs
KC cells	*Culicoides variipennis* insect cells
kDa	kilodalton
KOAc	potassium acetate
LB	Luria-Bertani
µg	microgram
µl	microlitre
µm	micrometre
µM	micromolar
M	molar
mg	milligram
min	minute
ml	millilitre
mM	millimolar
MOI	multiplicity of infection
mRNA	messenger ribonucleic acid
MVA	modified vaccinia Ankara
N	amino
NaOAc	sodium acetate
ng	nanogram
nm	nanometre
no.	number
NS	non-structural protein
NTP	nucleoside triphosphate
NTPase	nucleoside triphosphate phosphohydrolase
ºC	degrees Celcius
OD	optical density
OIE	*Office International des Epizootics* (*French:* World Organisation for Animal Health)
OsO_4	osmium tetraoxide
PAGE	polyacrylamide gel electrophoresis
PBS	phosphate-buffered saline
PCR	polymerase chain reaction
pfu	plaque forming units
pmol	picomole

poly(A)	poly-adenosine
poly(U)	poly-uracil
PSB	protein solvent buffer
RNA	ribonucleic acid
RNase	ribonuclease
rpm	revolutions per minute
RTPase	5'-RNA triphosphatase
s	second
S	Svedberg unit
SAXS	small-angle X-ray scattering measurements
SDS	sodium dodecyl sulphate
Ser	serine
spp.	species
ss	single-stranded
STI	soybean trypsin inhibitor
TEM	transmission electron microscopy
TEMED	N',N',N',N'-tetramethylethylenediamine
Tris	Tris(hydroxymethyl)aminomethane
Tris-HCl	Tris(hydroxymethyl)aminomethane hydrogen chloride
TRITC	tetramethyl rhodamine isothiocyanate
U	units
UHQ	ultra high quality
UV	ultraviolet
V	volts
v.	version
v/v	volume per volume
VIB	virus inclusion body
VP	virus protein
w/v	weight per volume
X-Gal	5-bromo-4-chloro-3-indolyl-β-D-galactopyranoside
α	alpha
β	beta
γ	gamma

LIST OF FIGURES

LIST OF TABLES

Chapter One
Preface

The genus *Orbivirus* of the family *Reoviridae* comprises a number of important animal pathogens, such as African horse sickness virus (AHSV) and bluetongue virus (BTV). In contrast to other family members, the orbiviruses are transmitted by haematophageous *Culicoides* spp. to vertebrate hosts, and have the ability to replicate in both insect and mammalian hosts (Calisher and Mertens, 1998). AHSV is the aetiological agent of African horse sickness (AHS), a highly infectious disease of equids of which the mortality rate in susceptible horse populations may reach 95% (Coetzer and Guthrie, 2004; Guthrie, 2007). The disease is enzootic in sub-Saharan Africa, although outbreaks, resulting in considerable economic loss to the equestrian industry, have occurred in the Middle East and in Europe (Howell, 1960; Mirchamsy and Hazrati, 1973; Rodriguez *et al.*, 1992; Coetzer and Guthrie, 2004).

Like bluetongue virus (BTV), the prototype orbivirus, AHSV consists of two concentric protein layers that encapsidate the genome of 10 double-stranded (ds) RNA segments (Oellerman *et al.*, 1970; Roy *et al.*, 1994; Manole *et al.*, 2012). The core particle is composed of two major (VP3 and VP7) and three minor (VP1, VP4 and VP6) structural proteins, and is surrounded by the outer capsid, composed of the two major structural proteins VP2 and VP5. In addition to these seven structural proteins, at least four non-structural proteins (NS1, NS2 and NS3/NS3A) are produced in infected cells at different stages of the infectious cycle (Roy *et al.*, 1994). Although the existence of a fifth non-structural protein, designated as NS4 and encoded by an overlapping reading frame in the VP6-encoding gene, was recently demonstrated for BTV, it is not yet known whether this is a general feature of orbivirus infections (Belhouchet *et al.*, 2011).

With the exception of NS4 that does not play a role in viral replication (Ratinier *et al.*, 2011), it is believed that the non-structural proteins are involved in the process of viral morphogenesis, leading to viral assembly and release. The non-structural proteins NS1 and NS2 are the first and second most abundant proteins in infected cells and their synthesis coincides with the appearance of two virus-specific intracellular structures, *i.e.* tubules and virus inclusion bodies (VIBs), respectively (Huismans and Els, 1979; Hyatt and Eaton, 1988; Brookes *et al.*, 1993). Although the function of the tubules is not clearly delineated, the NS1 protein has nevertheless been reported to be involved in viral morphogenesis (Owens *et al.*, 2004). The NS3/NS3A proteins, on the other hand, are synthesized in much smaller amounts

than NS1 and NS2, and play a role in the release of progeny viruses from infected cells (Hyatt *et al.*, 1993; Stoltz *et al.*, 1996; Celma and Roy, 2009).

Investigations of the NS2 protein of BTV have indicated that it is a multifunctional protein. Several properties of NS2 suggest that it might play an important role in the viral replication cycle, particularly with respect to the recruiting and packaging of BTV single-stranded (ss) RNA prior to encapsidation. The NS2 protein forms multimers and the size of the NS2 oligomers is likely to be between six and eight subunits (Taraporewala *et al.*, 2001), with more recent structural investigations favouring a decameric composition (Mumtsidu *et al.*, 2007). Compared with the other BTV proteins, NS2 appears to be unique by virtue of its ability to bind ssRNA, but not dsRNA. Although the NS2 protein was initially shown to have non-specific ssRNA binding properties (Huismans *et al.*, 1987; Thomas *et al.*, 1990; Taraporewala *et al.*, 2001), more recent evidence indicated that NS2 displays some preference for viral genomic segments (Theron and Nel, 1997; Lymperopoulos *et al.*, 2003, 2006). NS2 also has the enzymatic ability of hydrolyzing nucleotide triphosphates (NTPs) to nucleotide monophosphates (Horscroft and Roy, 2000; Taraporewala *et al.*, 2001). Although the significance of this activity is not clear, it can be envisaged that genome transportation and packaging are energy demanding processes in which NTP hydrolysis by NS2 may provide the required energy. Thus, it follows that these two properties of the NS2 protein might be important in the selection and/or packaging of the viral RNAs for replication. During the assembly of progeny virions, it is believed that the positive-strand RNA is packaged and then replicated to form the dsRNA genome segment by the RNA-dependent RNA polymerase (VP1) inside the progeny virions (Mertens and Diprose, 2004). However, the mechanism by which sorting and selection of the 10 mRNAs, to ensure the inclusion of only a single copy of each genome segment per virus particle, and the way in which packaging is carried out remains unknown.

As indicated above, a characteristic feature of NS2 is that it is predominantly associated with virus inclusion bodies (VIBs) formed in BTV-infected cells (Eaton *et al.*, 1987; Brookes *et al.*, 1993). Expression of BTV NS2 in both insect and mammalian cells results in the formation of inclusion bodies (IBs) that are indistinguishable from the VIBs found in virus-infected cells, indicating that NS2 is responsible for the formation of VIBs (Thomas *et al.*, 1990; Kar *et al.*, 2005). Since both viral structural proteins and newly assembled BTV core particles have been shown to localize within the VIBs (Hyatt and Eaton, 1988; Kar *et al.*,

2007), these structures are therefore believed to be the sites at which virus assembly occurs and are also the likely sites of RNA packaging. A distinctive feature of NS2 is that it undergoes phosphorylation in BTV-infected cells or when expressed in insect cells (Huismans *et al.*, 1987; Devaney *et al.*, 1988; Thomas *et al.*, 1990). It was reported that BTV NS2 purified by immunoprecipitation or by affinity chromatography could be phosphorylated *in vitro*, without the addition of an exogenous kinase (Huismans *et al.*, 1987). It has subsequently been shown that NS2 lacks autophosphorylation activity (Theron *et al.*, 1994; Taraporewala *et al.*, 2001) and that BTV NS2 is phosphorylated at two serines by a ubiquitous cellular kinase, most likely casein kinase 2 (Modrof *et al.*, 2005). The functional importance of NS2 phosphorylation has been investigated for BTV, and it was reported that phosphorylation of the NS2 protein is important for VIB formation but not for ssRNA binding (Thomas *et al.*, 1990; Modrof *et al.*, 2005).

In contrast to BTV, the properties and biological importance of the AHSV NS2 protein has not yet been investigated in great detail. Studies regarding AHSV NS2 have reported that it is phosphorylated (Devaney *et al.*, 1988; Theron *et al.*, 1994), able to self-associate to form multimeric assemblies in complex with ssRNA (Uitenweerde *et al.*, 1995) and is associated with the formation of VIBs (Uitenweerde *et al.*, 1995). In previous investigations, a combination of mutagenesis and re-expression of AHSV proteins in heterologous hosts has allowed progress to be made in relation to the structure-function relationships among some of the AHSV proteins, and has also allowed for mapping of the function of some of the proteins. Indeed, the expression of individual AHSV proteins by appropriately constructed baculovirus recombinants in *Spodoptera frugiperda* insect cell culture has made significant contributions to the structure-function relationships of non-structural proteins such as NS1 (Maree and Huismans, 1997), NS2 (Uitenweerde *et al.*, 1995) and NS3 (Van Staden *et al.*, 1995; Van Niekerk *et al.*, 2001), as well as structural proteins such as VP5 (Stassen *et al.*, 2011), VP6 (De Waal and Huismans, 2005) and VP7 (Burroughs *et al.*, 1994; Basak *et al.*, 1996). It can thus be envisaged that a similar strategy would allow for greater understanding of the functional importance of AHSV NS2 phosphorylation. Consequently, this dissertation reports on investigations undertaken to identify phosphate-acceptor residues within the AHSV NS2 protein and to determine the functional significance of NS2 phosphorylation with regards to VIB formation.

Chapter Two
Literature Review

2.1 GENERAL INTRODUCTION

African horse sickness (AHS), of which African horse sickness virus (AHSV) is the aetiological agent, is an infectious, non-contagious, arthropod-borne viral disease of equids. It is the most devastating and rapidly fatal disease of horses with a mortality rate of 70-95% in susceptible horse populations (Guthrie, 2007). The first reference to the disease concerns an epidemic that occurred in 1327 in Yemen (Mellor and Hamblin, 2004). However, the virus almost certainly originated in Africa and was first observed on the African continent after the introduction of horses from India in the 16th century for purposes of exploring central and east Africa. The first outbreak of AHS in southern Africa was recorded in 1719 when over 1 700 animals died of the disease in the then Cape of Good Hope. Subsequently, over the next 217 years, at least 10 major outbreaks of AHS have been recorded in southern Africa. The most severe outbreak occurred in the Cape of Good Hope in 1854-1855 in which more than 70 000 horses died (Coetzer and Erasmus, 1994). The frequency and severity of the outbreaks have, however, declined over the last century, probably due to improved surveillance and strict zoning measures, as well as vaccination of horses with polyvalent live attenuated vaccines (Mellor and Hamblin, 2004). Nevertheless, based on its potential economic and international importance, AHS has been classified as a notifiable disease by the Office International des Epizootics (OIE, 2004). Such diseases are defined as transmissible diseases that have the potential for very serious and rapid spread, they have particularly serious socio-economic or public health consequences and are of major importance in the international trade of animals and animal products.

AHSV was first identified as a non-filterable infectious agent in 1900, making it the fifth non-filterable infectious agent to be identified (McFaydean, 1900). Subsequently, much of the pioneering research on AHS was performed by Sir Arnold Theiler. His research indicated that there existed immunologically distinct strains of the AHS agent, since immunity acquired against one strain did not always protect the horse when challenged by a heterologous virus strain. In 1903, Theiler and Pitchford-Watkins established that AHSV may be transmitted by biting insects and in 1921, Theiler reported the first detailed descriptions of the clinical signs and lesions produced by infections with AHSV (reviewed in Coetzer and Erasmus, 1994). During the late 1960s and 1970s, several studies were undertaken aimed at characterizing the structure and morphology of AHSV (Verwoerd and Huismans, 1969; Oellerman *et al.*, 1970; Bremer, 1976). Consequently, AHSV has been classified as a member of the genus *Orbivirus*

in the family *Reoviridae*. Orbiviruses are characterized as non-enveloped, multi-layered virus particles that harbour a segmented double-stranded (ds) RNA genome, and are capable of infecting a broad range of vertebrate and insect hosts (Mertens *et al.*, 2005).

With the advent of gene cloning, genetic engineering and protein expression technologies, progress has been made regarding structure-function relationships of different AHSV genes and the encoded gene products (Uitenweerde *et al.*, 1995; Maree and Huismans, 1997; Van Niekerk *et al.*, 2001; De Waal and Huismans, 2005; Stassen *et al.*, 2011). Despite these advances, knowledge regarding the viral replication and morphogenesis processes of dsRNA viruses in general and AHSV specifically, as well as the role of the individual proteins in these processes has remained elusive. The non-structural proteins are thought to play an important role in these processes, especially the NS2 protein. Not only is NS2 the second most abundant viral protein present in infected cells (Huismans, 1979), but it possesses several unique properties that has led to it being regarded as a modulator of viral replication and assembly (Kar *et al.*, 2007).

This review will summarize the current literature concerning AHSV and will highlight the role of individual proteins in the infectious cycle of the virus. This will be followed by a discussion of the non-structural protein NS2 and its role in virus replication and morphogenesis. The literature review will be concluded by a brief description of the aims of this investigation.

2.2 AFRICAN HORSE SICKNESS (AHS)

2.2.1 Susceptible species

AHS affects mainly equine species (horses, zebras and donkeys), with horses being the most susceptible and the mortality rates may range between 70 to 95% (Mellor and Hamblin, 2004; Guthrie, 2007). Zebras are considered the natural vertebrate host and reservoir of AHSV, since they rarely exhibit clinical signs of infection (Barnard, 1998). The levels of viraemia in zebras are lower compared to horses, but last longer (four weeks) and occur in the presence of circulating antibodies (Erasmus *et al.*, 1978; Barnard *et al.*, 1994; Barnard, 1997). Consequently, zebras are believed to play an important role in the persistence of the virus in Africa (Barnard and Paweska, 1993; Barnard *et al.*, 1994; Lord *et al.*, 1997). Interestingly,

donkeys in South Africa appear to be naturally resistant to AHSV (mortality rate less that 10%) and animals that become infected, rarely display clinical symptoms. Therefore, donkeys, in addition to zebras, may also act as reservoir hosts in South Africa (Alexander, 1948; Hamblin *et al.*, 1998). In addition to the above equine species, dogs (Piercy, 1951; Haig *et al.*, 1956) and camels (Salama *et al.*, 1981) are the only other domestic animals known to occasionally contract AHS naturally through consumption of infected meat.

2.2.2 Epidemiology

AHS is endemic in tropical and sub-tropical areas of Africa south of the Sahara, occupying a broad band stretching from Senegal in the west to Ethiopia and Somalia in the east, and extending as far south as northern South Africa (Mellor and Hamblin, 2004). Of the nine AHSV serotypes, serotypes 1 to 8 are found in restricted areas of sub-Saharan Africa, while serotype 9 is more widespread (Mellor, 1993; Coetzer and Guthrie, 2004). In South Africa, AHS is confined mostly to the north-east of the country as the harsh Karoo conditions is thought to create a natural barrier against the *Culicoides* vectors (Du Toit, 1944; Rawlings *et al.*, 2003; White *et al.*, 2005).

Although AHS is believed to be confined largely to sub-Saharan Africa, except for occasional incursions into North Africa, there have been several outbreaks of the disease in European countries and countries of the Persian Gulf and Middle East. Outbreaks caused by AHSV-9 have occurred in Egypt (1928, 1943, 1953, 1958 and 1971) (Carpano, 1931; Coetzer and Guthrie, 2004), while AHSV-2 caused a recent (2008) outbreak in Ethiopia (OIE Information Database: www.oie.int/). In 2007, AHSV-4 was detected in Kenya and outbreaks caused by AHSV-2 and AHSV-7 occurred in West Africa where only serotype 9 had previously been detected (Wilson *et al.*, 2009). Countries where epizootics occurred outside the African continent include Yemen (1930), the Middle East (AHSV-9, 1959-1961), Israel (1944), Spain (AHSV-9, 1966; AHSV-4, 1987-1990) and Portugal (AHSV-4, 1989). The outbreak in 1959-1961 in Middle Eastern countries and the Persian Gulf (Iran, Saudi Arabia, Pakistan, Afghanistan, India, Turkey, Cyprus Iraq, Syria, Lebanon, and Jordan) was the most extensive epizootic to date (Howell, 1960, 1963; Mirchamsy and Hazrati, 1973). The extended epizootic in Spain (1987-1990) occurred after the importation of zebras from Namibia to a safari park outside Madrid (Rodriguez *et al.*, 1992; Mellor *et al.*, 1990).

2.2.3 Transmission

As early as the 1800s, it had already been established that AHS is non-contagious, climatic changes influence outbreaks and that stabling of horses from dusk until dawn reduces the incidence of infection (Coetzer and Guthrie, 2004). It was only decades later that *Culicoides imicola* midges were identified as a vector species and transmission of AHSV to horses was demonstrated (Du Toit, 1944; Wetzel *et al*., 1970). An adult *Culicoides* becomes infective eight days after feeding on a viraemic animal and stays infected until death. The virus replicates in the gut and salivary glands of the insect vector, without adversely affecting its insect hosts, and is subsequently transmitted from the *Culicoides* vector to a susceptible equine host when the midge takes a blood meal (Meiswinkel *et al.*, 2000) (Fig. 2.1). Experimental transmission to animals has been shown to occur more readily via the intravenous than the subcutaneous route (Henning, 1956), which is in agreement with the finding that AHS is a haematophagous arthropod-borne viral disease.

In Africa, *C. imicola* and *C. bolitinos* transmit AHSV (Meiswinkel *et al*., 2000; Venter *et al*., 2000), while *C. variipennis*, which is dominant in the USA, but not in South Africa, can experimentally transmit AHSV (Boorman *et al*., 1975). *C. bolitinos* has a wide distribution in southern Africa and is common in cooler highland areas where *C. imicola* is rare (Meiswinkel and Paweska, 2003). Epidemic outbreaks of AHS have been well correlated with climate conditions favoured by the *Culicoides* species, with early heavy rainfall followed by warm, dry spells generally considered as optimal breeding conditions (Venter and Meiswinkel, 1994). Several concerns have recently been raised that climate change may expand the range of the insect vector and therefore raises the possibility that AHS may spread more globally (Purse *et al.*, 2008; MacLachlan and Guthrie 2010; Thompson *et al.*, 2012).

It has been reported that mosquitoes of the genus *Aedes* could harbour AHSV for one week, but they could not transmit AHS (Nieschulz *et al*., 1934; Wetzel *et al*., 1970). Furthermore, infected dogs do not play a role in the spread of AHSV since midges do not feed on dogs (McIntosh, 1955). Although biting flies may play a minor role in transmission (Wetzel *et al*., 1970) and dog ticks may harbour and transmit the virus under experimental conditions (Salama *et al*., 1981; Hess, 1988), no arthropod species other than *Culicoides* is implicated in natural transmission.

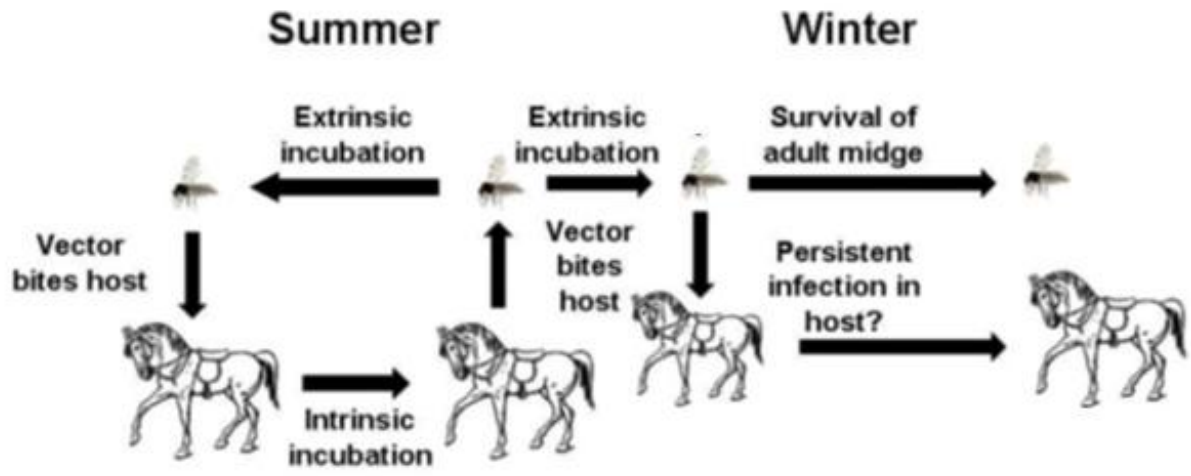

Fig. 2.1 Transmission of AHSV between equine and *Culicoides* vectors. (Adapted from Thompson *et al.*, 2012).

2.2.4 Pathogenesis and clinical indications

Following transmission of AHSV to horses the virus replicates in the regional lymph nodes from where the progeny viruses disseminate via the blood, giving rise to primary viraemia (Coetzer and Guthrie, 2004). Subsequent infection of the lungs, lymphoid tissues and endothelial cells leads to secondary viraemia. The duration and titer varies depending upon a number of factors, including the host species. Oedema of the lungs, pleura and subcutaneous tissues, transudation into the body cavities, and haemorrhages in various organs and tissues develop as a result of impaired function of the circulatory and respiratory systems (Erasmus, 1973; Coetzer and Guthrie, 2004).

According to the extent and severity of clinical symptoms caused by the infection, the disease is classified into four distinct forms, *i.e.* the pulmonary (acute), cardiac (subacute), mixed pulmonary and cardiac (cardio-pulmonary), and fever forms (Theiler, 1921). The least serious manifestation is African horse sickness fever, which is experienced as a mild fever and may include several mild symptoms such as appetite loss and increased heart rate. The illness is not severe and seldom lasts more than six days. African horse sickness fever usually affects horses that are partially immune to the infecting strain and is the only clinical manifestation of AHS among donkey and zebra, which are resistant to the more severe forms of the disease. The cardiac form of the disease is more severe and manifests as swelling of the subcutaneous

tissue around the head, neck and supraorbital fossae of the animal. In more severe infections, tissue in other areas may also appear swollen. The cardiac form of the disease has a mortality rate of *ca.* 50%. The pulmonary form of the disease is more severe. Clinical symptoms include a high fever, as well as coughing and discharge of copious amounts of serofibrinous fluid as froth from the nostrils. The onset of dyspnoea usually precedes death and can occur suddenly in an otherwise apparently healthy animal. The mortality rate is very high and fewer than 5% of infected horses recover. The mixed form of AHS refers to cases wherein the affected animal shows symptoms of both the cardiac and pulmonary form of the disease, and the mortality rate is *ca.* 70% with death occurring within 3-6 days after onset of fever (Coetzer and Guthrie, 2004).

2.2.5 Control and prevention of AHS

At present, there is no specific treatment available for AHS due to the rapid onset and severity of the disease. Consequently, great emphasis has been placed on the control of AHS incidence (House, 1998; Sanchez-Vizcaino, 2004). Since AHSV is non-contagious and can only spread via the bites of infected *Culicoides* species, control is effected through the use of insecticides and repellents to control the vector population, as well as by restricting animal movement to prevent infected animals from initiating new foci of infection, and, in some instances, by slaughtering of viraemic animals to prevent them acting as sources of virus for vector insects (Meiswinkel *et al.*, 2000; Mellor and Hamblin, 2004).

In addition to the above, control of AHS may be effected by vaccination of susceptible equines, which remains the most practical and effective measure (Van Dijk, 1998; Mellor and Hamblin, 2004; Patel and Heldens, 2009). In southern Africa, AHS is controlled by vaccination with polyvalent live attenuated vaccines that are administered twice in the first and second year of life of susceptible animals, and annually thereafter (Van Dijk, 1998). The vaccine is formulated into two components, *i.e.* trivalent (serotypes 1, 3 and 4) and quadrivalent (serotypes 2, 6, 7 and 8) combinations. The AHSV serotypes were selected based on cross-neutralization results and minimal inter-serotype interference post-vaccination, in order to allow antibody production to each of the AHSV serotypes. Due to the difficulties experienced in the attenuation of serotype 5 and because serotype 9 historically rarely causes disease in South Africa, these serotypes were excluded from the current vaccine

formulation. However, serotypes 8 and 6 afford a degree of cross-protection against respectively serotypes 5 and 9 in vaccinated animals (von Teichman *et al*., 2010).

Due to concerns regarding gene segment reassortment between virulent and avirulent strains (House, 1998; Venter and Paweska, 2007) and the fact that some strains of the virus in the vaccine might only be weakly immunogenic (Laegreid, 1996), research has been undertaken to develop alternative vaccines. Subunit vaccines, based on the use of baculovirus-expressed AHSV-4 VP7 (Wade-Evans *et al.*, 1997) and the outer capsid proteins VP2 and VP5 (Martinez-Torrecuadrada *et al.*, 1996; Scanlen *et al.*, 2002), have been investigated. A recombinant Venezuelan equine encephalitis virus-derived vector, expressing AHSV-4 VP2 and VP5, has also been developed but failed to induce neutralizing antibodies in horses (MacLachlan *et al.*, 2007). In contrast, immunization with a recombinant canarypox virus-vectored vaccine, co-expressing the AHSV outer capsid proteins (VP2 and VP5), was reported to induce complete protection in horses (Guthrie *et al*., 2009). Furthermore, a modified vaccinia Ankara (MVA) strain, which is replication deficient, was used for expression of different AHSV antigens (VP2, VP7 and NS3 of AHSV-4) and presented in ponies (Chiam *et al.*, 2009). Analysis of the antibody responses indicated that only the VP2 vaccine was capable of inducing a neutralizing antibody response. Despite these developments, none of the subunit vaccines have been commercialized, which could be a reflection of cost and/or difficulties associated with their large-scale production.

2.3 AFRICAN HORSE SICKNESS VIRUS (AHSV)

2.3.1 Classification

AHSV belongs to the genus *Orbivirus* in the family *Reoviridae*. This family encompasses viruses with a dsRNA genome (10-12 segments) encapsidated within single non-enveloped virus particles with a diameter of 60-80 nm and exhibit icosahedral symmetry (Mertens, 2000; Mertens *et al.*, 2005). Twelve genera are currently included in this family (Schiff *et al.*, 2006). Members of the *Reoviridae* infect humans and other mammals (colitiviruses, orbiviruses, orthoreoviruses, rotaviruses, seadornaviruses), fish and mollusks (aquareoviruses), birds and reptiles (orthoreoviruses), insects (cypoviruses, idnoreoviruses), plants (fijiviruses, oryzaviruses, phytoreoviruses), and fungi (mycoreoviruses).

Orbiviruses can be distinguished from other members of the *Reoviridae* in that they replicate in both insects and vertebrates, show greater sensitivity to lipid solvents and detergents, and virus infectivity is lost in mild acidic conditions (Calisher and Mertens, 1998). The prefix "orbi" in "orbiviruses" is derived from the Latin word "orbis", meaning ring or circle, and describes the characteristic pentameric or hexameric capsomers (rings) on the orbiviral core-surface (Borden *et al.*, 1971). AHSV has similar morphological and biochemical properties to other orbiviruses of agricultural importance, including bluetongue virus (BTV), the prototype orbivirus, and epizootic hemorrhagic disease virus (EHDV). Currently, 21 orbivirus serogroups are distinguished based on serologic cross-reactivities, while virus neutralization tests discriminate different serotypes within each serogroup (Gorman, 1979; Mertens *et al.*, 2005). To date, nine different serotypes of AHSV have been identified. Serotypes 1 to 7 were identified by Sir Arnold Theiler between 1908 and 1921 (Theiler, 1921), and the last two serotypes, 8 and 9, were identified later in 1962 (Howell, 1962).

2.3.2 Virion structure

The AHSV virion is non-enveloped and consists of two concentric protein layers that enclose the dsRNA genome consisting of 10 segments (Oellerman *et al.*, 1970; Manole *et al.*, 2012). The outer capsid of the virion is composed of the two major structural proteins VP2 and VP5. The inner capsid (core) is composed of the structural proteins VP7 and VP3, which enclose the three minor proteins, VP1, VP4 and VP6, as well as the dsRNA genome of the virus. A schematic diagram of the AHSV virion is presented in Fig. 2.2.

Using cryo-electron microscopy and three-dimensional image reconstruction, the architecture of an AHSV-4 reference strain was recently determined (Manole *et al.*, 2012). The structure of the AHSV particle was found to be comparable to that of BTV, of which the structure of single- and double-shelled virus particles has been determined by cryo-electron microscopy and by X-ray crystallography (Hewat *et al.*, 1992a; Prasad *et al.*, 1992; Grimes *et al.*, 1998; Stuart and Grimes, 2006). The AHSV core particle can be segregated into two distinct layers. The innermost layer of AHSV is a T=1 lattice composed of 60 asymmetric dimers of the triangular-shaped VP3 protein that forms a complete shell, while minimizing conformational distortion. The internal scaffold of VP3 is stabilized by the outer layer of the core which is composed of 780 monomers of VP7, arranged as 260 trimers on a T=13 lattice. The core contains the dsRNA genome and the transcription complexes consisting of VP1, VP4 and

VP6, each of which plays an important role in genome RNA replication (Stuart and Grimes, 2006). Cryo-electron microscopy and analyses have also revealed that the outer shell of AHSV is highly ordered, consisting of globular VP5 proteins that are located upon each of the six-membered rings of the VP7 trimers. Manole *et al.* (2012) suggested that AHSV VP5 is likely to be similar to the VP5 of BTV both in shape and fold topology, but they were unable to make a reliable homology model of AHSV VP5 to confirm this. Furthermore, VP2 is arranged as 60 triskelion-type motifs, formed by 180 copies of VP2, which are centred directly on top of the VP7 trimers. Together, VP2 and VP5 form a continuous layer surrounding the core. Interestingly, Manole *et al.* (2012) reported that a protein plugs the five-fold vertices of the AHSV VP3 layers. This is in contrast to results reported for BTV. Three types of channels have been distinguished in the BTV virion, depending on their location in the icosahedral layer, of which some extend into the VP3 layer. It has been proposed that the channels are involved in the passage of metabolites into and from the virus particle during replication (Diprose *et al*., 2001). Nascent mRNA transcripts are also thought to be extruded through pores in the VP3 layer at the five-fold axes (Gouet *et al*., 1999) and the VP7 channels located above these pores may act as portals for their release into the cytosol (Diprose *et al*., 2001; Mertens and Diprose, 2004).

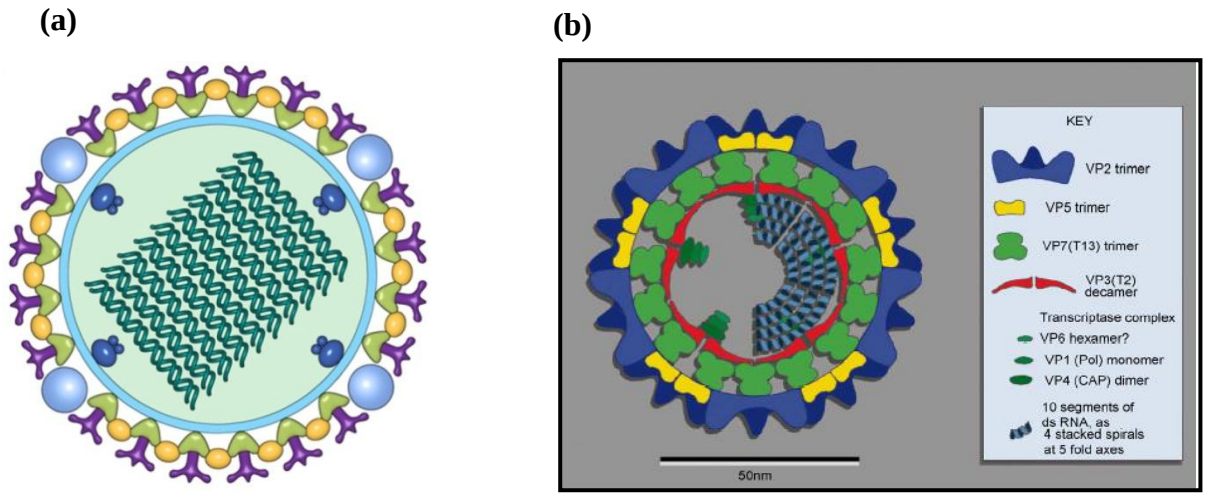

Fig. 2.2 Schematic representation of the AHSV-4 virion (a) and the BTV-1 virion (b). The structural arrangement of the AHSV virion was modelled based on data obtained from cryo-electron microscopy. The VP3 protein (light blue) encloses the dsRNA segments of the AHSV genome (forest green) and the proteins of the transcription complex, namely VP1, VP4 and VP6 (dark blue). Attached to the VP3 surface are the VP7 trimers (light green), upon which the VP2 protein (purple) is attached. The VP5 protein (yellow) is located in the spaces made by the VP2 lattice (Manole *et al.*, 2012). The structure of the AHSV virion reveals a similar structural arrangement as the BTV virion (b), which is shown for comparative purposes (Mertens and Diprose, 2004).

2.3.3 Viral genome

The genome of AHSV comprises 10 dsRNA segments, which are designated according to their migration rates through polyacrylamide gels (Oellerman, 1970). The genome segments are further grouped into three size classes, *i.e.* large (L1-3), medium (M4-6) and small (S7-10) (Bremer *et al.*, 1990). With the exception of S10, and possibly S9, each genome segment encodes for a single protein. It was recently reported that BTV S9 contains two overlapping open reading frames and, in addition to VP6, encodes a non-structural protein, NS4 (Belhouchet *et al.*, 2011; Ratinier *et al.*, 2011). S10 of BTV (Huismans, 1979; Van Dijk and Huismans, 1988) and AHSV (Van Staden and Huismans, 1991; Van Staden *et al.*, 1995), encodes for both NS3 and NS3A via different in-frame translation initiation sites. The different AHSV dsRNA segments with their encoded proteins are summarized in Table 2.1.

The molecular weight of the 10 AHSV genome segments range from 2.53 - 0.2 × 10^6 Da, with a total molecular weight of 13 × 10^6 Da (Bremer, 1976; Roy *et al.*, 1994). The 5' non-coding region of the genome segments ranges in size between 12 and 35 base pairs (bp), while the 3' non-coding regions are 29 to 100 bp in length (Roy *et al.*, 1994). In contrast to BTV, the terminal hexanucleotide sequences of AHSV are not conserved through all the segments (Rao *et al.*, 1983; Roy *et al.*, 1994). Nevertheless, the 5'- and 3'-terminal sequences of each genome segment display partial inverted complementarity and this feature is thought to play a role in determining the secondary structure of the viral mRNA. The segment-specific secondary structures have been postulated to act as sorting signals for the incorporation of each viral positive-strand ssRNA transcript into progeny viral capsids (Rao *et al.*, 1983; Markotter *et al.*, 2004). Alternatively, it has been suggested that these structures may facilitate second-strand synthesis by interacting via homologous base pairing, thus holding ssRNA in a panhandle structure to guide the RNA-dependent RNA polymerase viral enzyme (Mertens and Diprose, 2004).

2.3.4 Viral proteins

Bluetongue virus (BTV) has been the subject of extensive molecular, genetic and structural studies (Roy, 2008). As a consequence, it represents one of the best characterized viruses. Therefore, in the following sections, information on AHSV will be supplemented with that obtained from studies undertaken on BTV.

Table 2.1 AHSV genome segments and encoded proteins

AHSV genome segment allocations				
dsRNA segment	**Length (bp)**	**Protein**	**Protein size (amino acids)**	**Location, function, or property in analogy to BTV**
L1	3965 (3854)[a]	VP1	1305 (1302)	Subcore: minor structural protein; RNA-dependent RNA polymerase.
L2	3205 (2926)	VP2	1053 (956)	Outer capsid: structural protein (180; 60 trimers); Receptor-mediated virus entry; Haemagglutinin; Serotype-specific determinant; Highly variable; Serotype-specific neutralization; Virus egress (binds vimentin and NS3).
L3	2792 (2770)	VP3	905 (901)	Subcore layer: structural protein (120; 60 asymmetric decamers); Serogroup-specific antigen; Highly conserved; Scaffold for VP7; Interacts with genomic RNA.
M4	1978 (1981)	VP4	642 (644)	Subcore: minor core structural protein; Capping enzyme: guanylyl transferase, methyl transferases 1 and 2, NTPase.
M5	1748 (1769)	NS1	548 (522)	Major non-structural protein; Virus-specified tubules, function unknown; Hypothesized function: virus translocation; cytopathogenesis.
M6	1566 (1638)	VP5	505 (526)	Outer capsid: structural protein (360; 120 trimers); Virus entry: fusiogenic; membrane permeabilization; translocation of core into cytosol.
S7	1169 (1046)	VP6/NS4[b]	369/143 (329/77)	Minor core structural protein; Possible helicase; binds ssRNA and dsRNA.
S8	1167 (1156)	VP7	349 (349)	Core: surface layer structural protein (780; 260 trimers); Serogroup-specific antigen; Conserved; Core entry into arthropod vectors.
S9	1166 (1124)	NS2	365 (357)	Non-structural protein; Associated with virus inclusion bodies (VIBs); Phosphorylated; binds ssRNA; recruits RNA? Phosphohydrolase.
S10	765 (822)	NS3/NS3A	217/203 (229/216)	Minor non-structural protein; Membrane-associated; Aids virus release.

[a]: The sizes of the corresponding BTV genome segments and proteins are indicated in brackets.
[b]: Expression of an AHSV NS4 protein has yet to be confirmed experimentally.

2.3.4.1 Outer capsid proteins

The VP2 protein, one of the two outer capsid proteins, is the most exposed virus protein on the virion surface and is the most variable protein among different serotypes (Potgieter *et al.*, 2003). The VP2 protein is the major serotype-specific antigen (Huismans and Erasmus, 1981) and displays heamagglutinin activity (Cowley and Gorman, 1987; Hassan and Roy, 1999). Furthermore, VP2 is involved in attachment of the virus to cells and has been reported to bind to sialic acid moieties of cellular receptors prior to internalization of the virus particle (Hassan and Roy, 1999; Zhang *et al.*, 2010). In addition to its role in attachment, VP2 is also emerging as a key player in the control of BTV assembly and egress from infected cells. The amino (N)-terminal of the protein interacts with vimentin and this interaction is proposed to contribute to virus egress (Bhattacharya *et al.*, 2007; Celma and Roy, 2009). Neutralizing epitopes have been mapped on AHSV VP2 (Bentley *et al.*, 2000; Martínez-Torrecuadrada *et al.*, 2001) and antibodies raised in rabbits to VP2 of AHSV-4 have been reported to neutralize a virulent strain of AHSV-4 (Martínez-Torrecuadrada *et al.*, 1994). It has also been shown that vaccinia- and baculovirus-expressed AHSV VP2 can protect horses against a lethal challenge with the homologous virus serotype (Stone-Marschat *et al.*, 1996; Scanlen *et al.*, 2002).

Recent studies of VP5 of both BTV and AHSV showed that the protein permeabilizes host cell membranes (Hassan *et al.*, 2001; Stassen *et al.*, 2011) and has the ability to induce cell-cell fusion when expressed on the cell surface (Forzan *et al.*, 2004). Both of these activities are mediated by two N-terminal amphipathic helices and are believed to play a major role in destabilizing the membrane of the endocytosized vesicle, thus allowing release of the viral core into the cytoplasm (Forzan *et al.*, 2007; Zhang *et al.*, 2010). Furthermore, in contrast to BTV (Marshall and Roy, 1990), AHSV VP5 is able to induce neutralizing antibodies, albeit at lower levels than VP2 (Martínez-Torrecuadrada *et al.*, 1999). However, when used in conjunction with VP2, higher titers of neutralizing antibody, compared to immunization with VP2 only, have been reported (Martínez-Torrecuadrada *et al.*, 1996). Consequently, it was proposed that AHSV VP5 may play a supportive role to VP2 in enhancing the immune response.

2.3.4.2 Inner capsid proteins

- **Major core proteins**

The two major structural proteins VP3 and VP7 form the inner and outer layer, respectively, of the viral core particle. The most abundant structural protein in the virion is VP7 that self-assembles into trimers (Basak *et al*., 1992). In both BTV and AHSV, VP7 has been demonstrated to be a serogroup-specific antigen (Huismans and Erasmus, 1981; Chuma *et al*., 1992; Maree and Paweska, 2005). The crystal structure of BTV VP7 has been solved and revealed that each VP7 monomer has two distinct domains, *i.e.* an outer or top β-barrel domain and an inner or bottom α-helical domain that is formed by both the amino and carboxy termini of the molecule (Basak *et al*., 1992; Grimes *et al*., 1995). The X-ray structure of the top domain of AHSV-4 has also been solved and revealed a structural arrangement similar to that of BTV (Basak *et al*., 1996). The top domain contains a conserved surface-exposed Arg-Gly-Asp (RGD) tripeptide that is believed to mediate attachment and entry of cores into *Culicoides* host cells in the absence of the outer capsid proteins (Xu *et al*., 1997; Tan *et al*., 2001). The AHSV VP7 protein has been shown to form hexagonal crystals in the cytoplasm of mammalian cells infected with AHSV, as well as in *Spodoptera frugiperda* insect cells infected with recombinant baculoviruses (Chuma *et al*., 1992; Burroughs *et al*., 1994; Maree and Paweska, 2005). These VP7 crystalline structures have not been observed in BTV-infected cells and it is unknown what function, if any, these structures may have.

VP3 is the most conserved major capsid protein among different AHSV serotypes (Le Blois *et al*., 1991; Iwata *et al*., 1992). In addition to playing a crucial role in the structural integrity of the core particle by providing a scaffold for the VP7 trimers, the VP3 protein also contains group-specific antigenic determinants (Inumaru *et al*., 1987), and it is capable of binding to RNA (Loudon and Roy, 1992) and the non-structural protein NS2 (Kar *et al*., 2005). A model for the assembly of AHSV subcores has recently been proposed (Manole *et al*., 2012). The VP3 proteins were reported to occur in one of two forms, an A or B form, depending on their folding conformation. It was proposed that the VP3 proteins dimerize in groups of five of each VP3A and VP3B to form a decameric structure, and that 12 of these structures then coalesce to form the scaffold structure or subcore.

- **Minor core proteins**

Viral cores are transcriptionally active and have associated RNA-dependent RNA polymerase activity (Verwoerd and Huismans, 1972; Van Dijk and Huismans, 1980). The minor core proteins (VP1, VP4 and VP6) display independent enzyme activities and are collectively referred to as the "transcription complex" (Mertens *et al.*, 2004). In the case of BTV, the transcription complexes interact with the inner surface of VP3, immediately below a pore at the five-fold axes, and each dsRNA segment appears to associate with a different transcription complex (Grimes *et al*., 1995; Gouet *et al*., 1999; Nason *et al*., 2004). X-ray diffraction studies have indicated that the transcription complexes of AHSV are also located at the five-fold symmetry axis of the VP3 decamers (Manole *et al.*, 2012).

The largest of the minor core proteins, VP1, is considered to be the RNA-dependent RNA polymerase responsible for transcription of the viral dsRNA genome. BTV and AHSV VP1 possesses motifs characteristic of RNA polymerases, including a Glycine-Aspartic acid-Aspartic acid (GDD) motif (Roy *et al.*, 1988; Vreede and Huismans, 1998), and share homology with other prokaryotic or eukaryotic RNA polymerases (Kowalik and Li, 1989; Kowalik *et al*., 1990). By making use of lysates prepared from *S. frugiperda* cells infected with a recombinant baculovirus expressing BTV VP1, it was shown that poly(A) synthesis can occur *in vitro* when the extract is provided with a poly(A) primer and poly(U) template (Urukawa *et al*., 1989). More recently, it was reported that soluble recombinant BTV VP1 displayed a processive replicase activity, synthesizing complete complementary negative-strand RNA of *in vitro*-synthesized positive-strand virus RNA template (Boyce *et al*., 2004). However, the replicase activity associated with the recombinant BTV VP1 was low and exhibited little sequence specificity for BTV positive-strand templates.

Newly synthesized viral mRNA must be capped and methylated at the 5'-end in order to stabilize the mRNA synthesized during viral infection (Roy, 1992; Boyce *et al.*, 2008). The BTV VP4 protein has been reported to possess guanylyltransferase (Le Blois *et al*., 1992) and methyltransferases type 1 and 2 (Ramadevi *et al*., 1998) activities. Furthermore, BTV VP4 also binds to GTP and displays nucleoside triphosphate phosphohydrolase (NTPase) activity, which may be important for transcription and RNA processing (Ramadevi and Roy, 1998).

BTV VP6 is a highly basic protein that displays ATP binding, nucleoside triphosphatase, RNA binding and helicase activities (Roy *et al*., 1990; Stäuber *et al*., 1997). Regions in VP6 of BTV (Hayama and Li, 1994) and AHSV (Turnbull *et al*., 1996) share homology with ATPase domains of known helicases. Similar to other helicases, BTV VP6 catalyzes the unwinding of dsRNA in the presence of divalent cations such as Mg^{2+} or Mn^{2+} and forms stable hexamers in the presence of nucleic acids (Kar and Roy, 2003). This activity of VP6 may thus mediate unwinding of the dsRNA genome segments ahead of the transcriptase protein, and may also allow for separation of the parental and newly synthesized RNAs following transcription (Stäuber *et al*., 1997). AHSV VP6 contains two nucleic acid binding domains near the centre of the protein, as well as at the C-terminal of the protein (Hayama and Li, 1994; De Waal and Huismans, 2005). Due to its ability to bind RNA, VP6 is also considered to potentially be involved in the packaging of viral RNA during virus replication.

2.3.4.3 Non-structural proteins

The orbivirus non-structural proteins do not form part of the mature virion particle; however, they are thought to play important roles during virus replication and are responsible for the formation of several virus-associated structures in the cytoplasm of infected cells. The non-structural proteins include the NS1, NS2, NS3 and co-linear NS3A proteins, as well as the recently discovered NS4 protein.

The NS1 protein is expressed abundantly in infected cells and self-assembles into cytoplasmic tubules, which are morphologically and biochemically distinct from cellular microtubules and neurofilaments (Huismans and Els, 1979). The NS1 protein is rich in cysteine residues and contains several hydrophobic and hydrophilic regions spaced evenly throughout the protein, suggesting it has a highly ordered structure (Maree and Huismans, 1997). In AHSV-infected cells, the tubules display an interlaced, cross-weave appearance and are 23 nm in diameter and may be up to 4 µm in length (Maree and Huismans, 1997). In contrast, BTV tubules exhibit a defined ladder-like appearance and are 52.3 nm in diameter and do not exceed 1 µm in length (Hewat *et al*., 1992b). Although the function of the NS1 tubules in virus replication has not yet been elucidated, it has been proposed that they may be involved in the translocation of virus particles from virus inclusion bodies (VIBs) to the cell plasma membrane prior to virus release (Eaton *et al*., 1990), or, alternatively, that they function as a chaperone to prevent premature core particle assembly prior to encapsidation of

the subcore components (Hewat *et al.*, 1992b). More recent evidence suggests that the BTV NS1 protein is a major determinant of pathogenesis in the vertebrate host since it augments virus-cell association that ultimately leads to lysis of the infected cell (Owens *et al.*, 2004).

The NS2 protein is the predominant component of VIBs (Hyatt and Eaton, 1988; Brookes *et al.*, 1993). NS2 is also the only virus-specific protein that is phosphorylated in infected cells (Huismans *et al.*, 1987; Devaney *et al.*, 1988). Although the significance of NS2 phosphorylation is not understood completely, a recent report has indicated that BTV NS2 is phosphorylated by casein kinase 2 (CK2) and that phosphorylation of NS2 is important for VIB formation (Modrof *et al.*, 2005). In addition, NS2 has a strong affinity for ssRNA but not for dsRNA, suggesting that it may have a role in the recruitment and packaging of viral ssRNA prior to encapsidation (Huismans *et al.*, 1987). BTV NS2 also displays phosphohydrolase (NTPase) activity and can bind and hydrolyse ATP and GTP to their corresponding nucleotide monophosphates (Horscroft and Roy, 2000; Taraporewala *et al.*, 2001). However, the functional importance of this enzymatic activity is not yet known. The above-mentioned properties of NS2 will be discussed in greater detail, as they are closely related to the aims of this investigation (See Section 2.5).

The two closely related NS3 and NS3A proteins are synthesized much less abundantly than the NS1 and NS2 proteins in orbivirus-infected cells (Huismans, 1979; French *et al.*, 1989; Van Staden *et al.*, 1995). The AHSV NS3 and NS3A proteins are encoded by RNA genome segment 10 from alternate in-phase translation initiation codons, and differ only with respect to 10 amino acid residues present at the N-terminal end of NS3 (Van Staden and Huismans, 1991). The BTV NS3, in contrast to that of AHSV, has been shown to be glycosylated (Wu *et al.*, 1992), which may serve to protect it from degradation (Bansal *et al.*, 1998). Expression of AHSV NS3 by a baculovirus recombinant was reported to have a cytotoxic effect on the *S. frugiperda* insect cells (Van Staden *et al.*, 1995). Although the mechanism by which NS3 causes cell death is not known, it may be as a result of an alteration of the permeability of the cell membrane. Subsequently, it was shown that the cytotoxic effect was abrogated when mutations were introduced into either of the NS3 hydrophobic transmembrane domains, thus indicating that cytoxicity is dependent on the membrane association of the protein (Van Niekerk *et al.*, 2001). Transmission electron microscopy studies revealed that the NS3 proteins are localized to the sites of virus release in infected cells (Hyatt *et al.*, 1993; Stoltz *et al.*, 1996). NS3 has also been shown to interact specifically with VP2 in newly formed BTV

virions (Beaton *et al.*, 2002), an activity which has been mapped to highly charged lysine residues on the C-terminal of the protein (Celma and Roy, 2009). These findings therefore suggest a role for NS3 during the final stages of viral morphogenesis by facilitating the release of progeny virus from infected cells.

The NS4 protein was only recently described after bioinformatic analysis of the S9 genome segment of BTV detected an open reading frame overlapping the VP6 gene, as well as in the VP6 cistron of other orbiviruses including AHSV (Firth, 2008; Belhouchet *et al.*, 2011). NS4 rapidly accumulates in both mammalian and *Culicoides* insect cells after 4 h post-infection with BTV, giving rise to aggregates that are present throughout the cytoplasm, as well as in the nucleoli of infected cells (Belhouchet *et al.*, 2011; Ratinier *et al.*, 2011). The finding that NS4 localizes in the nucleus may be ascribed to the presence of nuclear localization signal in the S9 nucleotide sequence. This non-structural BTV protein is predicted to be structured as coiled-coils and, based on bioinformatic comparisons, may be functionally related to proteins involved in nucleic acid binding, or that are associated with lipids and membranes. In agreement with the latter, cell-localization studies indicated that the BTV NS4 protein is associated with lipid droplets within infected cells (Belhouchet *et al.*, 2011). At 72 h post-infection, BTV NS4 is associated with the cell membrane, suggesting that the protein may play a role, together with NS3, in virus exit. It was furthermore demonstrated that BTV NS4 protects DNA from degradation by DNase, but not dsRNA from RNase III cleavage (Belhouchet *et al.*, 2011). Although NS4 was shown to be dispensable for BTV replication, both in mammalian and insect cells, it nevertheless conferred a replication advantage to BTV-8, but not to BTV-1, in cells in an interferon (IFN)-induced antiviral state (Ratinier *et al.*, 2011). It was thus suggested that NS4 may play an important role in virus-host interaction and that it may be a possible mechanism, at least by BTV-8, to counteract the antiviral response of the host.

2.4 REPLICATION AND MORPHOGENESIS OF ORBIVIRUSES

Although orbiviruses are able to replicate in vertebrate hosts and arthropod vectors, the effect of orbivirus replication in these distinct host types is markedly different. For AHSV and BTV, replication of the virus in insect cells results in persistent infection with little or no cytopathic effect (CPE) (Homan and Yunker, 1988; Stassen *et al.*, 2012). However, infection

of mammalian cells results in cell death (Huismans, 1979; Wechsler and McHolland, 1988; Stassen *et al.*, 2012). Although it is likely that the basic replication strategies may be similar in the different host types, orbiviruses must have evolved specific replication mechanisms to enable the survival of its arthropod vector to ensure infection of a new vertebrate host. Using BTV as a model for orbivirus replication and morphogenesis, four major events in the replication cycle of orbiviruses have been identified (Fig. 2.3). These events are (i) adsorption and penetration, (ii) uncoating of the virion and formation of replicative complexes, (iii) formation of virus tubules and virus inclusion bodies, and (iv) transport of virus to and release from the cell surface (Gould and Hyatt, 1994; Mertens *et al.*, 2004; Roy, 2008).

BTV rapidly adsorbs to susceptible mammalian cells, with maximal adsorption occurring within 20 min (Huismans *et al.*, 1983). The binding and internalization of BTV in mammalian cells is mediated by the outer capsid protein VP2 (Huismans and Van Dijk, 1990; Hassan and Roy, 1999). Although the cellular receptors to which BTV binds have not yet been identified, it has been reported that the VP2 of BTV attaches to sialoglycoproteins of mammalian cells prior to internalization (Hassan and Roy, 1999; Zhang *et al.*, 2010). In contrast to mammalian cells, BTV virions bind *Culicoides* cells with low efficiency; however, core particles are highly infectious (Mertens *et al.*, 1996; Tan *et al.*, 2001). This suggests that the outer core protein VP7 may therefore be responsible for binding to insect cell receptors.

Following adsorption, the virus enters mammalian cells through AP2-dependent clathrin-mediated endocytosis and is incorporated into early endosomes (Forzan *et al*., 2007). The low pH environment within the endosome causes removal of VP2 and triggers conformational changes in VP5 that allows the protein to permeabilize the endosomal membrane (Hassan *et al*., 2001; Forzan *et al.*, 2004; Zhang *et al*., 2010). Subsequently, the transcriptionally active core is released into the cytoplasm (Huismans *et al.*, 1987; Forzan *et al*., 2007). Following the entry of cellular substrates into the viral core, the viral transcription complex is activated (Mertens and Diprose, 2004). Within the BTV core, VP6, the viral helicase, likely unwinds dsRNA duplexes ahead of the viral polymerase to enable transcription (Stäuber *et al*., 1997). The viral polymerase (VP1) transcribes ssRNA copies (positive-strand) of each of the 10 RNA genome segments simultaneously and repeatedly (Boyce *et al*., 2004), which are then capped and methylated by the viral capping enzyme VP4 (Sutton *et al.*, 2007).

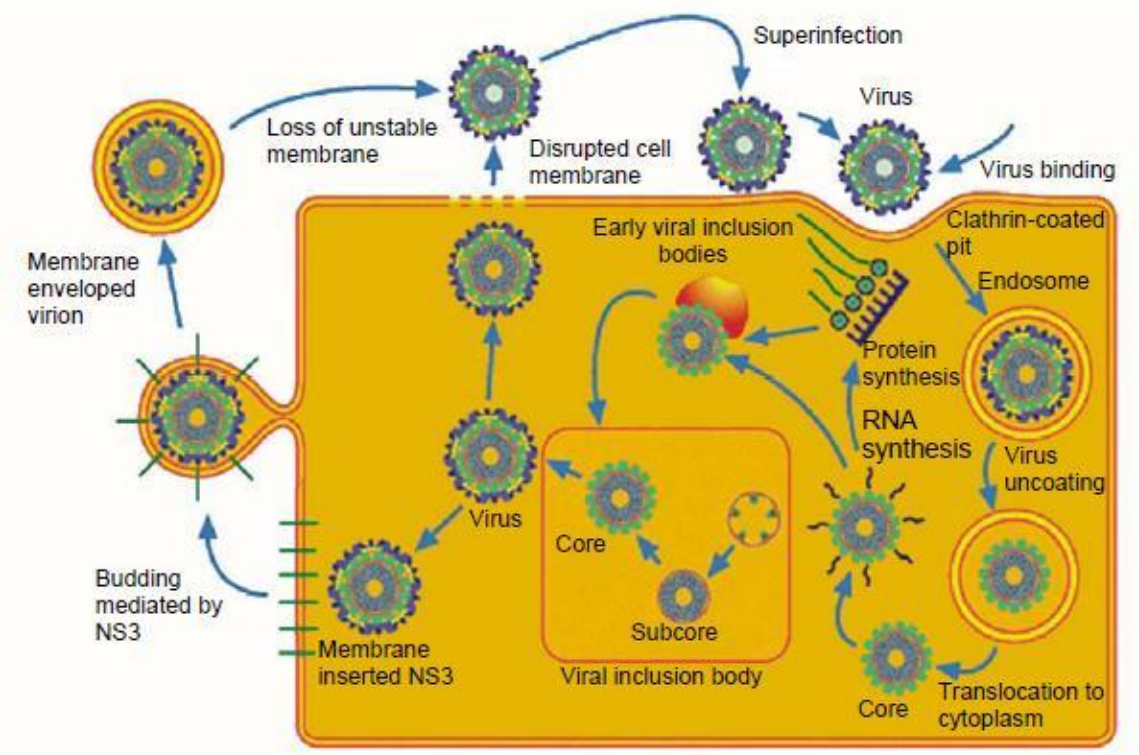

Fig. 2.3 Schematic representation of the replication cycle of an orbivirus, based on the model for BTV replication. The virus enters the cell by means of clathrin-mediated endocytosis. After uncoating, the transcriptionally active core begins ssRNA synthesis for early protein expression. Progeny virions are assembled within the VIBs and mature virus particles are released through either NS3-mediated budding or through disruption of the host cell membrane (Mertens *et al.*, 2004).

Conformational changes in VP3 and VP7 possibly mediates opening of a pore in the VP3 layer at the five-fold axes (Gouet *et al*., 1999) and enables extrusion of the stabilized mRNAs into the cytoplasm where they are translated into viral proteins (Diprose *et al*., 2001; Mertens and Diprose, 2004). Since AHSV appears to lack a pore at the five-fold axes at the VP3 layer (Manole *et al.*, 2012), it is unclear how these processes progress in AHSV. The first viral proteins can be detected between 2-4 h after infection, after which the rate of viral protein synthesis increases rapidly until 11-13 h post-infection, and then slows down until cell death (Huismans, 1979; Huismans and Van Dijk, 1990). The mRNA transcripts function not only to encode proteins, but also as templates for production of minus-strands to form the dsRNA genome segments encapsidated in the progeny virions (Mertens and Diprose, 2004). However, the mechanism by which viral mRNAs are selected and encapsidated prior to replication is not yet known.

Soon after the initiation of translation of viral transcripts, viral proteins condense with the viral ssRNA around the parental cores to form granular, early VIBs (Eaton *et al*., 1990; Brookes *et al*., 1993). The VIBs, which consist mainly of the ssRNA-binding phosphoprotein NS2 (Thomas *et al*., 1990), grow in size during the replication cycle (Eaton *et al*., 1990). The four subcore viral proteins (VP1, VP3, VP4 and VP6), as well as assembled cores and subcores have been identified in the VIBs and therefore appear to be the sites of early viral assembly (Hyatt and Eaton, 1988). More recently, co-expression of the BTV structural proteins with NS2 has indicated that VP7 requires co-expression of VP3 to be recruited to the VIBs and that neither of the outer capsid proteins VP2 and VP5 have an affinity for the VIBs (Modrof *et al.*, 2005; Kar *et al.*, 2007). Therefore, it would appear that progeny core particles are first produced in the VIBs, then moved to the periphery of the VIBs where they are coated by the outer capsid proteins VP2 and VP5 (Kar *et al.*, 2007). Little is known of the mechanism whereby VP2 and VP5 are added to the developing virus particle. However, it was reported that VP5 of BTV associates with lipid rafts in the plasma membrane and that the core particles are transported to these sites for the final assembly of the outer capsid proteins (Bhattacharya and Roy, 2008). Although the NS1-rich virus tubules are not observed within the VIBs, they are found associated with the cytoskeleton in BTV-infected cells (Eaton *et al*., 1987) and form part of the insoluble phase of the cell at an early stage of infection (Huismans and Els, 1979). BTV tubules have been reported to be a determinant of pathogenesis in the vertebrate host by leading to lysis of infected cells (Owens *et al*., 2004).

BTV utilizes different strategies to escape from vertebrate and invertebrate cells. Investigations regarding virus release from mammalian cells have demonstrated a strong correlation between the presence of NS3 and NS3A, and virus release (Hyatt *et al.*, 1989; Hyatt *et al.*, 1993). In addition, virions have been demonstrated to leave infected cells in two ways. Early after the infection, progeny virions have been observed to bud through the plasma membrane, acquiring a transient envelope. Alternatively, egress of virions can be accomplished by non-enveloped particles by extrusion through locally disrupted plasma membrane surfaces (Hyatt *et al.*, 1989). Although virus release is observed in mammalian cells, virions remain mainly associated with cellular components and only a minority of particles are found in the extracellular medium (less than 10%), presumably due to release as a consequence from CPE and death of infected cells (Guirakhoo *et al.*, 1994). In contrast to mammalian cells, infection of insect cells results in persistent infection with no CPE and the majority of progeny virions (90%) are released into the supernatant (Homan and Yunker, 1988; Guirakhoo *et al.*, 1994). The increased release of progeny virions in insect cell culture is also associated with increased NS3/NS3A expression (Guirakhoo *et al.*, 1994). Notably, the NS3 protein of BTV has also been shown to interact with the cellular proteins p11 and Tsg101, and these interactions were shown to assist in the egress of virus particles from infected cells in a non-lytic manner (Beaton *et al.*, 2002; Wirblich *et al.*, 2006; Celma and Roy, 2009).

2.5 THE NON-STRUCTURAL PROTEIN NS2

Since NS2 is the focus of this investigation, the following sections will focus in greater detail on its properties and possible roles in virus replication and morphogenesis. The information on AHSV NS2 will be supplemented, where applicable, with relevant information obtained from studies on NS2 of BTV and comparisons will also be made to the cognate non-structural proteins of other members of the *Reoviridae*.

2.5.1 Structure of NS2

Sedimentation analysis and non-reducing SDS-polyacrylamide gel electrophoresis revealed that the NS2 protein of BTV and AHSV is a 7S homo-multimer with both inter- and intra-molecular disulfide bonds, and consists of *ca.* six to eight NS2 molecules (Uitenweerde *et al.*, 1995; Taraporewala *et al.*, 2001). The tendency of the NS2 proteins to form higher oligomers

of variable size has precluded structural analysis of the full-length NS2 protein. Consequently, structural analysis has been limited to the N-terminal and C-terminal domains of the BTV NS2 protein. The high-resolution structure of the 182-amino-acid N-terminal domain of NS2 from BTV was reported by Butan *et al.* (2004). The crystal is composed of infinite chains of the protein domain that form a spiral. The structure is a β-sandwich and two extensive interfaces were described. One of these involves the extension of the β-sheet and the second involves an arm that links one protein molecule to the next, thus generating oligomers that span the crystal. A low resolution envelope, obtained from small-angle X-ray scattering measurements (SAXS), of the C-terminal segment (residues 178-354) of NS2 was reported by Mumtsidu *et al.* (2007). The C-terminal domain was modelled to likely be positioned on the inside of the spiral configuration, which would prevent the spiral from closing. This configuration would prevent the NS2 protein from forming oligomers consisting of more than 10 to 12 monomeric units. Crystallographic analysis of phosphorylated BTV NS2 has not yet been performed due to the non-uniformity of the samples' oligomer states and the flexibility of the two-domain configuration (Butan *et al.*, 2004; Mumtsidu *et al.*, 2007).

2.5.2 Properties of NS2

2.5.2.1 Virus inclusion body (VIB) formation

In AHSV- and BTV-infected cells, VIBs are observed as large, electron-dense perinuclear structures (Breese, 1969; Eaton *et al.*, 1988, 1990; Brookes *et al.*, 1993) that increase both in size and number as the infection progresses (Eaton *et al.*, 1990). The NS2 protein is the predominant component of VIBs and expression of NS2, in the absence of other viral proteins in both insect and mammalian cells, results in the formation of inclusion bodies (IBs) that are indistinguishable of VIBs found in virus-infected cells (Thomas *et al.*, 1990; Brookes *et al.*, 1993; Uitenweerde *et al.*, 1995; Modrof *et al.*, 2005). These results therefore indicate that the NS2 proteins are the minimal components required to form VIBs. In addition to NS2, the four subcore viral proteins (VP1, VP3, VP4 and VP6), as well as assembled cores and subcores have been identified in the VIBs (Hyatt and Eaton, 1988; Kar *et al.*, 2007). Consequently, the VIBs are thought to be the sites where early viral assembly occur. It has also been shown that truncated NS2 proteins lacking amino- (1-115, 1-237) and carboxyl- (116-357, 238-357) terminal fragments were impaired in their ability to form IBs. Interestingly, expression of the N-terminal (1-115) and C-terminal (116-357) deletion NS2

mutants in mammalian cells, which had been infected with BTV, was shown to result in a marked reduction in overall virus yield and thus indicates that virus replication was adversely affected (Kar *et al.*, 2007).

2.5.2.2 RNA binding activity of NS2

A central unresolved question regarding the morphogenesis of orbiviruses concerns the mechanism whereby individual segments are selectively recognized, sorted and assembled into mature virus particles. The lack of free pools of non-packaged dsRNA in infected cells has led to the assumption that the viral mRNA are encapsidated, with the minus-strands subsequently being made using packaged positive-strands as templates. Based on its ssRNA binding capability, several studies have linked NS2 with a function in viral mRNA selection and condensation.

Many early studies regarding the ssRNA binding ability of NS2 have indicated that the protein has a non-specific affinity for ssRNA. Non-specific binding of poly(U)-Sepharose by NS2 isolated from cells infected with BTV (Huismans *et al.*, 1987), as well as by NS2 of AHSV, BTV and EHDV expressed by recombinant baculoviruses (Uitenweerde *et al.*, 1995) has been demonstrated. Furthermore, BTV NS2 has also been reported to bind to *in vitro*-synthesized transcripts derived from plasmid DNA (Thomas *et al.*, 1990) and rotavirus gene 8 ssRNA (Taraporewala *et al.*, 2001). Although a condensing activity may only require non-specific ssRNA binding, selection of individual ssRNA segments would likely require a degree of specificity in the NS2-ssRNA interaction. Thus, binding should in addition to being specific for viral mRNA also be specific for each of the different mRNA transcripts. In this regard, competition UV cross-linking studies using radiolabelled BTV ssRNA and NS2 produced during virus replication in mammalian cells (Theron and Nel, 1997), as well as similar assays performed *in vitro* using purified baculovirus-expressed NS2 protein (Lymperopoulos *et al.*, 2003) concluded that NS2 bound preferentially to the BTV ssRNA. The specificity of interactions between NS2 and four BTV segments (S8, S9, S10 and M6) was also investigated in greater detail. Different stem-loop structures in the respective BTV RNA segments were shown to be recognized by NS2, suggesting that NS2-ssRNA interaction is dependent on the ssRNA structure and that the structural interactions between NS2 and the different BTV ssRNA segments are likely to be independent events (Lymperopoulos *et al.*, 2006).

Several studies aimed at identifying the ssRNA binding domains within NS2 have also been undertaken and these have indicated that the N terminus appears to be important for ssRNA binding. Truncated BTV NS2 with N-terminal deletions (up to residue 92) lost their ability to bind ssRNA (Zhao *et al.*, 1994). In addition, a short nine-amino-acid sequence, found within the NS2 of various orbiviruses and that resides within the N-terminal 92-amino-acid region, was shown through deletion and site-directed mutagenesis to be important for NS2 interaction with ssRNA (Theron *et al.*, 1996). However, more recently, three regions (residue positions 2-11, 153-166, and 274-286) within the BTV NS2 amino acid sequence were identified by deletion mutagenesis as being important for the binding of ssRNA (Fillmore *et al.*, 2002). Deletion of each domain reduced the affinity of NS2 toward ssRNA, and the deletion of all three domains completely eliminated the ability of NS2 to bind to ssRNA. This data therefore suggests that sequential domains of NS2 may bind ssRNA in a cooperative manner, rather than ssRNA binding being mediated by a single domain (Fillmore *et al.*, 2002).

2.5.2.3 Phosphorylation of the NS2 protein

The NS2 protein is the only orbivirus protein that undergoes phosphorylation during virus replication (Huismans *et al.*, 1987), and subsequent studies have indicated that NS2 expressed in insect cells by recombinant baculoviruses is also phosphorylated (Thomas *et al.*, 1990; Theron *et al.*, 1994). Notably, NS2 expressed in orbivirus-infected cells and NS2 expressed in insect cells shared the same phosphorylated peptides, indicating that phosphorylation of the same residues occurs in both cell types. Serine residues were identified as the phosphorylated amino acids in both BTV and AHSV NS2 hydrolysates (Devaney *et al.*, 1988), and the sites of BTV NS2 phosphorylation were recently identified as Ser-249 and Ser-259, located within the C-terminal segment of the protein (Modrof *et al.*, 2005; Mumtsidu *et al.*, 2007).

The NS2 protein lacks autokinase activity since an unphosphorylated form of EHDV NS2, obtained by expressing the NS2 gene in *Escherichia coli*, could only be phosphorylated *in vitro* by a protein kinase associated with the cytoplasm of insect cells (Theron *et al.*, 1994). Likewise, unphosphorylated BTV NS2, also expressed in *E. coli*, could be phosphorylated by cellular kinases when mixed with a cytoplasmic extract from uninfected mammalian cells (Taraporewala *et al.*, 2001). These results therefore ruled out the phosphorylation of NS2

protein by another orbivirus protein, but suggested that the NS2 protein is phosphorylated by a ubiquitous cellular protein kinase. The protein kinase responsible for BTV NS2 phosphorylation has since been identified as casein kinase 2 (CK2) (Modrof *et al.*, 2005). CK2 is ubiquitous among eukaryotic cells and is involved in the phosphorylation of many cellular proteins (Meggio and Pinna, 2003).

In contrast to EHDV, where phosphorylation of the NS2 protein appears to down-regulate its ssRNA binding ability (Theron *et al.*, 1994), the phosphorylation of BTV NS2 does not affect its ability to bind to ssRNA (Thomas *et al.*, 1990; Modrof *et al.*, 2005). However, phosphorylation of the BTV NS2 protein appears to be essential for the ability of the protein to form VIBs. In contrast to phosphorylated NS2 that exhibited VIB formation, an unphosphorylated version of the protein failed to assemble as VIBs and partially phosphorylated NS2 produced irregular VIB-like structures (Modrof *et al.*, 2005).

2.5.2.4 NTPase activity of NS2

As mentioned previously, BTV NS2 displays phosphohydrolase activity, and can bind and hydrolyze both ATP and GTP to their corresponding nucleotide monophosphates (Horscroft and Roy, 2000). It was furthermore reported that the hydrolysis of these substrates by NS2 is dependent on divalent ions (*e.g.* Ca^{2+}, Mg^{2+} and Mn^{2+}) and that ouabain, an inhibitor of cellular ATPases, did not abolish the ATPase activity of NS2 (Horscroft and Roy, 2000). In a subsequent study, purified *E. coli*-expressed BTV NS2 protein was shown to non-specifically hydrolyze the α-, β- and γ-phosphodiester bonds of nucleotide triphosphates to their corresponding nucleotide monophosphates (Taraporewala *et al.*, 2001). Of the four substrates tested, recombinant NS2 displayed higher efficiency for the hydrolysis of ATP as compared with the other nucleotides for which NS2 has a preference in the order GTP > UTP/CTP. The regions of NS2 responsible for this enzymatic activity have not yet been mapped, but a truncated BTV NS2 protein that lacked the first 177 amino acids at the N terminus was still able to hydrolyze NTPs (Mumtsidu *et al.*, 2007). Although the functional importance of the NTPase activity of NS2 is not yet known, it has been suggested that the enzyme activity may play a role in providing energy for the assortment, transportation, packaging or condensation of bound ssRNA (Horscroft and Roy, 2000).

2.5.3 Comparison to other *Reoviridae* proteins

The orbivirus NS2 protein shares several functional similarities with non-structural proteins of other members of the *Reoviridae* family, most notably the σNS-µNS protein pair of the reovirus genus and the NSP2-NSP5 protein pair of the rotavirus genus.

The σNS-µNS reovirus proteins, in combination, appear to be functional homologues of the orbivirus NS2 protein. The σNS protein associates with the µNS protein in reovirus viral factories (Miller *et al.*, 2003), which bear similar morphological properties as the VIBs of orbiviruses. However, when expressed alone in cells, µNS is capable of forming structures that resemble the viral factories in reovirus-infected cells, as assessed by light microscopy (Becker *et al.*, 2003). Like BTV NS2, σNS isolated from virus-infected cells is found in large complexes that dissociate upon treatment with RNase A to *ca.* four monomers (Huismans and Joklik, 1976; Gomatos *et al.*, 1981). Despite these similarities, there are also some differences between the orbivirus NS2 protein and the respective reovirus proteins. The σNS protein does not undergo phosphorylation and is incapable of hydrolyzing NTPs (Gillian *et al.*, 2000), whereas there are no reports regarding the phosphorylation status of the µNS protein or of its NTP hydrolysis capability.

The NSP2-NSP5 rotavirus protein pair plays a major role in the formation and structure of viroplasms in infected cells (Fabbretti *et al.*, 1999; Eichwald *et al.*, 2004). The viroplasms, similar to the VIBs observed in orbivirus-infected cells, are large cytoplasmic inclusion bodies that function as the sites of genome replication and packaging in rotavirus-infected cells (Silvestri *et al.*, 2004). Consequently, these proteins may be considered as possible functional homologues of BTV NS2. The NSP2 protein self-assembles into stable doughnut-shaped octamers (Taraporewala *et al.*, 2002) and, like BTV NS2, has non-specific ssRNA binding activity, forming large RNA-protein complexes (Taraporewala *et al.*, 1999, 2006). However, in contrast to BTV NS2, which has nucleotidyl phosphatase activity, NSP2 exhibits only NTPase activity and cleaves the terminal phosphate from NTPs without any specificity for a particular base (Taraporewala *et al.*, 1999, 2001). More recent studies have shown similar triphosphatase activity with pppRNA as a substrate, suggesting that NSP2 can be considered a 5'-RNA triphosphatase (RTPase) (Vasquez-Del Carpio *et al.*, 2006), and NSP2 also exhibits an NDP-kinase activity (Kumar *et al.*, 2007). How the various enzymatic activities of NSP2 are utilized in the context of genome replication remains unclear. The

rotavirus NSP5 protein has been reported to have both ssRNA and dsRNA binding affinities (Vende *et al.*, 2002) and, in the infected cell, the protein undergoes phosphorylation (Gonzalez and Burrone, 1991; Afrikanova *et al.*, 1996). However, variation in the phosphorylation of the protein is observed that generates NSP5 isomers *in vivo*, ranging from 28-kDa hypophosphorylated forms to 32- to 34-kDa hyperphosphorylated forms (Afrikanova *et al.*, 1996). Hyperphosphorylation of NSP5 requires NSP2 (Afrikanova *et al.*, 1998), whereas the conversion from hypo- to hyperphosphorylated NSP5 appears to be mediated by cellular kinase enzymes (Eichwald *et al.*, 2004; Campagna *et al.*, 2007). In contrast to BTV NS2, NSP5 phosphorylation is not important for viroplasm formation (Contin *et al.*, 2010) and the functional significance of NSP5 phosphorylation in the rotavirus infectious cycle is not yet known.

2.6 AIMS OF THIS INVESTIGATION

Although orbiviruses and especially AHSV are important pathogens of domestic and native animals, little is known about the mode whereby these viruses replicate and assemble in infected cells. The non-structural proteins are thought to play an important role in the replication cycle of these viruses. Information obtained for BTV has indicated that the NS2 protein may be of particular importance in these processes. In contrast, limited information is available on the function of the NS2 protein of AHSV. Studies have shown that the NS2 protein is phosphorylated, capable of binding ssRNA and is closely associated with the formation of VIBs, which are believed to be the sites in which virus morphogenesis occurs. It can be envisaged that a combination of mutagenesis and re-expression of phosphorylation-deficient AHSV NS2 protein would allow for greater understanding of the functional importance of NS2 phosphorylation. Towards the long-term goal of mapping the role of NS2 in the AHSV replication cycle, the specific aims of this investigation were as follow:

- To identify phosphorylated serine residues within the AHSV NS2 protein.
- To evaluate the importance of AHSV NS2 phosphorylation for VIB formation during expression in *S. frugiperda* cells and in virus-infected *C. variipennis* cells.

Chapter Three
Materials and Methods

3.1 Bacterial strains and plasmids

Escherichia coli strains were cultured in LB broth (1% [w/v] tryptone, 1% [w/v] NaCl, 0.5% [w/v] yeast extract; pH 7.4) (Sambrook and Russell, 2001) at 37°C with shaking at 200 rpm, and maintained at 4°C on LB agar plates (LB broth containing 1.2% [w/v] bacteriological agar) or at -70°C as glycerol cultures. For plasmid DNA selection and maintenance in *E. coli*, the following concentrations of antibiotics were used: 50 µg/ml for ampicillin, 50 µg/ml for kanamycin, 10 µg/ml for tetracycline and 7 µg/ml for gentamycin. All antibiotics were obtained from Sigma-Aldrich. Recombinant plasmid pGEX-AHSVNS2, which contains a full-length cDNA copy of AHSV-9 genome segment 8, was obtained from Prof. J. Theron (Department of Microbiology and Plant Pathology, University of Pretoria). The pGEM®-T Easy cloning vector and pFastBac™1 bacmid donor plasmid were obtained from Promega and Invitrogen, respectively.

3.2 Bioinformatic analyses

It has been reported previously that the AHSV NS2 protein is phosphorylated at serine residues only (Devaney *et al.*, 1988). To identify putative phospho-acceptor serine residues, the amino acid sequence of the AHSV-9 NS2 protein (Van Staden *et al.*, 1991; GenBank Acc. no. M69090) was subjected to bioinformatic analyses using different computer prediction programes, *i.e.* NetPhosK (Blom *et al.*, 2004), Group-based prediction system (GPS) v.2.0 (Xue *et al.*, 2008) and Scansite 2.0 (Obenauer *et al.*, 2003). These programs are available online and can be accessed through the ExPASy server (http://ca.expasy.org).

3.3 Site-directed mutagenesis of the AHSV-9 NS2 gene

3.3.1 Primers

Primers used to amplify the full-length AHSV-9 NS2 gene, as well as those used to introduce site-specific mutations into the NS2 gene were designed, based on the available nucleotide sequence of the AHSV-9 NS2 gene (Van Staden *et al.*, 1991; GenBank Acc. no. M69090), by making use of the Primer3 software program (Rozen and Skaletsky, 2000). To facilitate cloning of the amplicons, unique restriction endonuclease recognition sites were incorporated at the 5' terminus of selected primers. The primers, indicated in Table 3.1, were obtained from Integrated DNA Technologies.

Table 3.1 Primers used for DNA amplification, mutagenesis and sequencing reactions

Primer	Nucleotide sequence	Remarks
Primers for PCR amplification and mutagenesis of the NS2 gene[a]		
NS2F	5'-**ggatcc**ATGGCAGAGGTCAGA-3'	*Bam*HI site included
NS2R	5'-**gaattc**TCAACCGCTCCCCCC-3'	*Eco*RI site included
NS2A256	5'-GTGTCAA**GC**TGATAGTGATGA-3'	Ser-256 to Ala
NS2A258	5'-GTGTCAAAGTGAT**GC**TGATGATCAATC-3'	Ser-258 to Ala
NS2A262	5'-CAAAGTGATAGTGATGATCAA**G**CTG-3'	Ser-262 to Ala
NS2A256/258	5'-GTGGTGTCAA**GC**TGAT**GC**TGATGATCAATC-3'	Ser-256+258 to Ala
NS2A256/262	5'-GTCAA**GC**TGATAGTGATGATCAA**G**CTG-3'	Ser-256+262 to Ala
NS2D256	5'-GTGTCAA**GA**TGATAGTGATGA-3'	Ser-256 to Asp
NS2D258	5'-GTGTCAAAGTGAT**GA**TGATGATCAATC-3'	Ser-258 to Asp
NS2D262	5'-CAAAGTGATAGTGATGATCAA**GA**TGATGA-3'	Ser-262 to Asp
NS2D256/258	5'-GGTGTCAA**GA**TGAT**GA**TGATGATCAATC-3'	Ser-256+258 to Asp
NS2D256/262	5'-GTCAAGAT**GA**TAGTGATGATCAA**GA**TGATG-3'	Ser-256+262 to Asp
Primers for nucleotide sequencing		
pUC/M13F	5'-TGTAAAACGACGGCCAGT-3'	Sequencing and bacmid analyses
pUC/M13R	5'-CAGGAAACAGCTATGAC-3'	

[a]: In primer sequences, the restriction endonuclease recognition sequences are indicated in bold lower case letters and the site-specific mutations in bold capital letters.

3.3.2 Polymerase chain reaction (PCR)

Each of the NS2 site-specific mutants were constructed by the "megaprimer" method, in which three primers and two PCRs were used (Landt *et al.*, 1990). The first PCR reaction (20 µl) contained 50 ng of pGEX-AHSVNS2 as template DNA, 50 pmol of the 3'-specific antisense primer NS2R, 50 pmol of the sense mutagenic primer, 1 × PCR buffer, 1.5 mM $MgCl_2$, 1 mM of each deoxynucleotide triphosphate (dNTP) and 1 U of SuperTherm™ *Taq* DNA polymerase (Seperations). The tubes were placed in a Perkin-Elmer GeneAmp® 2700 thermal cycler. Following initial denaturation at 90°C for 2 min, the samples were subjected to 30 cycles of denaturation at 90°C for 1 min, annealing at 50°C for 30 s and elongation at 55°C for 30 s. After the last cycle, the reactions were kept at 55°C for 5 min to complete synthesis of all strands. Following electrophoresis on a 1% (w/v) agarose gel, in the presence of an appropriate DNA molecular weight marker, the 300-bp amplicon was purified from the agarose gel with a Zymoclean™ Gel DNA Recovery Kit, as described below. The purified amplicon (1 µg) was used as a "megaprimer", along with 50 pmol of the 5'-specific sense primer NS2F, in the second PCR reaction as described above, except that the cycling conditions were as follow: 1 min at 90°C, 1 min at 50°C and 1 min at 55°C (30 cycles), followed by a final extension step at 55°C for 10 min. Following PCR, aliquots of the reaction mixtures were analyzed by agarose gel electrophoresis in the presence of an appropriate DNA molecular weight marker.

3.4 Agarose gel electrophoresis

DNA was analyzed by agarose gel electrophoresis (Sambrook and Russell, 2001). For this purpose, horizontal 0.8% (w/v) agarose gels were cast and electrophoresed at 100 V in 1 × TAE buffer (40 mM Tris-HCl, 20 mM NaOAc, 1 mM EDTA; pH 8.5). The agarose gels were supplemented with ethidium bromide (0.5 µg/ml) and the DNA visualized by UV fluorescence on a UV transilluminator. Where appropriate, DNA fragments were sized according to their migration in the agarose gel as compared to that of a standard DNA molecular weight marker, namely O'GeneRuler™ 1-kb DNA Ladder (Fermentas Life Sciences). Gel images were captured with a digital gel documentation system (Vilber Lourmat).

3.5 Purification of DNA fragments from agarose gels

DNA fragments were purified from agarose gel slices with the Zymoclean™ Gel DNA Recovery Kit (Zymo Research Corporation) according to the instructions of the manufacturer. The DNA fragment of interest was excised from the agarose gel using a scalpel blade, placed into a 1.5-ml Eppendorf tube and mixed with 3 µl of agarose digestion buffer (ADB) per 1 mg of agarose gel. The agarose was melted by incubation at 55°C, centrifuged through a DNA-binding column at 8000 rpm for 60 s and washed with 200 µl of DNA wash buffer. Following brief centrifugation to remove residual buffer, the DNA was eluted from the column with 6 µl of UHQ water. An aliquot of the sample was analyzed by electrophoresis on a 0.8% (w/v) agarose gel to assess the purity of the DNA, and the DNA concentration was determined with a Nanodrop® ND-1000 spectrophotometer.

3.6 Cloning of DNA fragments into plasmid vectors

3.6.1 Ligation reactions

For cloning of PCR amplicons, the pGEM®-T Easy vector system (Promega) was used according to the manufacturer's instructions. Briefly, the gel-purified amplicon (250 ng) and pGEM®-T Easy vector DNA (50 ng) were ligated at 15°C for 16 h in a reaction mixture that contained 5 µl of a 2 × Rapid ligation buffer, 1 µl of T4 DNA ligase (3 U/µl) and UHQ water to a final volume of 10 µl. For cloning of DNA fragments into pFastBac™1 bacmid donor plasmid, the DNA fragments of interest and restricted vector DNA were ligated at 15°C for 16 h in a 10-µl reaction volume, containing 1 µl of a 10 × DNA ligase buffer and 1 µl of T4 DNA ligase (5 U/µl; Fermentas Life Sciences). The ratio of insert to vector DNA was typically in excess of 5:1.

3.6.2 Preparation of competent *E. coli* JM109 cells

Competent *E. coli* JM109 cells were prepared according to method described by Dagert and Ehrlich (1979). A single colony of a freshly streaked culture of *E. coli* JM109 was inoculated into 50 ml of LB broth and cultured overnight at 37°C with shaking. Following incubation, 1 ml of the overnight culture was inoculated into 100 ml of pre-warmed (37°C) sterile LB broth and incubated at 37°C until an OD_{600} of 0.9 was reached. The cells from 50 ml of the culture were harvested by centrifugation at 8000 rpm for 8 min at 4°C. The cell pellet was suspended in 10 ml of an ice-cold solution comprising 80 mM $CaCl_2$ and 50 mM $MgCl_2$, incubated on

ice for 10 min and then pelleted as above. This step was repeated once more, after which the cell pellet was suspended in 10 ml of ice-cold 100 mM $CaCl_2$. Following the addition of 1.5 ml of 50% (v/v) glycerol, the cells were pipetted in aliquots of 200 µl into 1.5-ml Eppendorf tubes, snap-frozen in liquid nitrogen and stored at -70°C until needed.

3.6.3 Transformation of competent cells

After allowing the competent *E. coli* JM109 cells to thaw on ice, the cells were transformed by the heat shock-method, as described by Sambrook and Russell (2001). The competent *E. coli* JM109 cells (200 µl) and the ligation reaction mixture (2 µl) were mixed, and incubated on ice for 30 min. The tubes were then incubated at 42°C for 90 s in a water bath and immediately placed on ice for 2 min. Subsequently, 800 µl of LB broth was added and the cells were incubated at 37°C for 1 h with shaking. A positive control (2 ng of pGEM $3Zf^+$ plasmid DNA) and negative control (competent cells only) were included to determine the competency of the *E. coli* JM109 cells and to test for contamination, respectively. The transformation mixtures were plated in volumes of 100 µl onto LB agar supplemented with the appropriate antibiotic. For plasmids containing a *lacZ'* marker gene (pGEM®-T Easy), the cells were plated together with 10 µl of 100 mM IPTG and 50 µl of 2% (w/v) X-Gal to identify recombinant clones, based on insertional inactivation of the *lacZ'* marker gene. All agar plates were incubated overnight at 37°C.

3.7 Plasmid DNA extraction

Plasmid DNA was extracted with the alkaline lysis method, as described by Sambrook and Russell (2001). Single bacterial colonies were inoculated into 10 ml of LB broth supplemented with the appropriate antibiotic, and cultured overnight at 37°C with shaking. The cells from 1.5 ml of the overnight culture were collected by centrifugation at 13 400 rpm for 1 min in a 1.5-ml Eppendorf tube. The cell pellet was suspended in 100 µl of ice-cold Solution I (50 mM glucose, 10 mM EDTA, 25 mM Tris; pH 8) and incubated at room temperature for 5 min. The cells were lysed by addition of 200 µl of Solution II (0.2 N NaOH, 1% [w/v] SDS) and after incubation on ice for 5 min, 150 µl of ice-cold Solution III (3 M NaOAc; pH 4.8) was added. After incubation on ice for 10 min, the insoluble aggregate that formed was removed by centrifugation at 13 400 rpm for 5 min. The plasmid DNA was precipitated from the recovered supernatants by addition of 2 volumes of absolute ethanol and incubation on ice for 30 min. The precipitated plasmid DNA was collected by

centrifugation at 13 400 rpm for 15 min, rinsed with 1 ml of 70% ethanol, air-dried and then suspended in 30 µl of 1 × TE buffer (10 mM Tris-HCl, 1 mM EDTA; pH 8.0). To remove contaminating RNA, extracted plasmid DNA was incubated at 37°C for 30 min with 1 µl of RNase A (100 µg/µl).

3.8 Restriction endonuclease digestion

Approximately 500 ng to 1 µg of plasmid DNA was digested with 5 U of enzyme in the appropriate concentration of salt (using the 10× buffer supplied by the manufacturer). The reaction volumes were typically 20 µl and incubation was at 37°C for 1 h. For digestions involving two different restriction enzymes, the buffer that results in the most activity for both enzymes was selected for use in the digestion reactions. All the restriction endonucleases were supplied by Roche Diagnostics. Following digestion, the restriction products were analyzed by agarose gel electrophoresis in the presence of an appropriate DNA molecular weight marker.

3.9 Nucleotide sequencing and sequence analysis

Nucleotide sequencing of cloned insert DNA was performed with the ABI-PRISM® BigDye™ Terminator Cycle Sequencing Ready Reaction kit v.3.1 (Perkin-Elmer Applied Biosystems) according to the manufacturer's instructions. The universal pUC/M13 forward and reverse primers were used as sequencing primers (Table 3.1). Each sequencing reaction consisted of 50-100 ng of purified recombinant plasmid DNA, 2 µl of Big Dye™ 3.1 Reaction mix, 3.6 pmol of sequencing primer, 2 µl of 5 × Big Dye™ Terminator Sequencing buffer and UHQ water to a final volume of 10 µl. Cycle sequencing reactions were performed in a GeneAmp® 2700 thermal cycler (Applied Biosystems) and consisted of 25 cycles of denaturation at 96°C for 10 s, annealing at 50°C for 15 s and extension at 60°C for 4 min. The extension products were precipitated by addition of 2 µl of 3 M NaOAc (pH 4.6) and 60 µl of 96% ethanol. Following incubation at room temperature for 15 min in the dark, the tubes were centrifuged at 13 400 rpm for 15 min and the supernatant carefully aspirated. The pellet was washed twice with 250 µl of 70% ethanol and allowed to air dry. The samples were then submitted to the University of Pretoria's sequencing facility for sequencing on an ABI PRISM® Model 3100 DNA sequencer. The nucleotide sequences obtained were analyzed with BioEdit Sequence Alignment Editor v.5.0.6 (Hall, 1999) software. The nucleotide and deduced amino acid sequences were compared against entries in the GenBank database with the BLAST-N

and BLAST-P programs (Altschul *et al*., 1997), respectively, available on the National Centre for Biotechnology Information web page (http://www.ncbi.nlm.nih.gov/). The nucleotide and deduced amino acid sequences of the wild-type and mutant NS2 genes were aligned using the Pairwise alignment function included in the BioEdit software package.

3.10 Plasmid constructs

All molecular cloning techniques used in the construction of the different recombinant plasmids were performed in accordance to the procedures described in the preceding sections. The construction of the desired recombinant bacmid donor plasmids entailed a strategy whereby the wild-type or mutant AHSV-9 NS2 amplicons, obtained by the megaprimer PCR-based mutageneis strategy, was first cloned into pGEM® T-Easy vector DNA. The full-length wild-type and mutant NS2 genes were subsequently recovered by digestion with *Bam*HI and *Eco*RI and then recloned into the identical sites of the bacmid donor plasmid pFastBac™1. In total, 11 recombinant plasmids were prepared. These harboured the wild-type NS2 gene or 10 different mutant NS2 genes in which specific serine residues were mutated to either alanine or aspartate (Table 3.1). The plasmid constructs were confirmed by agarose gel electrophoresis following restriction endonuclease digestions, and by nucleotide sequencing.

3.11 Engineering and characterization of recombinant bacmids

3.11.1 Transposition

An overview of the Bac-to-Bac® baculovirus expression system is provided in Fig. 3.1. An overnight culture of *E. coli* DH10Bac™ cells, containing the bacmid genome and helper plasmid, was prepared by inoculating a single colony in LB broth supplemented with kanamycin (50 µg/ml) and tetracycline (10 µg/ml). Competent *E. coli* DH10Bac™ cells were prepared and transformed, as described previously (Sections 3.6.2 and 3.6.3), except that 400 ng of the recombinant pFastBac™1 donor plasmid DNA was mixed with 100 µl of the competent *E. coli* DH10Bac™ cells and the transformation mixtures were incubated at 37°C for 4 h to allow transposition to occur. The transformation mixtures were plated in aliquots of 100 µl onto LB agar supplemented with 50 µg/ml of kanamycin, 7 µg/ml of gentamycin and 10 µg/ml of tetracycline in the presence of 10 µl of 100 mM IPTG and 50 µl of 2% (w/v) X-Gal. The agar plates were incubated at 37°C for at least 24 h. Transformants displaying a white colony-phenotype were selected and re-streaked onto the same agar medium, as above, to confirm the recombinant phenotype.

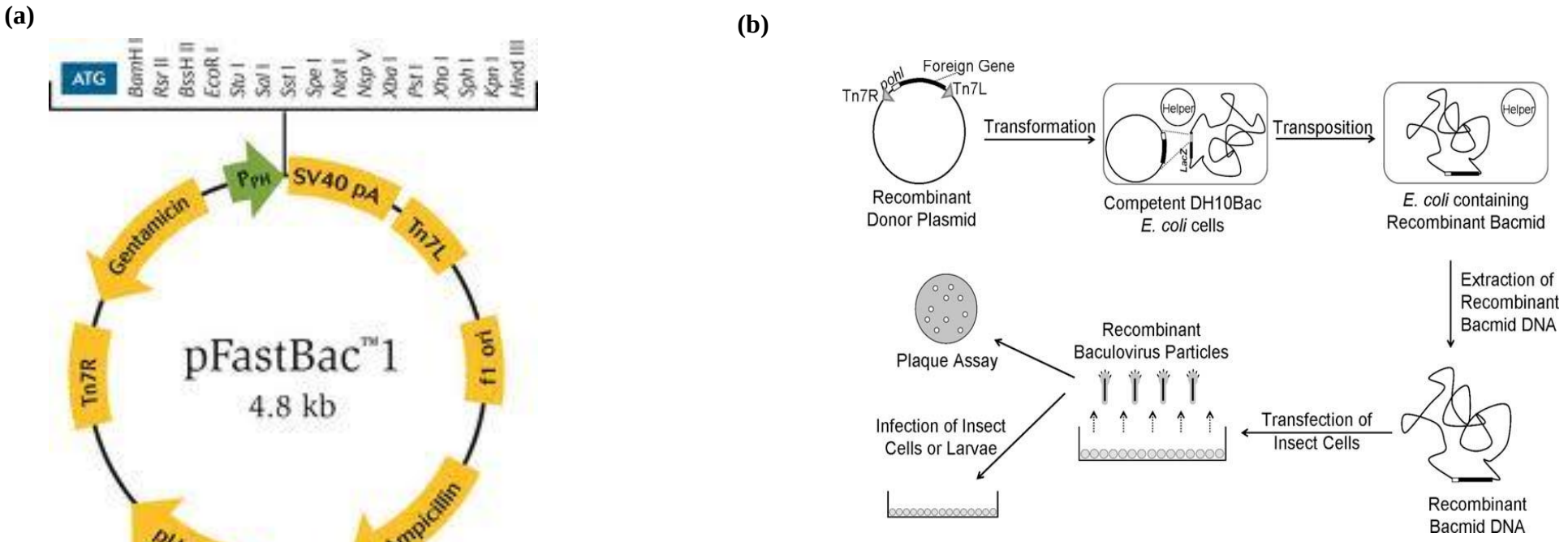

Fig. 3.1 Overview of the Bac-to-Bac® baculovirus expression system (Invitrogen). (a) The gene of interest is cloned into the multiple cloning site of the pFastBac™1 vector, located between the Tn7R and Tn7L transposase recognition sites. (b) The recombinant plasmid is transformed into *E. coli* DH10Bac™ cells, which contain the bacmid backbone and helper plasmid encoding for the transposase. The gene of interest is then transposed from the pFastbac™1 to the bacmid. After purification, the recombinant bacmid DNA is transfected into *S. frugiperda* cells from which recombinant baculovirus is produced. The recombinant baculovirus can then be used for subsequent infection of cells to produce the protein of interest.

3.11.2 Extraction of recombinant bacmid DNA

Selected colonies were inoculated into 2 ml of LB broth containing antibiotics (50 µg/ml kanamycin, 7 µg/ml gentamycin, 10 µg/ml tetracycline) and cultured overnight at 37°C with shaking. The recombinant bacmid DNA was isolated using a modified alkaline lysis protocol for isolation of large plasmids (Fawcett, 1999) that had been adapted for the extraction of bacmid DNA (Invitrogen). The bacterial cells from the overnight culture were harvested by centrifugation at 13 400 rpm for 1 min and the cell pellet suspended in 300 µl of Solution I (15 mM Tris-HCl [pH 8.0], 10 mM EDTA, 100 µg/ml RNase A). A volume of 300 µl of Solution II (0.2 N NaOH, 1% [w/v] SDS) was added, followed by incubation at room temperature for 5 min. Subsequently, 300 µl of 3 M KOAc (pH 5.5) was added and the tubes were incubated on ice for 10 min. Following centrifugation at 13 400 rpm for 10 min, the bacmid DNA was precipitated from the recovered supernatant by addition of 800 µl of isopropanol and incubation on ice for 10 min. The precipitated bacmid DNA was collected by centrifugation at 13 400 rpm for 15 min, washed with 500 µl of 70% ethanol, air-dried and then suspended in 40 µl of 1 × TE buffer. An aliquot of the extracted bacmid DNA was analyzed by electrophoresis in a 0.8% (w/v) agarose gel at 90 V for 30 min in 1 × TAE buffer.

3.11.3 Analysis of recombinant bacmid DNA

Successful transposition of the AHSV-9 NS2 and mutated NS2 genes into the bacmid DNA was verified by PCR analysis of the extracted bacmid DNA. For this purpose, the universal pUC/M13 primers, which anneal at sites flanking the mini-*att*Tn7 site, were used. Each of the PCR reaction mixtures (20 µl) contained 20 ng of bacmid DNA, 1 × PCR buffer, 1.5 mM $MgCl_2$, 25 pmol of each of the primers, 1 mM of each dNTP and 1 U of SuperTherm™ *Taq* DNA polymerase (Seperations). The PCR was performed in a GeneAmp® 2700 thermal cycler (Applied Biosystems). After initial denaturation at 94°C for 2 min, the reactions were subjected to 30 cycles of denaturation at 94°C for 1 min, primer annealing at 50°C for 1 min and elongation at 55°C for 1 min. To test for contamination, reaction mixtures from which the template DNA was omitted were also included. Following PCR, aliquots of the reaction mixtures were analyzed by agarose gel electrophoresis in the presence of an appropriate DNA molecular marker.

3.12 Generation of recombinant baculoviruses

3.12.1 Cell culture

Spodoptera frugiperda clone 9 insect cells were propagated and maintained as monolayers in 75-cm^3 tissue culture flasks or as suspension cultures in Spinner flasks at 28°C in TC-100 medium (Lonza, BioWhittaker®). The medium was supplemented with 10% (v/v) foetal bovine serum (FBS), 10 000 U/ml of penicillin, 10 000 µg/ml of streptomycin and 25 µg/ml of amphotericin B. The cell densities of the suspension cultures were determined with a haemocytometer. Cell viability was determined by staining the cells with Trypan Blue (0.4% [w/v] in 1 × PBS), as described by Drews *et al.* (1995). Suspension cultures were seeded at an initial density of 0.3 × 10^6 cells/ml and subcultured when they reached 2 × 10^6 cells/ml.

3.12.2 Transfection of *S. frugiperda* cells with recombinant bacmid DNA

Recombinant bacmid DNA was transfected into *S. frugiperda* cells with CellFECTIN® Reagent (Invitrogen) according to the manufacturer's instructions. The cells were seeded in six-well tissue culture plates (9 × 10^5 cells/well) and allowed to attach at 28°C for 1 h. For each transfection, *ca*. 50 ng of recombinant DNA and 6 µl of CellFECTIN® Reagent (Invitrogen) were separately diluted in 100 µl of incomplete TC-100 medium (lacking FBS and antibiotics). The two solutions were then mixed and, following incubation at room temperature for 45 min, 800 µl of incomplete TC-100 medium was added. The *S. frugiperda* cells were prepared for transfection by aspirating the medium from the attached cells and the cells were rinsed twice with 1 ml of incomplete TC-100 medium. The cells were then overlaid with the lipid-DNA complexes and the tissue culture plate incubated at 28°C for 5 h in a humidified environment. Following incubation, the transfection mixtures were removed and replaced with 2 ml of complete TC-100 medium (containing FBS and antibiotics). The tissue culture plate was subsequently incubated at 28°C for 72 h, after which the supernatants were removed and stored at 4°C until use. Mock-transfected cells and cells transfected with wild-type bacmid DNA were included as controls whereby infection of the cells could be monitored.

3.12.3 Preparation and titration of virus stocks

To prepare virus stocks, 500 µl of the supernatants obtained following transfection of *S. frugiperda* cells was used to infect cell monolayers in six-well tissue culture plates (1.2 × 10^6

cells/well) using a procedure similar to that described above. The cells were harvested at 72 h post-infection by centrifugation at 8000 rpm for 2 min and the cell-free supernatants, containing recombinant baculovirus, were stored at 4°C. To determine the virus titre, plaque assays were performed as described by Browne and Faulkner (1977) with modifications. *S. frugiperda* cells were seeded in six-well tissue culture plates (1×10^6 cells/well) and after adsorption at room temperature for 1 h, the medium was replaced with 900 µl of serial 10-fold dilutions of virus in 2 mM Tris. After incubation at room temperature for 1 h to allow virus particles to infect the cells, the virus dilutions were removed and the cells gently overlaid with 2 ml of a sterile solution of agarose (1:1 ratio of 0.7% [w/v] agarose and 2 × concentrated Earle's salt containing 10% [v/v] FBS and antibiotics). The tissue culture plates were incubated at 28°C for 96 h in a humidified environment. Following incubation, the monolayers were flooded with Neutral Red (0.1% [w/v] in sterile UHQ water) and incubated for a further 24 to 48 h until plaques became visible.

3.13 Analysis of recombinant baculovirus-expressed proteins

3.13.1 Preparation of cell lysates

Monolayers of *S. frugiperda* cells (1.2×10^6 cells/well) were infected at a multiplicity of infection (MOI) of 5 pfu/cell with the respective recombinant baculoviruses and incubated at 28°C for 72 h. As controls, mock-infected and wild-type baculovirus-infected *S. frugiperda* cells were included in the analysis. Following incubation, detached and adherent cells were harvested using a syringe, collected by centrifugation at 8000 rpm for 2 min and the cell pellet was suspended in 50 µl of 1 × Phosphate Buffered Saline (PBS: 137 mM NaCl, 2.7 mM KCl, 4.3 mM $Na_2HPO_4.2H_2O$, 1.4 mM KH_2PO_4; pH 7.4). Aliquots of the whole-cell lysate (5 µl) from each sample were mixed with an equal volume of 2 × Protein Solvent Buffer (PSB: 125 mM Tris-HCl [pH 6.8], 4% [w/v] SDS, 20% [v/v] glycerol, 10% [v/v] 2-mercaptoethanol, 0.001% [w/v] bromophenol blue). The samples were heated for 10 min in boiling water prior to SDS-PAGE analysis.

3.13.2 SDS-polyacrylamide gel electrophoresis (SDS-PAGE)

Protein samples were analyzed by SDS-PAGE, as described by Laemmli (1970). A 5% (w/v) acrylamide stacking gel and 12% (w/v) acrylamide separating gel was used, of which the acrylamide:bisacrylamide ratio was 30:0.8. The low-porosity separating gel (0.375 M Tris-

HCl [pH 8.8], 0.1% [w/v] SDS) and high-porosity stacking gel (0.125 M Tris-HCl [pH 6.8], 0.1% [w/v] SDS) were each polymerized by the addition of 100 µl of 10% (w/v) ammonium persulphate and 10 µl of TEMED. The TGS electrophoresis buffer consisted of 25 mM Tris-HCl (pH 8.3), 192 mM glycine and 0.1% (w/v) SDS. Electrophoresis was performed in a Hoefer Mighty Small™ SE260 electrophoresis unit for 3 h at 100 V. After electrophoresis, the gels were stained for 20 min with 0.125% (w/v) Coomassie Blue G-250 (prepared in 50% [v/v] methanol, 10% [v/v] acetic acid) and then counterstained by soaking the gels in destaining solution (5% [v/v] methanol, 7% [v/v] acetic acid). The sizes of the resolved proteins were determined by comparison to reference molecular mass proteins (PageRuler™ Prestained Protein Ruler; Fermentas Life Sciences).

3.14 Immunoblot analysis

For immunoblot analysis (Ausubel *et al.*, 2002), proteins from an unstained SDS-polyacrylamide gel were electroblotted onto a Hybond™-C^+ nitrocellulose membrane (Amersham Pharmacia Biotech). Two sheets of filter paper and the nitrocellulose membrane, cut to the same size as the gel, were equilibrated for 30 min in transfer buffer (25 mM Tris, 192 mM glycine). The proteins were electroblotted onto the membrane at 28 V for 90 min with a Mighty Small™ Transphor blotting apparatus (Hoefer). Following transfer, the membrane was rinsed in 1 × PBS for 5 min and non-specific binding sites were blocked by immersing the membrane at 4°C overnight in blocking solution (1% [w/v] non-fat milk powder in 1 × PBS). The membrane was transferred to 1 × PBS containing AHSV-9 NS2 antiserum (diluted 1:500; Uitenweerde *et al.*, 1995). Following incubation at room temperature for 2 h with gentle agitation, the unbound primary antibodies were removed by washing the membrane three times for 5 min each with wash buffer (0.005% [v/v] Tween-20 in 1 × PBS). The secondary antibody, Protein-A conjugated to horseradish peroxidase (Calbiochem) diluted 1:1000 in 1 × PBS, was added to the membrane and then incubated at room temperature for 1 h with gentle agitation. Following incubation, the membrane was washed three times for 5 min each with wash buffer and once with 1 × PBS for 5 min. To detect immune-reactive proteins, freshly prepared enzyme substrate solution (60 mg 4-chloro-1-naphtol in 20 ml of ice-cold methanol and 60 µl of H_2O_2 in 100 ml of 1 × PBS, mixed just before use) was added to the membrane, followed by incubation at room temperature in the dark until the protein bands became visible. The membrane was then rinsed with dH_2O and allowed to air dry.

3.15 Phosphoprotein staining assay

Monolayers of *S. frugiperda* cells were mock-infected and infected with recombinant baculoviruses expressing the wild-type or mutant NS2 proteins, as described above (Section 3.12.1). At 72 h post-infection, cell lysates were prepared and subjected to SDS-PAGE. To identify phosphorylated proteins, the SDS-polyacrylamide gel was stained using the GelCode™ Phosphoprotein Staining Kit according to the manufacturer's instructions (Pierce). Following electrophoresis, the gel was placed in a tray and washed with dH_2O for 10 min with mild agitation. The gel was then incubated in Reagent 1 (sulfosalicylic acid solution) for 15 min, followed by incubation in Reagent 2 (sulfosalicylic acid and $CaCl_2$ solution) for 30 min. The gel was subsequently rinsed with dH_2O to remove any traces of $CaCl_2$ and then incubated in Reagent 3 (0.5 N NaOH) for 20 min in an oven pre-heated to 60°C. Following incubation, the gel was incubated twice in Reagent 4 (ammonium molybdate solution) for 10 min. After discarding Reagent 4 for the second time, the gel was incubated in Reagent 5 (ammonium molybdate and HNO_3 solution) for 20 min, followed by incubation in Reagent 6 (Methyl green) for 20 min. The gel was finally destained with Reagent 1 for 15 min and then incubated overnight in Reagent 7 (7% [v/v] acetic acid) to completely destain the gel. After the gel became green in colour, the solution was discarded and the gel rinsed with dH_2O. Samples of Phosvitin and Soybean Trypsin Inhibitor (supplied in the kit) were loaded onto the gel as positive and negative controls, respectively.

3.16 Transmission electron microscopy (TEM)

Monolayers of *S. frugiperda* cells seeded in six-well tissue culture plates at 1.2×10^6 cells/well were either mock-infected or infected with the recombinant baculoviruses at a MOI of 1 pfu/cell and incubated at 28°C for 72 h. The cells were subsequently harvested, collected by centrifugation at 8000 rpm for 2 min and rinsed twice with 1 ml of 1 × PBS. The cells were fixed at room temperature for 30 min in a fixative solution (2.5% [v/v] formaldehyde, 2.2% [v/v] gluteraldehyde, 50% [v/v] 1 × PBS), after which the cells were pelleted by centrifugation at 8000 rpm for 5 min and the supernatant discarded. The cells were washed three times for 15 min each with 250 µl of 0.075 M NaP buffer (pH 7.4) and then post-fixed in 0.5% osmium tetraoxide (OsO_4) at room temperature for 1 h. After fixing, the cells were collected by centrifugation and washed with NaP buffer, as described above, prior to dehydration for 15 min each in 50%, 70%, 90% and 100% acetone. The treatment with 100% acetone was repeated two more times to ensure complete dehydration of the samples. The

cells were then infiltrated for 1 h each in different percentages of Quetol (33% and 66% prepared in acetone), followed by incubation overnight at room temperature in 100% Quetol. The cells were collected by centrifugation, added to fresh Quetol and polymerized at 60°C for 48 h. Ultrathin sections were obtained on an ultramicrotome and collected on copper grids. The samples were stained with 4% uranyl acetate for 3 min, rinsed in dH_2O and counterstained in 3% Reynolds' lead citrate for 3 min. Following rinsing in dH_2O, the samples were viewed with a JEOL JEM 2100 F transmission electron microscope.

3.17 Indirect immunofluorescence analyses

3.17.1 Cells and virus

Embryonic *Culicoides variipennis* (KC) cells were propagated as monolayers in 75-cm^3 tissue culture flasks at 28°C in modified Schneider's *Drosophila* medium (Highveld Biological) supplemented with 10% (v/v) FBS and antibiotics (120 mg/ml of penicillin, 120 mg/ml of streptomycin, 35.5 µg/ml of Fungizone). African horse sickness virus serotype 9 (AHSV-9) was provided by Mr. Flip Wege (Department of Genetics, University of Pretoria). AHSV-9 was propagated in confluent KC cell monolayers using a KC cell-adapted stock virus as inoculum. In all of the experiments described below, KC cells were seeded at 20% confluence on glass cover slips in six-well tissue culture plates and infected with AHSV-9 at a MOI of 0.1 pfu/cell when the cell monolayers were 50% confluent. Prior to infection, the cell monolayers were washed with FBS-free growth medium and then incubated with AHSV-9 at the indicated MOI. Virus adsorption was carried out for 1 h at 28°C, followed by incubation in complete Schneider's *Drosophila* medium (containing FBS and antibiotics).

3.17.2 Detection of NS2 in virus-infected KC cells treated with an inhibitor of casein kinase 2 (CK2)

To treat KC cells with myricetin (Sigma-Aldrich), which inhibits CK2 activity (Modrof *et al.*, 2005), the cell monolayers were rinsed once with complete Schneider's *Drosophila* medium. The cell monolayers were then exposed to 10 µM myricetin in complete growth medium for 2 h prior to AHSV-9 infection or at 96 h following AHSV-9 infection. The myricetin inhibitor was aspirated from the cells prior to virus infection. Following virus adsorption, the inoculum was aspirated, the cells rinsed twice with complete growth medium and then 2 ml of complete Schneider's *Drosophila* medium containing 10 µM myricetin was added. Mock-

infected KC cells and untreated KC cells infected with AHSV-9 were included in the assay as controls. The tissue culture plates were incubated at 28°C for a further 72 h.

Following incubation, the cell monolayers were processed for intracellular staining of NS2 according to the procedures described by Bhattacharya *et al.* (2007). The cell monolayers were rinsed twice for 5 min each with 1 ml of 1 × PBS and then permeabilized by ice-cold methanol:acetone (1:1 [v/v]) at room temperature for 3 min. Subsequently, the cell monolayers were rinsed twice with 1 × PBS and incubated for 30 min in 1 ml of blocking buffer (5% [w/v] fat-free milk powder in 1 × PBS). The cell monolayers were then incubated overnight at 4°C with 200 µl of a rabbit monospecific anti-NS2 serum (Uitenweerde *et al.*, 1995), which was diluted 1:500 in 1% (w/v) blocking buffer. After removal of the unbound antibodies by three washes for 5 min each with 1 ml of wash buffer (0.5% [v/v] Tween-20 in 1 × PBS), the cell monolayers were incubated for 1 h at room temperature with 200 µl of a labelled secondary antibody. This comprised of FITC-conjugated goat anti-rabbit IgG (Sigma-Aldrich), which was diluted 1:200 in 1% (w/v) blocking buffer. Following incubation, the cell monolayers were washed twice with wash buffer and twice with 1 × PBS. The coverslips were mounted on glass slides and the cells were examined with a Zeiss LSM S10 META confocal laser scanning microscope, using bypass filters for fluorescein (505-550 nm). Images were captured with a Zeiss Axiocam Series 5 digital camera, and processed with Zeiss LSM v.5 Image Examiner and Adobe Photoshop v.11.0 software packages.

3.17.3 Detection of newly synthesized RNA *in vivo*

At 96 h post-infection of KC cells grown on glass coverslips in six-well tissue culture plates, the medium was aspirated from the cells and replaced with complete Schneider's *Drosophila* medium containing 10 µg/ml of Actinomycin D (Sigma-Aldrich) to arrest cellular transcription. Following incubation at 28ºC for 1 h, the cells were transfected with BrUTP to enable the detection of newly synthesized RNA (Silvestri *et al.*, 2004). The cell monolayers were prepared for transfection by rinsing the cells twice with incomplete Schneider's *Drosophila* medium. For each transfection, 5 µl of 100 mM BrUTP (Sigma-Aldrich) and 4 µl of CellFECTIN® Reagent (Invitrogen) were each diluted in 100 µl of incomplete growth medium. The two solutions were mixed, incubated at room temperature for 45 min and following the addition of 800 µl of incomplete growth medium was then used to overlay the KC cells. The tissue culture plates were incubated at 28ºC for 5 h, after which the transfection

mixtures were replaced with 2 ml of complete Schneider's *Drosophila* medium containing 10 mg/ml Actinomycin D and incubation was continued for a further 72 h. Mock-infected KC cells and untreated KC cells infected with AHSV-9 were included in the assay as controls. For intracellular staining of newly synthesized RNA, the cell monolayers were processed as described above, except that immunofluorescence analysis was performed with mouse bromodeoxyuridine (BrdU) monoclonal antisera, followed by TRITC-conjugated goat anti-mouse IgG as the secondary antibody. The antibodies, obtained from Sigma-Aldrich, were each diluted 1:1000 in 1% (w/v) blocking buffer. The cells were examined with a Zeiss LSM S10 META confocal laser scanning microscope, using bypass filters for rhodamine (560-615 nm).

Chapter Four
Results

4.1 Identification of putative phosphorylated serine residues within the AHSV-9 NS2 protein

The NS2 protein of epizootic hemorrhagic disease virus (EHDV), African horse sickness virus (AHSV) and bluetongue virus (BTV) is the only virus-specified protein that is phosphorylated (Huismans *et al.*, 1987; Theron *et al.*, 1994). Phosphoamino acid analysis revealed that serine residues located in the C terminus of the BTV and AHSV NS2 proteins were the only phosphate acceptor sites and that neither phosphothreonine nor phosphotyrosine was identified (Devaney *et al.*, 1988). It has subsequently been reported that BTV NS2 is phosphorylated at serine (Ser) residues 249 and 259 by the ubiquitous cellular protein, casein kinase 2 (CK2) (Modrof *et al.*, 2005). Amino acid sequence alignments indicated that Ser-249 is conserved in at least 80% of BTV NS2 sequences and is conserved in all EHDV and AHSV NS2 sequences (corresponding to position 256). In contrast, the second phosphorylation site, Ser-259, is conserved within BTV NS2 sequences but not in other orbivirus NS2 sequences (Van Staden *et al.*, 1991; Butan and Tucker, 2010). There are 28 serine residues within the AHSV-9 NS2 protein, and these are distributed throughout the protein without showing any identifiable clustering (Van Staden *et al.*, 1991). Thus, to identify serine residues that may represent potential targets for phosphorylation by CK2, the amino acid sequence of AHSV-9 NS2 was analyzed by using three different computer prediction programs. A kinase landscape of the NS2 protein is presented in Fig. 4.1.

A total of six serine residues were identified in the AHSV-9 NS2 protein that represent potential phosphorylation sites of CK2 (Table 4.1). However, a serine residue at position 84 was disregarded since it was localized to the N terminus of the NS2 protein, and a serine residue located at position 221 was identified with only one of the prediction programs (GPS v.2.1). Although the serine at position 223 was identified as a potential phosphorylation site with both GPS v.2.1 and NetPhosK, its score was the lowest of the putative sites identified with the GPS v.2.1 prediction program. Therefore, based on these analyses, three serine residues of AHSV-9 NS2 were selected as potential phosphorylation sites, *i.e.* residues 256, 258 and 262. In all of the analyses, the serine residue located at position 262 within the NS2 protein sequence demonstrated the highest likelihood of being phosphorylated, while the serine residues located at positions 256 and 258 were also likely candidates but with comparatively lower scores (Table 4.1).

Table 4.1 Putative CK2-phosphorylated serine residues within the AHSV-9 NS2 protein, as identified with different computer prediction programs

Scansite 2.0[a]					
Position	**Amino acid**	**Kinase**	**Percentile**	**Sequence**	**Score**
256	S	CK2	2.522%	TESMWCQ**S**DSDDQSD	0.5672
258	S	CK2	1.535%	SMWCQSD**S**DDQSDED	0.5362
262	S	CK2	0.146%	QSDSDDQ**S**DEDHEVG	0.3912
Group-based Prediction System v.2.1[b]					
Position	**Amino acid**	**Kinase**		**Sequence**	**Score**
221	S	CK2		LSVQSNE**S**RSDDVAR	5.83
223	S	CK2		VQSNESR**S**DDVARRH	5.786
256	S	CK2		TESMWCQ**S**DSDDQSD	9.292
258	S	CK2		SMWCQSD**S**DDQSDED	9.17
262	S	CK2		QSDSDDQ**S**DEDHEVG	12.164
NetPhosK[c]					
Position	**Amino acid**	**Kinase**		**Sequence**	**Score**
84	S	CK2		LSLMITE**S**GIEVTQNR	0.53167
223	S	CK2		VQSNESR**S**DDVARRH	0.555
256	S	CK2		TESMWCQ**S**DSDDQSD	0.52367
258	S	CK2		SMWCQSD**S**DDQSDED	0.65730
262	S	CK2		QSDSDDQ**S**DEDHEVG	0.707

[a]: Scansite 2.0 predicts potential phosphorylation sites based on sequence comparisons between the protein of interest and the optimal motif sequence. A score of 0.0000 is considered a perfect match to the consensus sequence. The percentage score ranks the analyzed sequence compared to the consensus motif of vertebrate protein sequences of the Swiss-Prot database. The lower the score, the better the ranking, with less than 0.2% being considered "high stringency".

[b]: Group-based Prediction System (GPS) v.2.1 predicts locations for serine phosphorylation by CK2 according to a hierarchical model, using data from the Phospho.ELM database of experimentally verified eukaryotic phosphorylation sites to which the sequence of interest is compared. The evolutionary likelihood of a specific amino acid mutating into a different residue is calculated, allowing for a score to be awarded based on the hypothesis that closely related sequences would likely have similar three-dimensional structures and biochemical properties. The scores are calculated as an average of the substitution scores of the sequence of interest compared with the known target sequences. The higher the final score, the more similar the sequence is to other known sequences (Xue *et al.*, 2008).

[c]: NetphosK predicts the likelihood of phosphorylation of serine residues by various cellular kinases using an artificial neural network approach. A score is assigned to the candidate site that reflects the likelihood of it being phosphorylated, with 0.000 being most unlikely and 1.000 being most likely (Blom *et al.*, 2004).

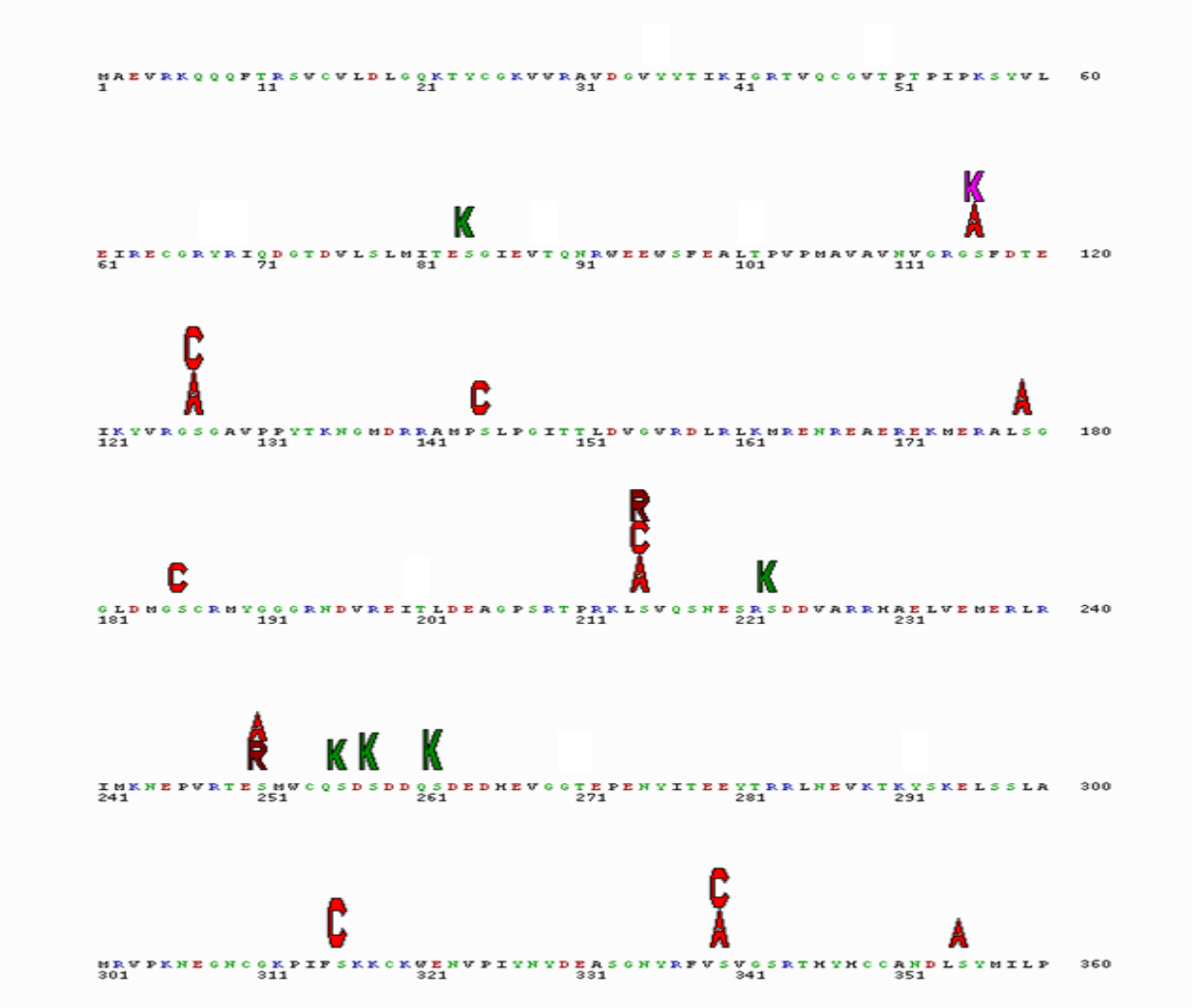

Fig. 4.1 Kinase landscape depiction of the AHSV-9 NS2 protein. Various serine kinases are depicted by the assorted coloured letters. The length of the letter reflects the likelihood of a specific serine residue being phosphorylated by a particular kinase. The represented kinases are depicted as **A,** protein kinase A; **C**, protein kinase C; **K**, casein kinase I; **K**, casein kinase II (CK2); and **R**, ribosomal s6 kinase.

4.2 Construction of site-directed mutants of the AHSV-9 NS2 gene

To examine whether the identified serine residues are the phosphorylation sites of the AHSV-9 NS2 protein, NS2 mutants were generated by substituting the respective serine residues with alanine residues singularly (residues 256, 258 and 262) and in combination (residues 256 and 258, and 256 and 262). To characterize further the phosphorylation of NS2, additional NS2 mutants were generated in which the above-indicated serine residues were substituted with aspartate residues. An aspartate residue is considered to mimic a phosphoserine residue due to its negative charge (Sarcevic *et al.*, 2002; Reddy *et al.*, 2004; Lewellyn and Loeb, 2011).

Site-directed mutagenesis was performed in a two-step PCR process. In the first round of amplification, the internal mutagenic primer and one external flanking primer were used to make an intermediate primer product. The intermediate DNA fragment was purified from excess primers to avoid the generation of wild-type fragments in the second PCR. The purified primer product intermediate was then used in a second PCR reaction with the other external flanking primer to yield a full-length internally mutagenized product.

Using pGEX-AHSVNS2 as template, and the PCR conditions described in Section 3.3, an amplicon of *ca.* 1.2 kb was synthesized in each case, the sizes of which are in agreement with that of the full-length AHSV-9 NS2 gene. In contrast, no amplification products were observed in the negative control reaction in which template DNA was omitted (Fig. 4.2a). The amplicons were subsequently purified from the agarose gel and ligated into pGEM® T-Easy vector DNA. Following transformation of competent *E. coli* JM109 cells, recombinant transformants with a Lac^- phenotype were selected from X-Gal indicator plates and cultured in LB broth supplemented with ampicillin. The extracted plasmid DNA was analyzed by agarose gel electrophoresis and by restriction endonuclease digestion.

Plasmid DNA migrating slower than the parental pGEM®-T Easy vector DNA on agarose gels were selected and analyzed for the presence of a cloned insert DNA by using restriction endonucleases of which the recognition sites had been incorporated during the design of the external flanking primers. The putative recombinant plasmid DNA was therefore digested with both *Bam*HI and *Eco*RI. Following agarose gel electrophoresis, restriction fragments of *ca.* 3.0 and 1.2 kb, respectively, were observed, which are in agreement with the expected size of the pGEM®-T Easy vector DNA (3.0 kb) and insert DNA (1.166 kb) (Fig. 4.2b).

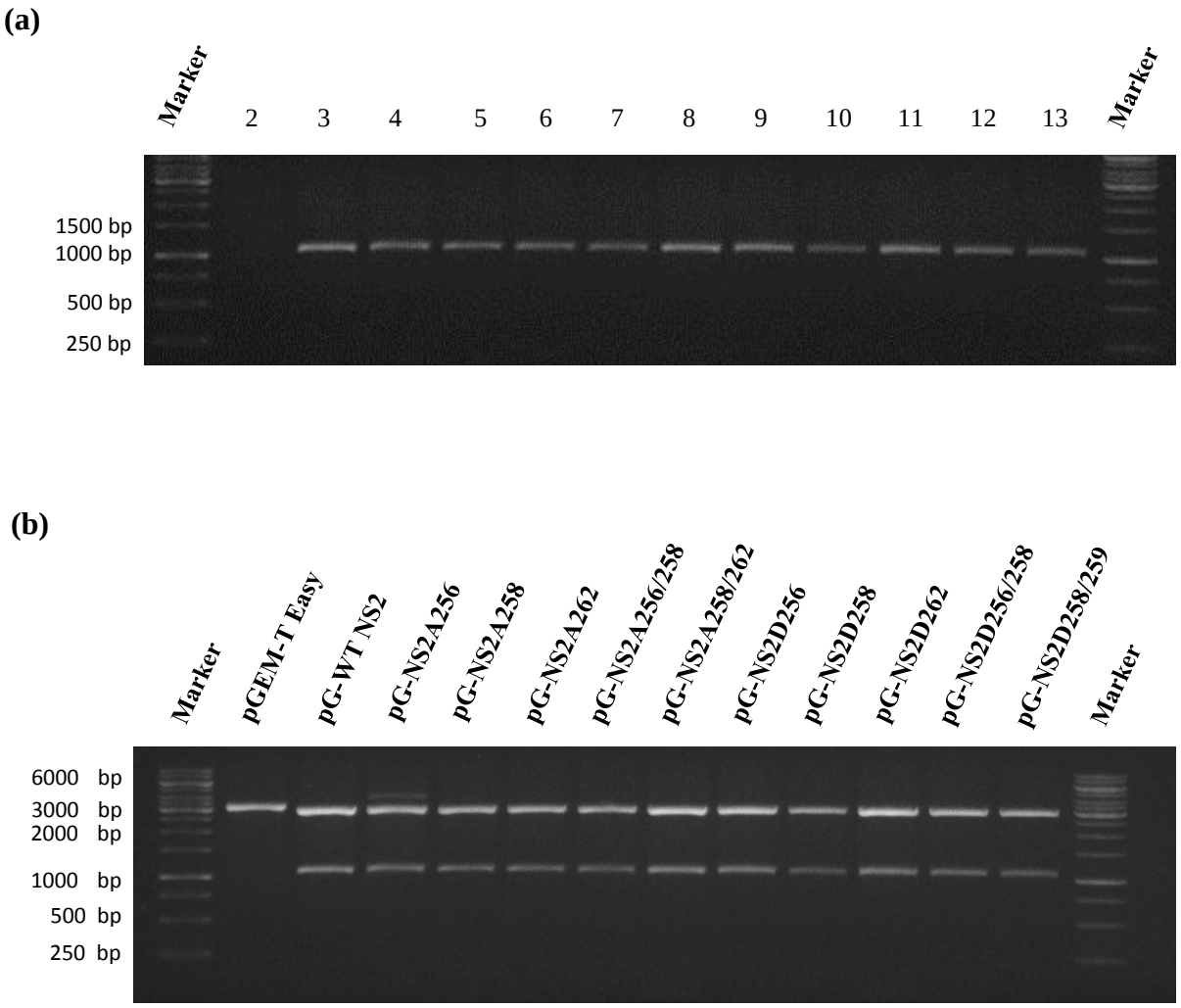

Fig. 4.2 Characterization of mutant AHSV-9 NS2 genes generated by PCR-based site-directed mutagenesis. (a) Amplicons of the different mutant NS2 genes (lanes 4 through 13), corresponding in size to the full-length wild-type NS2 gene (lane 3), were obtained after PCR amplification by making use of pGEX-AHSVNS2 plasmid DNA as template, together with a 5'-end gene specific primer and appropriate megaprimer. A negative control PCR reaction lacking template DNA (lane 2) was included in the analysis. (b) Agarose gel electrophoretic analysis of recombinant plasmid DNA constructs obtained by cloning the respective gel-purified amplicons into the pGEM®-T Easy vector. The derived recombinant plasmid DNAs, as indicated in the figure, were digested with both *Bam*HI and *Eco*RI, and non-recombinant pGEM®-T Easy vector DNA was included as an additional size marker. The sizes of the DNA molecular weight marker, O'GeneRuler™ 1-kb DNA Ladder (Fermentas Life Sciences), are indicated to the left of the figures.

Recombinant clones were selected and the integrity of the cloned insert DNA, as well as the presence of the newly introduced site-specific mutations was verified by nucleotide sequencing. Pairwise alignments of the nucleotide sequences of the wild-type and 10 mutant NS2 genes revealed no nucleotide differences other than the newly introduced site-specific mutations (Fig. 4.3). The complete nucleotide sequence and deduced amino acid sequence of the respective NS2 genes are provided in the Appendix to this dissertation.

4.3 Construction of recombinant bacmid donor plasmids harbouring wild-type and mutated NS2 genes

To facilitate studies regarding the identification of AHSV-9 NS2 phosphorylated residues and the importance of NS2 phosphorylation in virus inclusion body (VIB) formation, the Bac-to-Bac® baculovirus expression system was exploited for synthesis of the different NS2 proteins. To enable cloning of the wild-type and mutant NS2 genes into the bacmid donor plasmid pFastBac™1 (Fig. 4.4a), both the recombinant pGEM® T-Easy and pFastBac™1 plasmid DNA were digested with *Bam*HI and *Eco*RI. The excised NS2 genes and digested donor plasmid DNA were purified from an agarose gel and ligated overnight. Following transformation of competent *E. coli* JM109 cells, a number of ampicillin-resistant transformants were selected randomly and the extracted plasmid DNA was subsequently characterized by restriction enzyme digestion.

Digestion of the recombinant bacmid donor plasmids with both *Bam*HI and *Eco*RI resulted in the excision of a 1.2-kb DNA fragment, indicating that the full-length wild-type and mutant NS2 genes had been cloned successfully (Fig. 4.4b). To verify the correct transcriptional orientation of the cloned NS2 gene, the recombinant bacmid donor plasmids were furthermore characterized by restriction enzyme mapping with *Hind*III, which recognizes a site within the multiple cloning site of the vector and cuts asymmetrically within the NS2 gene, *i.e.* 253 bp from the 5' end. Digestion of the recombinant plasmids with *Hind*III excised an expected DNA fragment of 913 bp (Fig. 4.4c). These recombinant donor plasmids were subsequently used to generate recombinant bacmids, as described in the following section.

(a)

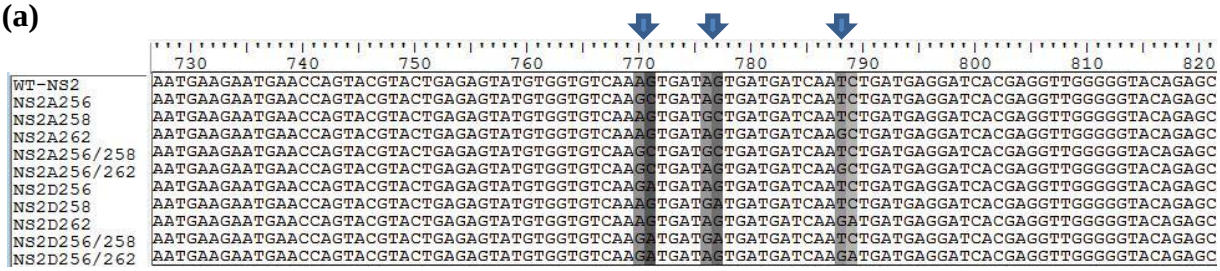

(b)

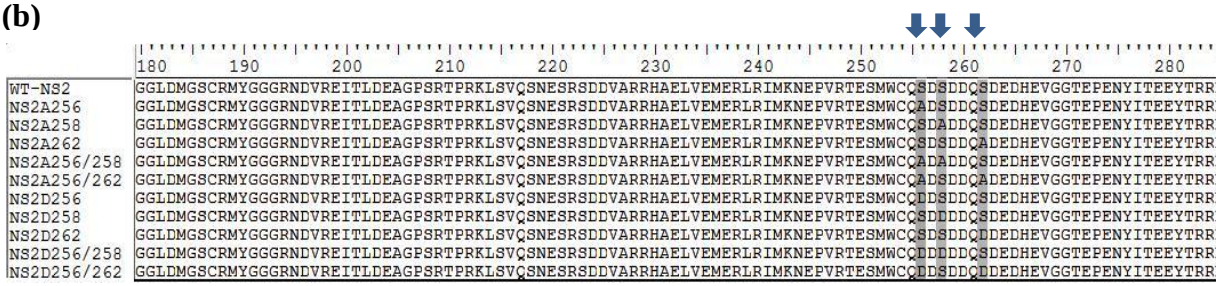

Fig. 4.3 Partial nucleotide (a) and amino acid (b) sequence alignments of the wild-type and mutant NS2. The specified site-specific mutations are indicated by arrows, indicating that the targeted serine codons (AGT or TCT) of the wild-type NS2 gene were mutated successfully to either alanine (GCT or AGA) or aspartic acid (GAT). Full-length alignments of the respective NS2 genes, indicating no other differences between their nucleotide and deduced amino acid sequences, are included in the Appendix.

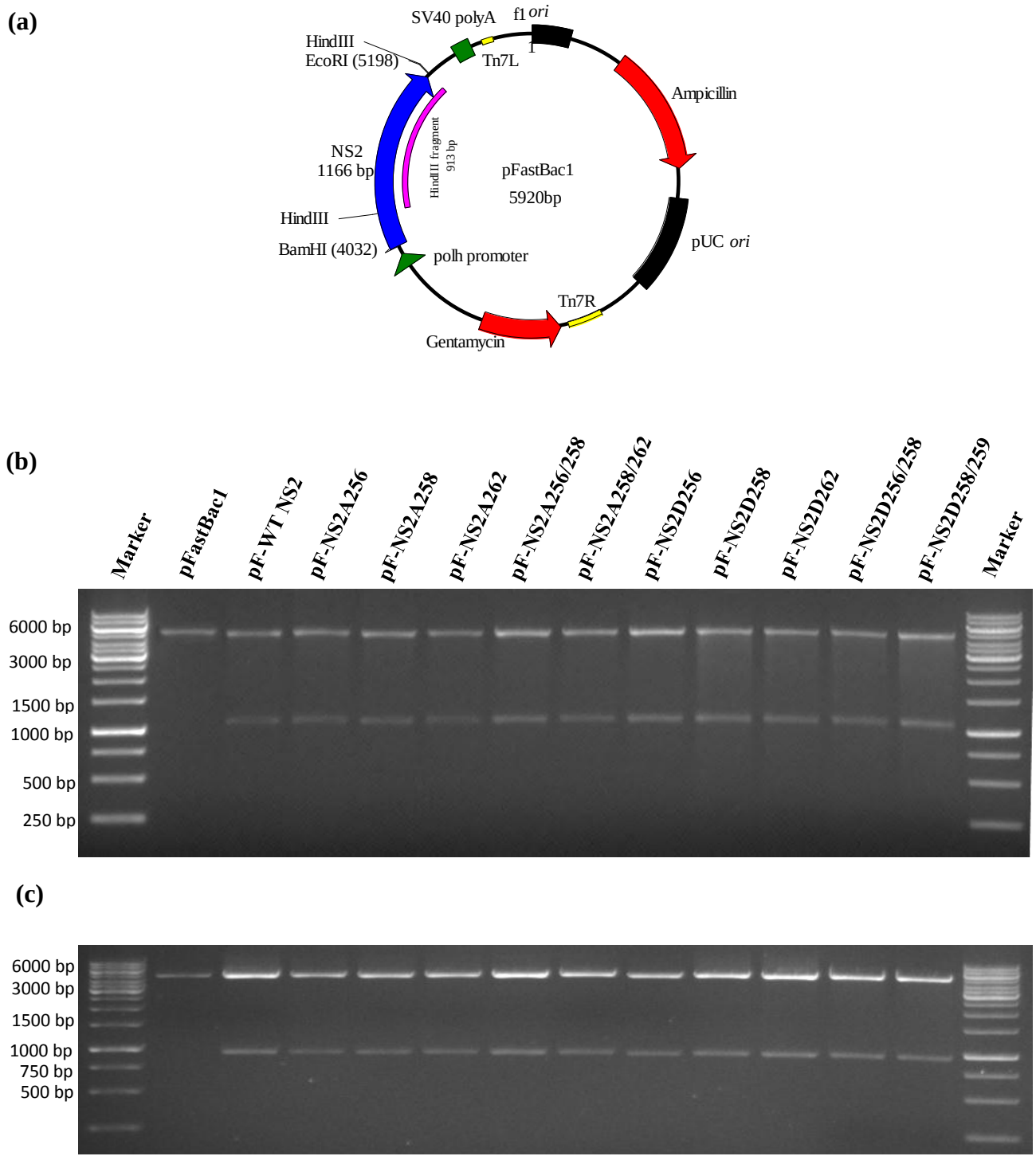

Fig. 4.4 Agarose gel electrophoretic analysis of recombinant pFastBac™1 plasmids harbouring wild-type and mutant NS2 gene-specific inserts. (a) Plasmid map of the recombinant pFastBac™1 donor plasmid, indicating relevant restriction endonuclease cleavage sites. The recombinant bacmid donor plasmids, as indicated in the figure, were digested either with both *Bam*HI and *Eco*RI to excise the NS2-specific insert DNA (b) or with *Hind*III to verify the transcriptional orientation of the cloned insert DNA (c). Non-recombinant pFastBac™1 vector DNA was included as an additional size marker. The sizes of the DNA molecular weight marker, O'GeneRuler™ 1-kb DNA Ladder (Fermentas Life Sciences), are indicated to the left of the figures.

4.4 Engineering and characterization of recombinant bacmids

The bacmid DNA propagates as a large plasmid (135 kb) in *E. coli* DH10Bac™ cells and confers resistance to kanamycin, as well as complements a *lacZ'* deletion present on the *E. coli* chromosome to form colonies that are blue in the presence of X-Gal. During site-specific transposition of the recombinant donor plasmid, the mini-Tn7 cassette is inserted from the donor plasmid into the mini-*att*Tn7 attachment site on the bacmid DNA, thereby disrupting expression of the LacZα peptide. Thus, colonies containing the recombinant bacmid display a white colony-phenotype and can be readily distinguished from the blue colonies that harbour the unaltered bacmid DNA. The transposase required for the transposition is encoded by the pMON7124 helper plasmid present in the *E. coli* DH10Bac™ cells, which also confers resistance to tetracycline (Luckow *et al*., 1993; Ciccarone *et al*., 1997).

Recombinant bacmid DNA was engineered by transforming competent *E. coli* DH10Bac™ cells with the respective recombinant pFastBac™1 donor plasmids, and selecting for recombinant bacmids by plating the transformed cells onto a selective agar medium. The high-molecular-weight recombinant bacmid DNA was subsequently extracted from selected transformants and used as template DNA in PCR assays to confirm successful transposition of the respective NS2 genes into the bacmid DNA. For this purpose, the universal pUC/M13 forward and reverse primers were used. These primers anneal to sequences flanking the mini-*att*Tn7 attachment site within the *lacZ'* gene of the bacmid DNA (Fig. 4.5a).

By making use of recombinant bacmid DNA transposed with the respective recombinant donor plasmids as template DNA for PCR, bands of *ca*. 3.4 kb were obtained (Fig. 4.5b). The size of the observed amplicons corresponded with the size of the NS2 gene (1.166 kb), together with the size of the transposed mini-Tn7 cassette (2.253 kb). No amplicons were observed in the control reaction from which template DNA was omitted. Recombinant bacmids were selected and used in all subsequent experiments.

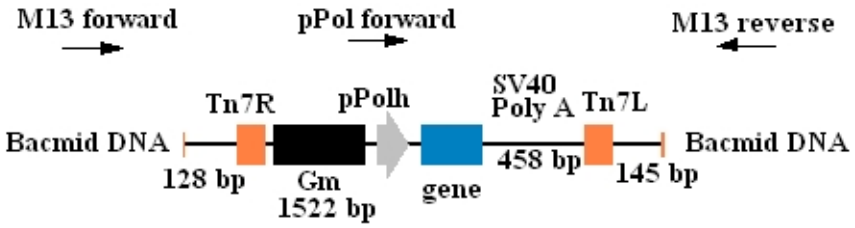

Fig. 4.5a Schematic representation of transposed bacmid DNA. The annealing positions of the pUC/M13 forward and reverse primers are indicated, as well as the size of the mini-*att*Tn7 cassette DNA and the bacmid DNA flanking the cassette. The position of the transposed AHSV-9 NS2 genes within the bacmid DNA is indicated in blue.

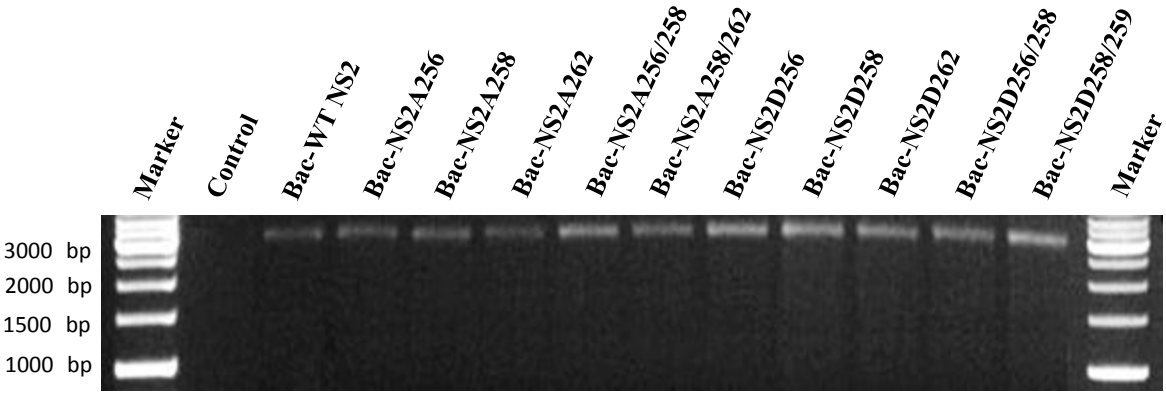

Fig. 4.5b Agarose gel electrophoretic analysis of amplicons derived from recombinant bacmid DNA following PCR analysis. Wild-type bacmid DNA and recombinant bacmid DNA, as indicated in the figure, were used as template in PCR analysis together with the universal pUC/M13 forward and reverse primers. A control reaction from which DNA template was omitted was included in the assay. The sizes of the DNA molecular weight marker, O'GeneRuler™ 1-kb DNA Ladder (Fermentas Life Sciences), are indicated to the left of the figure.

4.5 Analyses of proteins synthesized in recombinant baculovirus-infected *S. frugiperda* cells

The recombinant bacmid DNA was isolated from *E. coli* DH10Bac™ cultures and subsequently transfected into *S. frugiperda* cells. Progeny baculoviruses, resulting from each transfection, were propagated in monolayer cultures and the titer of the recombinant virus stocks was determined by plaque assays. To determine whether the wild-type and mutant NS2 proteins were synthesized in recombinant baculovirus-infected cells, monolayers of *S. frugiperda* cells were mock-infected or infected with the respective baculovirus recombinants at a MOI of 5 pfu/cell. At 72 h post-infection, the cells were harvested and the cell lysates were analyzed by SDS-PAGE and immunoblot analyses.

Analysis of the Coomassie-stained gel (Fig. 4.6a) indicated the presence of an over-expressed protein in the lysates prepared from cells infected with the baculovirus recombinants, which co-migrated with a wild-type baculovirus-expressed protein. The estimated molecular mass of the proteins was in agreement with the predicted molecular mass of NS2 (41 kDa). To confirm the identity of the over-expressed proteins, duplicate unstained SDS-polyacrylamide gels were subjected to immunoblot analysis. Depending on the nature of the introduced mutation, the primary anti-AHSV-9 NS2 antibody reacted either with a single protein or with two proteins (Fig. 4.6b). In the case of mutant NS2 proteins in which Ser-256, Ser-258 or Ser-262, as well as both Ser-256 and Ser-262 were substituted with alanine, the primary antibody reacted with two proteins of approximate sizes of 38 and 41 kDa, respectively. This result is in agreement with that obtained for the wild-type NS2 protein. However, for the mutant NS2 protein in which both Ser-256 and Ser-258 were substituted with alanine, as well as all other instances where the targeted serine residues were substituted with aspartate, the primary antibody reacted with a single protein with a molecular mass of 41 kDa. Notably, no cross-reactions with similarly sized proteins were observed in lysates prepared from mock-infected or wild-type baculovirus-infected cells (Fig. 4.6b). From these results it could thus be concluded that the wild-type NS2 protein and different mutant NS2 proteins were expressed successfully in *S. frugiperda* cells by means of the constructed baculovirus recombinants.

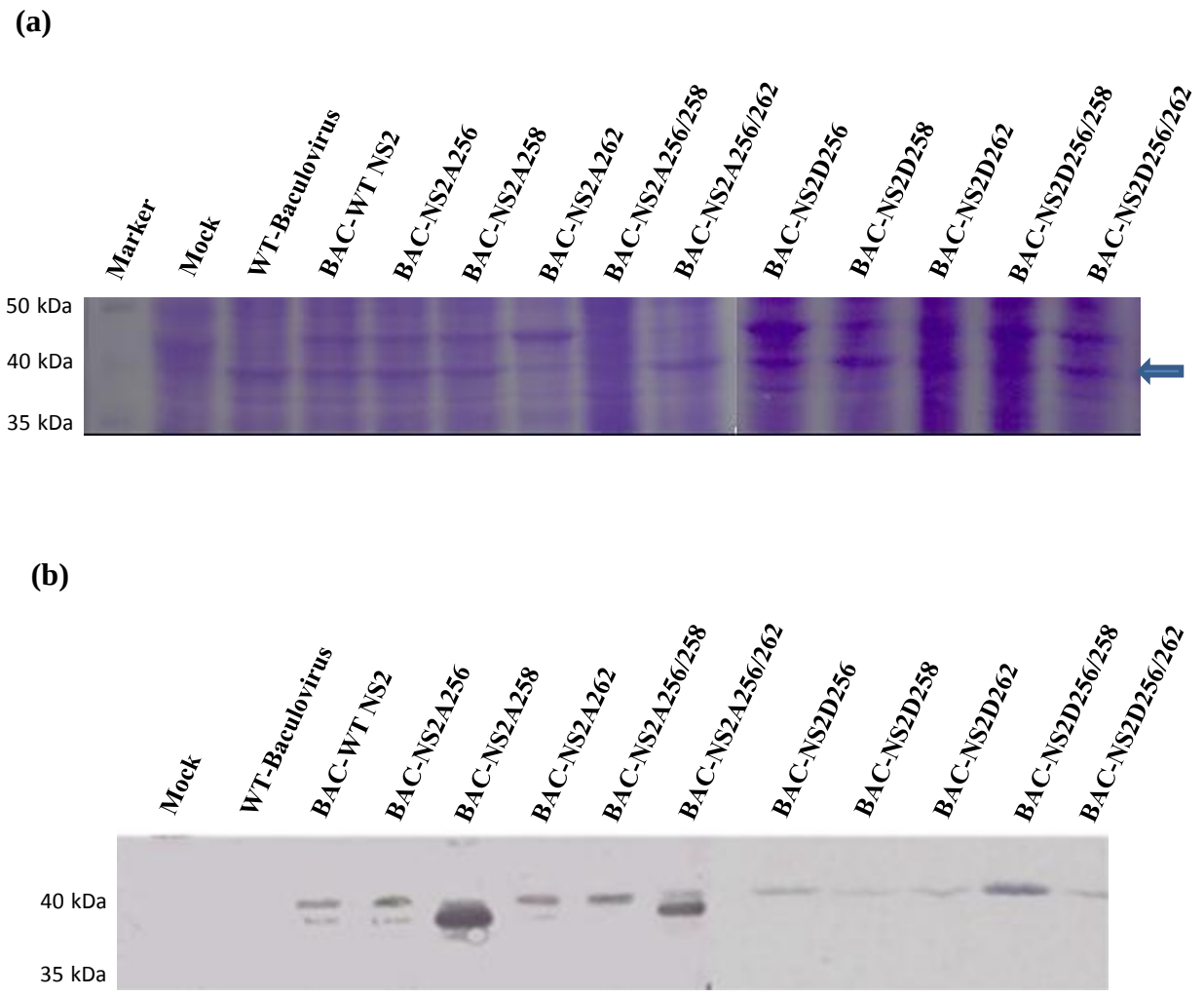

Fig. 4.6 SDS-PAGE and immunoblot analyses of whole-cell lysates prepared from *S. frugiperda* cells infected with recombinant baculoviruses. *S. frugiperda* cells were mock-infected and infected with the wild-type baculovirus or recombinant baculoviruses, and analyzed for protein expression at 72 h post-infection. Whole-cell lysate proteins were resolved by SDS-PAGE (a) and proteins from a duplicate, unstained gel were electroblotted onto a nitrocellulose membrane and subjected to immunoblot analysis with an anti-AHSV-9 NS2 antibody (b). The sizes of the protein molecular mass markers, PageRuler™ Prestained Protein Ruler (Fermentas Life Sciences), are indicated to the left of the figures. The arrow indicates the position of NS2 in cell lysates infected with the recombinant baculoviruses.

4.6 Phosphoprotein staining assays

To determine the phosphorylation status of the wild-type and mutant NS2 proteins expressed in *S. frugiperda* cells, cell lysates were prepared at 72 h post-infection from mock-infected and recombinant baculovirus-infected cells. The cell lysates were resolved by SDS-PAGE and the SDS-polyacrylamide gel was subjected to a phosphoprotein staining assay using a commercial kit. A duplicate gel was stained with Coomassie Blue G-250 in order to confirm that the wild-type and mutant NS2 proteins were indeed expressed (results not shown).

The staining kit that was used in this investigation is based on the colorimetric detection of phosphoproteins directly on gels (Cutting and Roth, 1973). Staining is achieved by first hydrolyzing the phosphoprotein phosphoester linkage with NaOH in the presence of Ca^{2+} ions. The gel containing the newly formed insoluble calcium phosphate is then treated with ammonium molybdate in dilute nitric acid and the resultant insoluble nitrophospho-molybdate complex is finally stained with the basic dye, Methyl Green. Thus, phosphoproteins are visualized as protein bands that are green in appearance.

Analysis of the stained gel indicated that in contrast to the non-phosphorylated protein Soybean Trypsin Inhibitor (STI), a blue-green band was visible corresponding to the band for Phosvitin, a highly phosphorylated protein used as a positive control in these assays. The wild-type NS2 protein and three of the mutant NS2 proteins (NS2A256, NS2A262 and NS2A256/262) also stained as green bands, indicating that these proteins were indeed phosphorylated. However, it appeared that the respective proteins were stained to different extents (Fig. 4.7a). Analysis of the remainder of the mutant NS2 proteins using a second, identical staining kit failed to indicate the presence of phosphorylated wild-type or mutant NS2 proteins, despite the assay being repeated several times (Fig. 4.7b).

Since the results therefore precluded definitive conclusions to be drawn regarding the importance of the respective serine residues as potential NS2 phosphorylation sites, all of the mutant NS2 proteins were included in subsequent analyses.

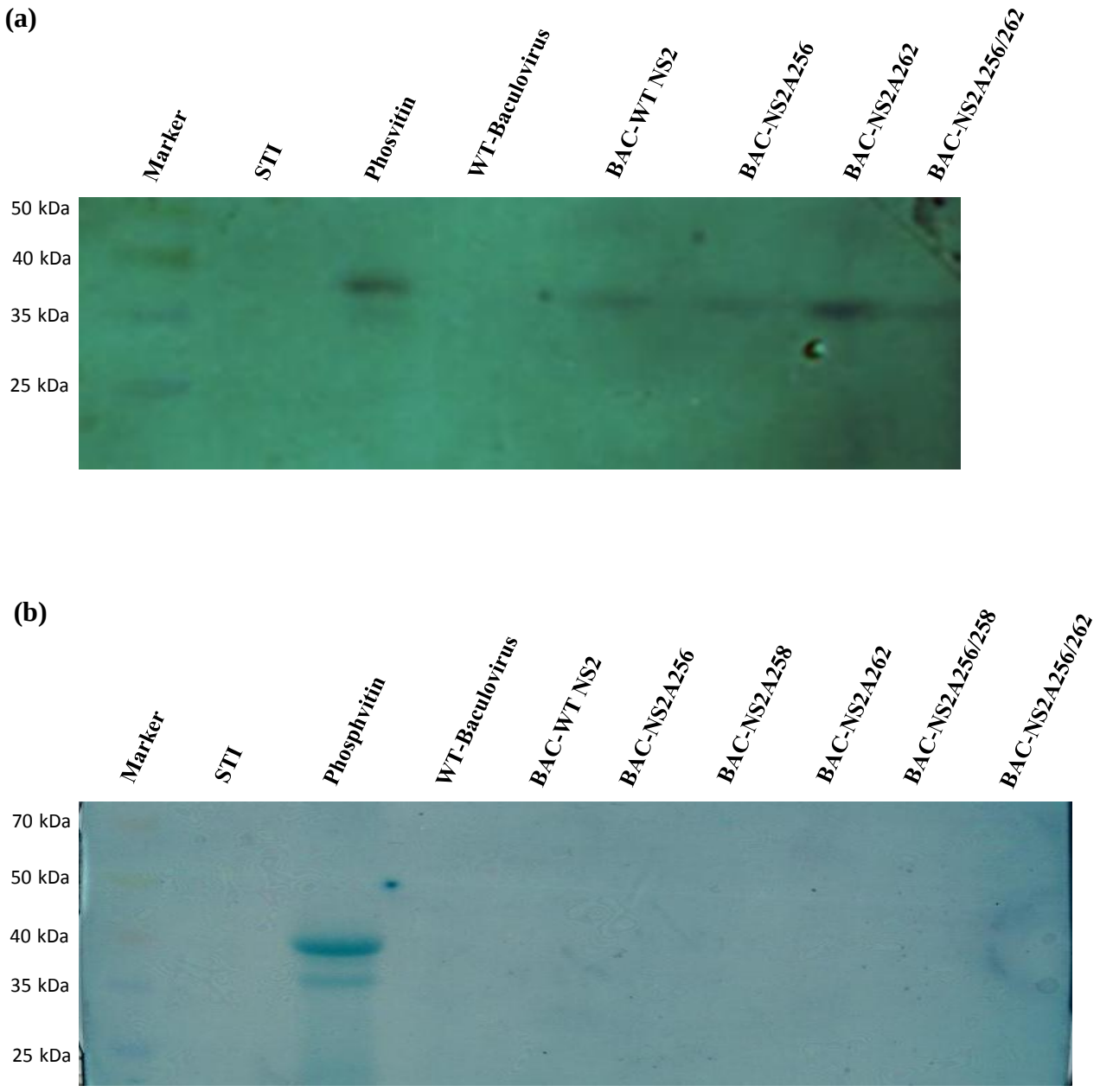

Fig. 4.7 Phosphorylation state analysis of the wild-type and mutant NS2 proteins expressed in *S. frugiperda* cells. Lysates prepared from cells infected with the wild-type or recombinant baculoviruses, as indicated in the figures, were subjected to SDS-PAGE. The SDS-polyacrylamide gels were subsequently stained with the GelCode® Phosphoprotein Staining Kit (Pierce) to identify phosphorylated proteins. Phosvitin, a hyperphosphorylated protein, and Soybean Trypsin Inhibitor (STI), a non-phosphorylated protein, were included as positive and negative controls, respectively. Representative results are shown. Protein bands that are stained green in colour represent phosphorylated proteins. (a) Initial experiments indicated apparent differences in the phosphorylation state of selected NS2 proteins. (b) However, the phosphorylation sate of the remainder of the mutant NS2 proteins could not be determined using a second, identical staining kit.

4.7 Electron microscopy of recombinant baculovirus-infected *S. frugiperda* cells

The NS2 protein is the main component of virus inclusion bodies (VIBs) that appear in the cytoplasm of BTV-infected mammalian cells (Hyatt and Eaton, 1987; Kar *et al.*, 2007), and it has been reported that baculovirus-expressed NS2 of BTV and AHSV can form similar inclusion bodies (IBs) (Brookes *et al.*, 1993; Uitenweerde *et al.*, 1995). To determine whether the targeted substitution of serine residues with either alanine or aspartate influenced the ability of NS2 to form IBs, monolayers of *S. frugiperda* cells were infected with the respective recombinant baculoviruses and processed at 72 h post-infection for microscopy.

The results from the transmission electron microscope analysis (Figs. 4.8 and 4.9) indicated that granular electron-dense structures were present in the cytoplasm of *S. frugiperda* cells infected with the baculovirus recombinant expressing wild-type AHSV NS2 protein. No similar structures were observed in control mock-infected or in wild-type baculovirus-infected cells. Interestingly, differences were observed regarding the size and morphology of the IBs formed by the mutant NS2 proteins. These differences appeared to be dependent on the type and nature of the mutation introduced into the NS2 protein.

S. frugiperda cells infected with baculovirus recombinants expressing NS2 proteins in which the serine residue at position 256 or 258 were mutated to alanine formed IBs that appeared elongated (NS2A256) or smaller (NS2A258) compared to the IBs formed by the wild-type NS2 protein. Cells expressing mutant NS2 harbouring an alanine substitution of Ser-262 formed IBs that resembled those formed in cells expressing wild-type NS2 (Fig. 4.8). Notably, no discernible IBs could be observed in cells infected with the baculovirus recombinant expressing a mutant NS2 protein in which Ser-256 and Ser-258 were both substituted with alanine (NS2A256/258). It therefore appears that IB formation was abrogated, despite productive infection of the cell as evidenced by the enlarged nucleolus of the cell. In contrast, substitution of both Ser-256 and Ser-262 with alanine did not appear to have the same effect on IB formation. In this case, the mutant NS2 protein (NS2A256/262) was capable of forming IBs, albeit that they were less defined, having no distinct size or shape as compared to the IBs formed by the wild-type NS2 protein (Fig. 4.8). In the case of *S. frugiperda* cells infected with baculovirus recombinants expressing mutant NS2 proteins in which the targeted serine residues were substituted with aspartate, all of the mutant NS2 proteins were capable of forming IBs. However, the IBs were generally smaller compared to the IBs formed in cells expressing wild-type NS2 protein (Fig. 4.9).

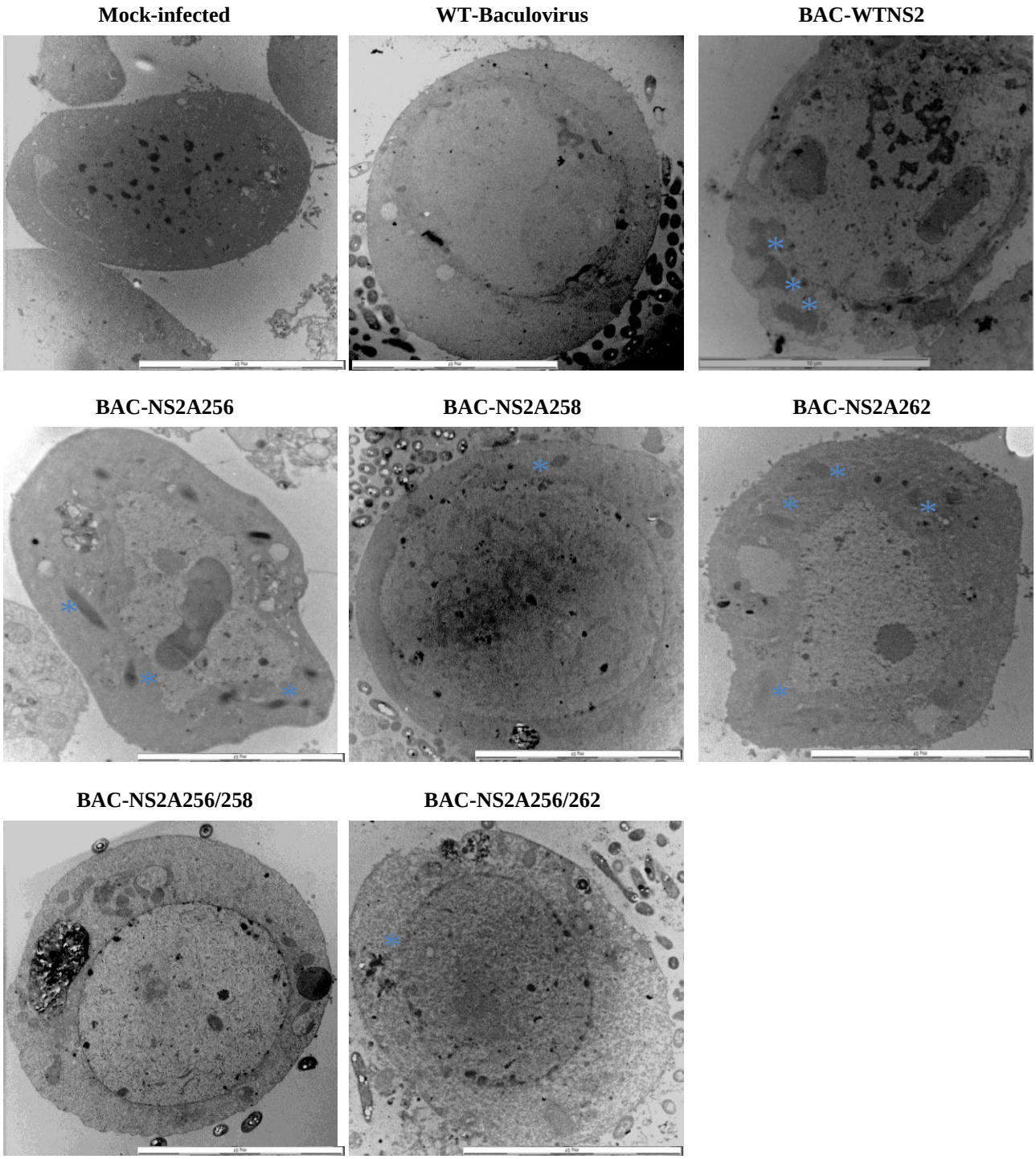

Fig. 4.8 Transmission electron micrographs of ultrathin sections of *S. frugiperda* cells infected with different baculovirus recombinants. *S. frugiperda* cells were infected with recombinant baculoviruses expressing the wild-type NS2 protein or mutant NS2 proteins in which selected serine residues were substituted with alanine residues, as indicated. Mock-infected cells and cells infected with the wild-type baculovirus were included as controls. The cells were processed for TEM at 72 h post-infection and examined with a JEOL transmission electron microscope. The inclusion bodies are indicated by asterisks and the scale bars represent 10 µm.

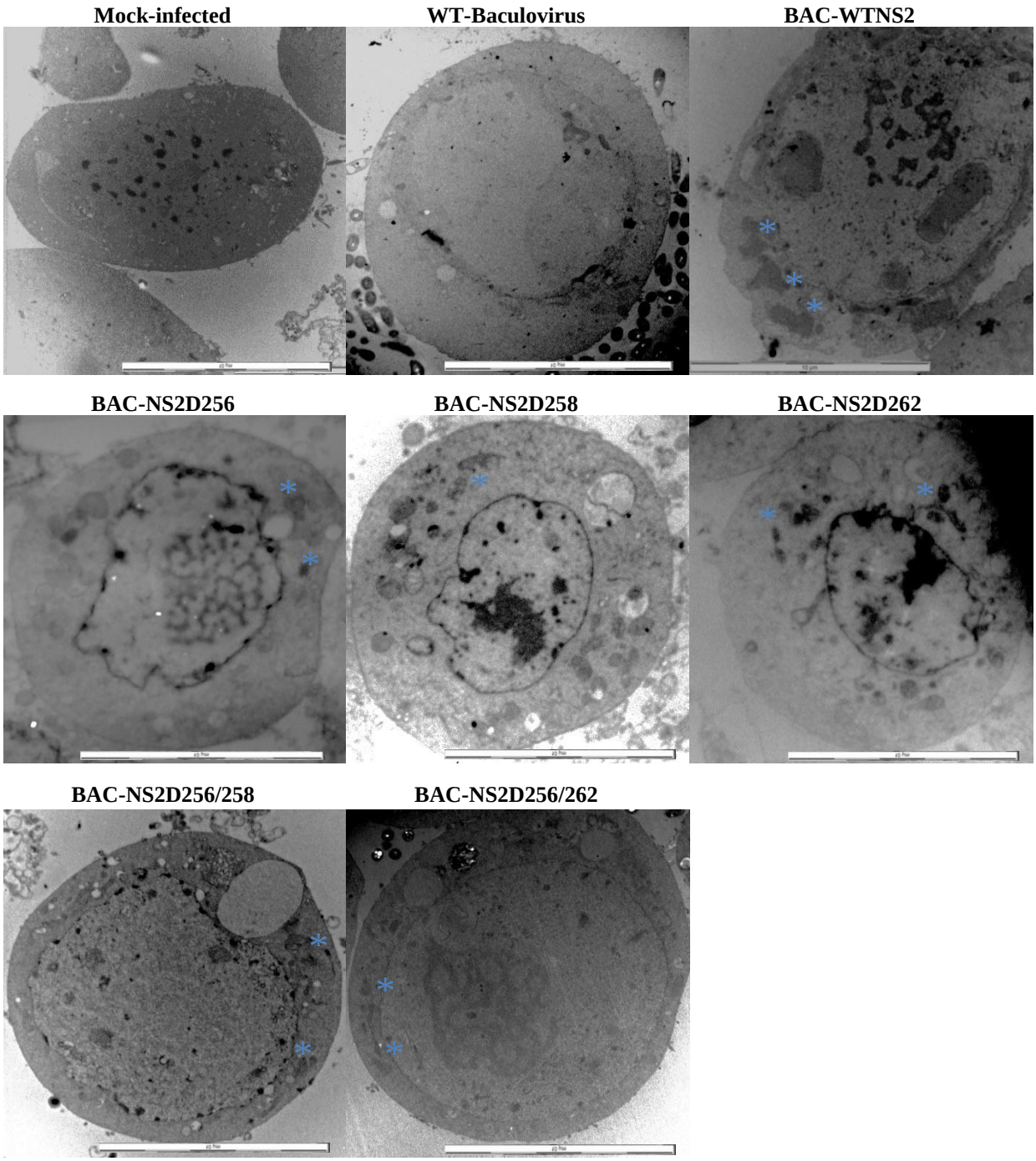

Fig. 4.9 Transmission electron micrographs of ultrathin sections of *S. frugiperda* cells infected with different baculovirus recombinants. *S. frugiperda* cells were infected with recombinant baculoviruses expressing mutant NS2 proteins in which selected serine residues were substituted with aspartate residues, as indicated. Micrographs of mock-infected cells and cells infected with the wild-type baculovirus or recombinant baculovirus expressing the wild-type NS2 protein, as presented in Fig. 4.8, are shown for comparative purposes. The inclusion bodies are indicated by asterisks and scale bars represent 10 µm.

4.8 Influence of NS2 phosphorylation on the formation of VIBs in *Culicoides variipennis* (KC) cells

The results obtained by transmission electron microscopy indicated that substitution of both Ser-256 and Ser-258 with alanine resulted in the absence of intracellular aggregates in the cytoplasm of *S. frugiperda* cells infected with the baculovirus recombinant. Since it has been reported that an unphosphorylated version of the BTV NS2 protein does not form VIBs (Modrof *et al.*, 2005), the results suggest that the above serine residues may be potential AHSV NS2 phosphorylation sites. Furthermore, these two serine residues have been identified as potential CK2 phosphorylation sites using different computer prediction software (Table 4.1). Thus, to determine whether CK2 could be responsible for the phosphorylation of NS2 of AHSV and to address the question of whether phosphorylation of NS2 is required for the formation of VIBs, an *in vivo* experiment was performed using KC cells infected with AHSV-9. To investigate, KC cells were treated with myricetin either prior to or during infection of the cells with AHSV-9, and the NS2 protein was detected by immunofluorescence analysis using confocal microscopy. Myricetin is a specific inhibitor of CK2 (Ong and Khoo, 1997; Lolli *et al.*, 2012) and has been used successfully to inhibit phosphorylation of the BTV NS2 protein (Modrof *et al.*, 2005).

The results indicated the presence of globular, dense inclusions in untreated virus-infected cells (Fig. 4.10b). Expression of NS2 in virus-infected KC cells treated at 96 h post-infection with myricetin resulted in the formation of NS2 aggregates similar to those observed in untreated AHSV-infected KC cells (Fig. 4.10d). These VIBs were likely formed by NS2 protein that had been expressed and phosphorylated before the addition of the CK2 inhibitor. In contrast, expression of NS2 in KC cells treated with myricetin prior to virus infection did not show this distinct aggregation. Instead, the NS2 aggregates appeared to be less dense and more diffuse (Fig. 4.10c). The globular structures were not produced in mock-infected cells treated with the anti-NS2 serum, confirming the specificity of NS2 labelling in infected KC cells (Fig. 4.10a). The results suggest that CK2 likely phosphorylates NS2 and that NS2 phosphorylation may be required for formation of VIBs.

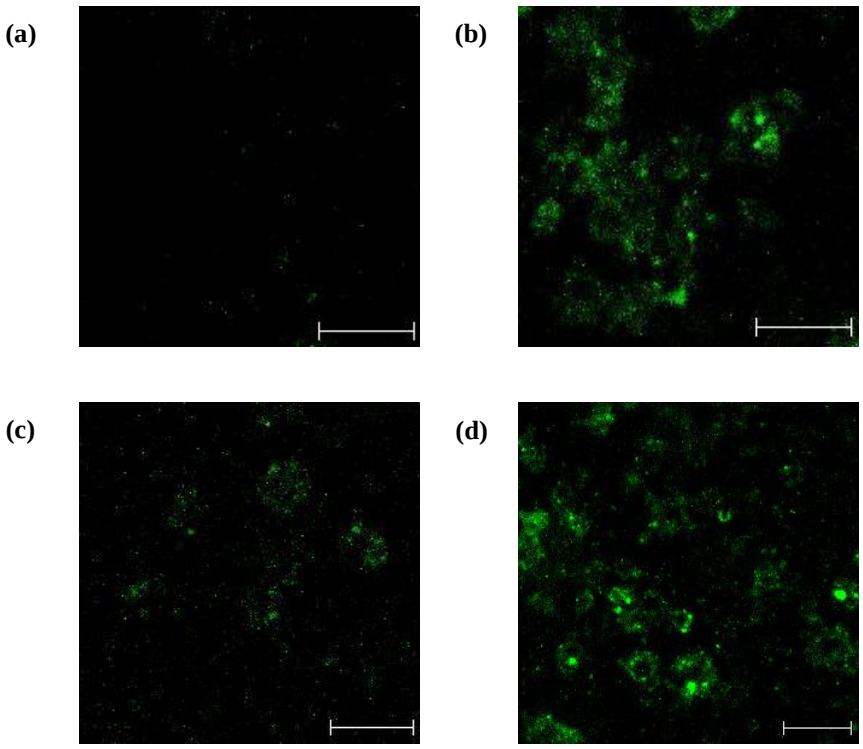

Fig. 4.10 Formation of VIBs by NS2 in *C. variipennis* (KC) insect cells in the absence and presence of myricetin. The KC cells were treated with the CK2 inhibitor prior to infection of the cells with AHSV-9 (c) or at 96 h post-infection (d). As controls, mock-infected cells (a) and untreated KC cells infected with AHSV-9 (b) were also subjected to immunofluorescence analysis. The NS2 protein was visualized using a FITC-conjugated secondary antibody (green) with a Zeiss LSM S10 META confocal microscope fitted with bypass filters for fluorescein (505-550 nm). Scale bars represent 10 µm.

4.9 Localization of RNA transcription *in vivo*

The NS2 protein has been reported to have an affinity for ssRNA transcripts (Huismans *et al.*, 1987; Thomas *et al.*, 1990), but displays preferential binding to viral transcripts (Theron and Nel, 1997; Lymperopoulos *et al.*, 2006). NS2 is therefore likely to be involved in the recruitment of viral transcripts during virus morphogenesis. Consequently, it was of interest to determine whether the viral transcripts could be identified within the VIBs of virus-infected cells. To investigate, AHSV-infected KC cells were treated at 96 h post-infection with actinomycin D to block host replication and transcription and then transfected with bromouridine triphosphate (BrUTP). After fixation and permeabilization of the cells, the location of newly made RNA was determined by using an anti-bromodeoxyuridine (BrdU) antibody and the location of NS2 VIBs was determined by using an anti-NS2 antibody.

The analysis showed that BrUTP-labelled RNA accumulated in areas of the cells corresponding to the location of cytoplasmic inclusion bodies, suggesting that these inclusions represented sites of viral RNA synthesis (Fig. 4.11a). In comparison, no anti-BrdU immunofluorescence signal (red) was detectable in cells that had been mock-transfected and thus lacked BrUTP (Fig. 4.11b). The absence of signal in the mock-transfected cells confirmed that the anti-BrdU antibody specifically recognized BrUTP-labelled RNA and did not cross-react with viral proteins or RNA lacking the nucleotide analogue.

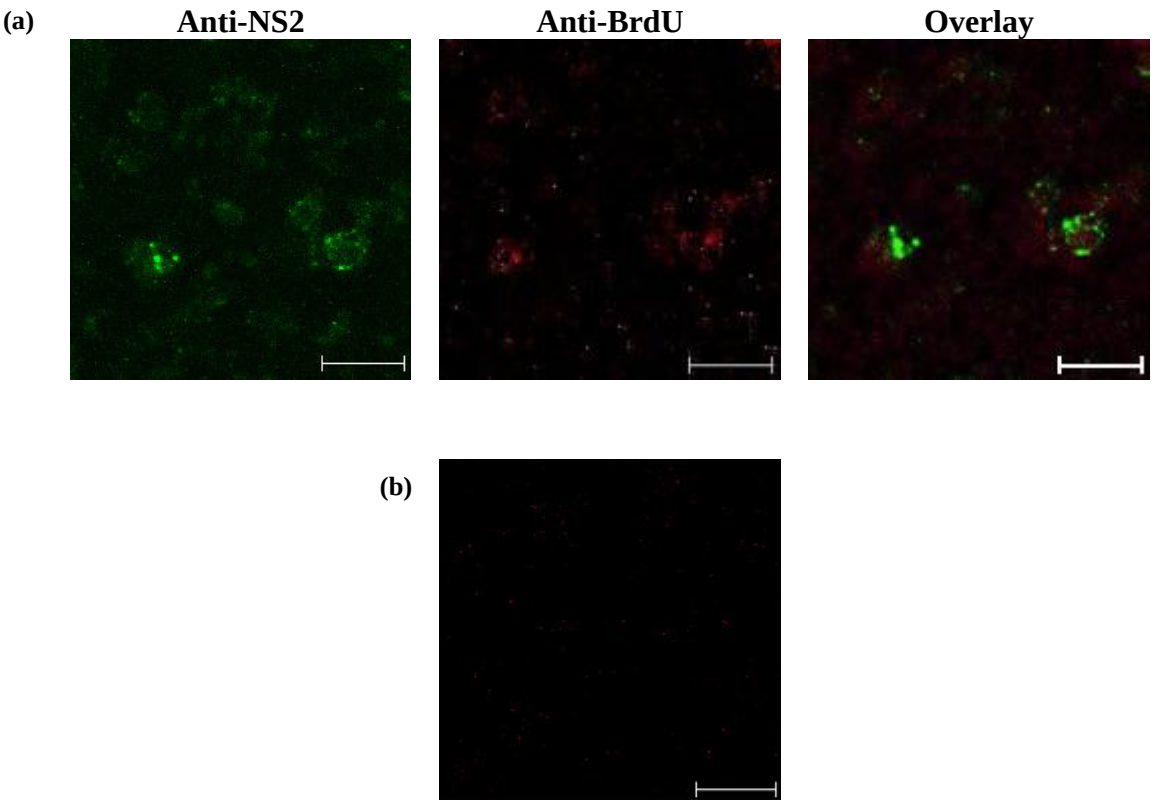

Fig. 4.11 Intracellular sites of RNA synthesis in AHSV-infected *C. variipennis* (KC) cells. The cells were treated with Actinomycin D and then processed for immunofluorescent analysis using NS2- and BrdU-specific antibodies (a). Mock-transfected cells, thus lacking BrUTP, were included as a control in the analysis (b). The localization of NS2 (green) and BrUTP-labelled RNA (red) in KC cells infected with AHSV-9 was examined with a Zeiss LSM S10 META confocal microscope fitted with bypass filters for fluorescein (505-550 nm) and rhodamine (560-615 nm). Scale bars represent 10 µm.

Chapter Five
Discussion

Non-structural proteins play key roles in the replication cycle of viruses. Although they are encoded by the viral genome and synthesized within infected cells, non-structural proteins do not form part of the virions and therefore do not enter with the viral particles into susceptible host cells. However, at each round of infection, non-structural proteins play important roles in assisting the assembly of progeny virions (Levy *et al.*, 1994; Fillmore *et al.*, 2002). The non-structural protein NS2 has been proposed to fulfill such a role within the orbivirus replication and assembly process. Prior investigations have established that the African horse sickness virus (AHSV) NS2 protein binds single-stranded RNA (ssRNA), is associated with the virus inclusion bodies (VIBs) present in infected cells, and is the only phosphorylated AHSV protein (Theron *et al.*, 1994; Uitenweerde *et al.*, 1995). Although the first two properties of the NS2 protein suggest that it may interact with viral mRNAs at the sites of assembly of new viral particles, not much is known regarding the functional importance of AHSV NS2 protein phosphorylation. Consequently, this investigation was aimed primarily at mapping phosphorylated sites within AHSV NS2 and to investigate the importance of NS2 phosphorylation in its ability to form intracellular inclusion bodies.

Protein phosphorylation is a ubiquitous protein modification and in eukaryotic systems, phosphorylation occurs almost exclusively on serine, threonine or tyrosine residues (Johnson and Barford, 1993). However, earlier studies reported that only serine residues located in the C terminus of AHSV and BTV NS2 proteins are phosphorylated (Devaney *et al.*, 1988), and it has been suggested that the ubiquitous cellular kinase, casein kinase 2 (CK2), is responsible for this post-translational modification (Modrof *et al.*, 2005). Using these criteria and different computer prediction programs, three serine residues (*i.e.* residues Ser-256, Ser-258 and Ser-262) that are present in CK2 consensus phosphorylation sites were identified in the AHSV-9 NS2 C terminus and thus selected for further analysis. To determine whether these serine residues constitute phosphorylation sites within the AHSV-9 NS2 protein, site-specific mutations were introduced into the NS2 gene by first generating an intermediate "megaprimer" product, which was subsequently used, together with an external flanking primer in a second PCR, to amplify the full-length internally mutagenized gene. In this investigation serine residues were replaced with alanine that can mimic dephosphorylated serine and aspartate that can mimic phosphorylated serine (Sarcevic *et al.*, 2002; Lewellyn and Loeb, 2011).

To map the phosphorylated sites within AHSV NS2, the NS2 mutants lacking the predicted phosphorylated serine residues were expressed by means of the baculovirus-insect cell expression system. The first manipulation of a baculovirus for the expression of non-baculovirus DNA was described almost 30 years ago (Smith *et al.*, 1983). Since then the baculovirus expression system has become one of the most powerful and versatile eukaryotic expression systems for heterologous protein expression (O'Reilly *et al.*, 1992; Yin *et al.*, 2007; Jarvis, 2009; Van Oers, 2011). Indeed, the synthesis of individual AHSV proteins by baculovirus recombinants in insect cell culture has made significant contributions to the understanding of AHSV morphology, as well as the function of individual proteins (Basak *et al.*, 1996; Maree and Huismans, 1997; Maree *et al.*, 1998; Van Niekerk *et al.*, 2001; De Waal and Huismans, 2005; Stassen *et al.*, 2011). Notably, it was reported that both BTV NS2 derived from virus-infected mammalian cells and NS2 expressed in insect cells are phosphorylated at identical sites in the C terminus of these proteins (Modrof *et al.*, 2005; Mumtsidu *et al.*, 2007). Therefore, the use of recombinant AHSV-9 NS2 expressed in the baculovirus-insect cell expression should allow for the accurate mapping of phosphorylated residues within the NS2 protein. Consequently, recombinant baculoviruses were engineered that harboured a transposed copy of the wild-type and respective mutant NS2 genes under the transcriptional control of the polyhedron promoter. This promoter directs high-level protein synthesis during the late stages of baculovirus infection and it has been reported that the expression of heterologous proteins can represent 20-50% of the total proteins of the infected host cell (Matsuura *et al.*, 1987; Possee, 1997).

Analysis of cell lysates prepared from recombinant baculovirus-infected *S. frugiperda* cells indicated that the wild-type NS2 protein (and several of the serine-to-alanine mutant NS2 proteins) electrophoresed as a diffuse band in SDS-polyacrylamide gels that occasionally separated as a noticeable doublet. Both bands of *ca.* 41 and 38 kDa, respectively, unequivocally reacted with anti-NS2 antibody. It is unlikely that the 38 kDa NS2 band may be due to proteolytic cleavage of the full-length protein by a ubiquitous cellular protease, since it was absent in recombinant baculovirus-infected *S. frugiperda* cells expressing mutant NS2 proteins in which selected serine residues were mutated to aspartate. Also, the NS2 sequence of AHSV-9 (Van Staden *et al.*, 1991) does not contain any overlapping reading

frames, thus the possibility that the different AHSV NS2 species originated as an artifact of *in vivo* translation by separate translation events could be excluded. Furthermore, the migration of different orbivirus NS2 as two distinct bands has been noted in previous studies. It has been reported that in addition to AHSV NS2 (Uitenweerde *et al.*, 1995), both EHDV NS2 (Theron *et al.*, 1994) and BTV NS2 (Taraporewala *et al.*, 2001; Butan *et al.*, 2004) can be presented as two closely separated bands upon electrophoresis in SDS-polyacrylamide gels. Therefore, considering that these orbivirus proteins are all phosphoproteins, one factor likely to influence their electrophoretic mobility may be differential phosphorylation of the NS2 protein.

To identify which, if any, of the selected serine residues within the AHSV-9 NS2 protein are phosphorylated, a phosphoprotein staining assay was performed that allows for staining of phosphorylated proteins directly on SDS-polyacrylamide gels (Cutting and Roth, 1973). It was demonstrated that wild-type NS2 and a mutant NS2 protein in which Ser-262 was substituted with alanine (NS2A262) were phosphorylated. Mutant NS2 proteins in which Ser-256 (NS2A256) or both Ser-256 and Ser-262 (NS2A256/262) were substituted with alanine stained less intensely compared to the above proteins and thus suggested a decrease in the level of phosphorylation of these mutant NS2 proteins. Subsequent analysis using a new, identical staining kit failed to indicate the phosphorylation status of the respective NS2 proteins since neither the wild-type NS2 nor the mutant versions of the NS2 protein could be stained. The reasons for this lack of staining with the second kit remain obscure, but due to its high cost this approach was not pursued further. Nevertheless, based on the obtained results, it is tempting to suggest that Ser-256 is potentially phosphorylated, but not Ser-262. Since both the single NS2A256 and dual NS2A256/262 mutant proteins stained faintly in the phosphoprotein staining assay, it therefore follows that other serine residue(s) are likely phosphorylated and may include the serine at position 258 in NS2. Indirect supporting evidence is provided by the results obtained in immunoblot analysis. It is interesting to note that, in contrast to the wild-type NS2 and other serine-to-alanine substitution mutant NS2 proteins, the anti-NS2 antibody reacted only with a single band in the case of the dual mutant NS2 protein (NS2A256/258), thus indicating that Ser-258 may indeed be phosphorylated.

Although a multitude of viral proteins have been reported to be phosphorylated, the actual number of viral non-structural proteins phosphorylated is much smaller (Butan and Tucker, 2010). In addition to the orbivirus NS2 protein, other examples include the rotavirus non-structural proteins NSP2 (Taraporewala *et al.*, 1999) and NSP5 (Afrikanova *et al.*, 1996; Eichwald *et al.*, 2004), which co-localize in the viroplasms of infected cells (Fabbretti *et al.*, 1999). Not only does NS2 share a striking similarity with NSP5 in its localization to VIBs, but recent reports have indicated that impaired phosphorylation of the rotavirus NSP5 protein is associated with a morphological change in the viroplasms (Campagna *et al.*, 2007), whereas an unphosphorylated version of the BTV NS2 protein was unable to form VIBs (Modrof *et al.*, 2005).

Based on the above, differences in the morphology of inclusion bodies (IBs) formed by the wild-type and mutant AHSV NS2 proteins were used as a guide in an attempt to delineate phosphorylated serine residues, and also to investigate whether NS2 protein phosphorylation plays a role in inclusion body formation. For this purpose, *S. frugiperda* cells infected with recombinant baculoviruses expressing the wild-type or mutant NS2 proteins were examined by transmission electron microscopy. Most strikingly, when both Ser-256 and Ser-258 were substituted with alanine, the mutant NS2A256/258 protein did not form any visible IBs in the cytoplasm of infected cells. However, engineered mutation of these serine residues to aspartate, mimicking a phosphorylated state, resulted in the formation of inclusion body structures. These results are in agreement with those reported for BTV NS2 in which mutagenesis of two phosphorylated serine residues (amino acids 249 and 259) to alanine was shown to abrogate the formation of VIBs in mammalian cells (Modrof *et al.*, 2005). The results obtained in this investigation therefore indicate that phosphorylation of Ser-256 and most likely also Ser-258 are important for the formation of AHSV NS2 intracellular aggregates, and furthermore suggests that it is the negative charges introduced by phosphorylation rather than the serine residues that are important for IB formation. To confirm further, additional data was obtained in immunofluorescence assays using *C. variipennis* cells that were treated with myricetin, an inhibitor of casein kinase 2 activity (Lolli *et al.*, 2012), prior to infection with AHSV-9. The results indicated that NS2 aggregates formed in the treated cells, but they were generally diffuse and distributed throughout the cytoplasm. This data therefore not only confirmed that phosphorylation of NS2 is important

for the formation of intracellular aggregates, but also implicate CK2 as a kinase involved in AHSV NS2 protein phosphorylation.

As indicated previously, NS2 binds ssRNA and is predominantly associated with VIBs in infected cells. The VIBs formed during virus infection are considered to be the putative sites of orbivirus replication and early virus assembly. This hypothesis is based on immunofluorescence analyses (Kar *et al.*, 2005, 2007) and immuno-electron microscopic analysis (Hyatt and Eaton, 1988) showing the presence of replication intermediates in the VIBs. However, the source of viral mRNAs that accumulate in VIBs and function as templates for dsRNA synthesis has not been established. A favoured idea has been that virus plus-strand RNAs are made by cores located at or near the VIBs. Subsequently, the plus-strand RNAs are either incorporated into polysomes, thereby driving protein synthesis or are transported by viral ssRNA-binding proteins, such as NS2, to the VIBs, where they undergo packaging and replication (Lymperopoulos *et al.*, 2003; Mertens and Diprose, 2004).

Towards delineating the involvement of the NS2 protein in this process, an immunofluorescence assay was performed to identify intracellular sites of RNA synthesis in AHSV-infected *C. variipennis* cells. The location of newly synthesized RNA was determined by using the UTP analogue, BrUTP, and a monoclonal antibody recognizing the analogue, while the location of VIBs was determined by using an anti-NS2 antibody. Prior to transfection of BrUTP into the cells, the host cell RNA synthesis was inhibited by addition of Actinomycin D, an inhibitor of RNA polymerase II (Sobell, 1985). Thus, the anti-BrdU immunofluorescence signal can be predicted to reflect only the location of newly synthesized RNA in the infected cell. The anti-BrdU signal was detected in VIBs, suggesting that these structures represent the sites of viral RNA synthesis. These results therefore imply that transcriptionally active cores associated with VIBs are the source of newly synthesized viral RNA. If this is indeed the case, it would negate the need for NS2 to transport to the VIBs the many copies of plus-strand RNAs that would be required to form genome segments of progeny virions. However, before such a conclusion can be reached, further co-localization studies of the VIBs and core proteins need to be performed.

Chapter Six
Concluding Remarks

The aims of this investigation were (i) to identify phosphorylated serine residues within the AHSV NS2 protein and (ii) to evaluate the importance of AHSV NS2 phosphorylation for virus inclusion body (VIB) formation, the presumed sites of virus replication and early virus assembly. The information that has evolved during the course of this investigation is summarized briefly in the following sections and suggestions regarding future research will be made.

Based on bioinformatic analyses of the AHSV-9 NS2 protein, three putative phosphorylated serine residues (Ser-256, Ser-258 and Ser-262) were identified within the C terminus of the NS2 protein. The serine residues were substituted with alanine residues, and the single and dual mutant NS2 proteins were subsequently expressed by means of recombinant baculoviruses in *Spodoptera frugiperda* insect cells. The phosphorylation status of the wild-type and some of the mutant NS2 proteins was assessed in a phosphoprotein staining assay. The results obtained during the course of this investigation did not allow for an unambiguous conclusion to be drawn as to whether the targeted serine residues are phosphorylated or not. However, indirect evidence has been presented, as highlighted in the previous Chapter, to suggest that Ser-256 and Ser-258 are most likely phosphorylated. Although it had previously been reported that the C terminus of AHSV NS2 is phosphorylated (Devaney *et al.*, 1988), note should be taken that this region of the protein (residues 220-360) contains seven serine residues of which four residues are present in casein kinase 2 (CK2) consensus phosphorylation sites, and the remainder are localized in protein kinase C and protein kinase A consensus phosphorylation sites. Thus, future studies should aim to definitively determine whether the serine residues targeted in this investigation are indeed phosphorylated and whether other serine residues may also be phosphorylated. For this purpose, methods that rely on metabolic labelling of the baculovirus-expressed NS2 proteins with [^{32}P] orthophosphate in *S. frugiperda* cells (Thomas *et al.*, 1990; Theron *et al.*, 1994) or *in vitro* phosphorylation of the respective proteins with [γ-^{32}P] ATP in the presence and absence of the appropriate kinase inhibitors (Blackhall *et al.*, 1998; Eichwald *et al.*, 2004; Modrof *et al.*, 2005) can be used. Alternatively, purified non-radioactively labelled NS2 protein can be subjected to analysis by mass spectrometry. This approach has been applied successfully in studies regarding the identification of phosphorylated residues within the rotavirus NSP5 protein (Sotelo *et al.*, 2010).

An interesting observation was the separation of AHSV NS2 as a doublet in SDS-polyacrylamide gels, of which both bands reacted specifically with an anti-NS2 antibody. The latter was observed, with the exception of the NS2A256/258 double mutant, for all of the other mutant NS2 proteins in which the targeted serine residues were substituted with alanine. The NS2 proteins of several orbiviruses (Theron *et al.*, 1994; Uitenweerde *et al.*, 1995; Butan *et al.*, 2004), as well as corresponding proteins of other members of the *Reoviridae* family (Afrikanova *et al.*, 1998; Kumar *et al.*, 2007) have been observed to form doublets when examined by SDS-polyacrylamide gel electrophoresis. It is possible that variable phosphorylation of the serine residues of the AHSV NS2 protein influences its electrophoretic mobility, as is the case for rotavirus NSP2 (Kumar *et al.*, 2007) and NSP5 (Blackhall *et al.*, 1998). If the phosphorylation state of the NS2 protein is responsible for the formation of the doublet in SDS-polyacrylamide gel, this might explain the uniformity of the NS2 bands representing the aspartic acid mutations, wherein the protein mimics the electrochemical properties of the phosphorylation state regardless of its actual level of phosphorylation. This would also lend support to the hypothesis of the serine residues at positions 256 and 258 being targets for phosphorylation, since the NS2A256/258 mutant produces only a single band, possibly representing a uniform, non-phosphorylated form of the protein. Future studies to determine whether the phosphorylation state of AHSV NS2 is responsible for the formation of the doublet could involve treating the NS2 protein samples with a phosphatase to remove phosphate groups from NS2 and subsequently examining whether the NS2 banding pattern has been affected.

It has been shown previously that recombinant AHSV NS2, expressed by the recombinant baculovirus expression system, forms intracellular aggregates in insect cells that resemble VIBs of AHSV-infected mammalian cells (Uitenweerde *et al.*, 1995). The data therefore indicate that NS2 is responsible for the formation of VIBs. In this regard, a particularly interesting result obtained during the course of this investigation was the observation that the dual mutant protein NS2A256/258, in contrast to the corresponding single mutant NS2 proteins, appeared to be incapable of forming inclusion bodies in the cytoplasm of recombinant baculovirus-infected cells. Notably, when both of these serine residues were replaced with aspartate, a phosphomimicking amino acid, the mutant NS2 protein was able to form discernible intracellular aggregates. These results suggest that phosphorylation of the AHSV NS2 protein is important for the formation of VIBs. This finding was confirmed in a second independent assay by making use of myricetin-treated *Culicoides variipennis* cells

infected with AHSV. Since myricetin is an inhibitor of CK2, the results furthermore implicate CK2 as a cellular kinase responsible for phosphorylation of the AHSV NS2. As the formation of VIBs appears to require phosphorylated NS2, it is reasonable to assume that newly synthesized, not yet phosphorylated NS2 might take on other functions prior to its association to VIBs. What such a role might be is not yet clear. However, one possibility, which is consistent with a model proposed for rotavirus viroplasms (Silvestri *et al.*, 2004), could be that unphosphorylated NS2 may bind to core proteins in the cell cytoplasm and upon phosphorylation NS2 recruit these components to the arising VIBs. However, neither the mechanism of protein trafficking that leads to the accumulation of viral proteins in VIBs nor the role of NS2 in such processes has been delineated for AHSV, and thus requires further investigation. Co-localization studies of transiently expressed viral proteins in the presence of phosphorylated and unphosphorylated NS2 proteins may aid these types of studies and could also generate data that may contribute to the understanding of AHSV morphogenesis.

Considering the important role that VIBs may play in orbivirus replication, a preliminary investigation was initiated to determine whether VIBs are the sites for viral RNA synthesis. In addition to directing protein synthesis, the viral positive-strand RNA also act as templates for minus-strand RNA synthesis to form the dsRNA genome segments in progeny viruses (Mertens and Diprose, 2004). Immunofluorescence analysis of bromouridine (BrU)-labelled RNA made in AHSV-infected *C. variipennis* cells provided evidence that viral RNA are localized within VIBs, thus indicating that they are the likely sites for RNA replication. This observation therefore suggests that the viral RNA required for replication originates from within the VIBs rather than being transported to these sites by single-stranded RNA binding proteins such as NS2, as had been suggested previously (Lymperopoulos *et al.*, 2003). It is conceivable that transcriptionally active core particles associated with the VIBs, either following infection or newly assembled, may serve as the source of newly synthesized viral RNA. However, before a definite conclusion in this regard can be drawn, the possibility that positive-strand RNAs were initially made elsewhere and then rapidly transported to the VIBs needs to be excluded. To assess whether pathways exist that transport positive-strand RNAs to VIBs, BrU-labelled positive-strand viral RNA could be synthesized *in vitro* and transfected into virus-infected cells. The location of the virus RNA and VIBs can then be determined using the same methodology as described in this dissertation.

In conclusion, the orbivirus NS2 phosphoprotein is a multifunctional protein and possesses different properties (ssRNA binding, VIB formation, nucleotidyl phosphatase activity) that suggest it may play a central role in the virus infectious cycle. Despite its potential importance, limited research has been performed on AHSV NS2 and these reports date from the 1990s. This study therefore aimed to redress this imbalance by taking the first steps towards delineating the role of phosphorylation in the structure-function relationships of the protein. Future studies, as highlighted in the sections above, together with studies aimed at better understanding the different functional properties of the protein should contribute greatly to unravelling the role of NS2 in the processes of viral replication and morphogenesis.

References

Afrikanova, I., Fabbretti, E., Miozzo, M.C. and Burrone, O.R. (1998). Rotavirus NSP5 phosphorylation is up-regulated by interaction with NSP2. *J. Gen. Virol.* 79, 2679-2686.

Afrikanova, I., Miozzo, M.C., Giambiagi, S. and Burrone, O. (1996). Phosphorylation generates different forms of rotavirus NSP5. *J. Gen. Virol.* 77, 2059-2065.

Alexander, R.A. (1948). The 1944 epizootic of horse sickness in the Middle East. *Onderstepoort J. Vet. Sci. Anim. Indus.* 2, 375-391.

Altschul, S.F., Madden, T.L., Schaffer, A.A., Zhang, J., Zhang, Z., Miller, W. and Lipman, D.J. (1997). Gapped BLAST and PSI-BLAST: a new generation of protein database search programs. *Nucl. Acids Res*. 25, 3389-3402.

Ausubel, F.M., Brent, R. and Kingston, R.E. (2002). Short Protocols in Molecular Biology. In: *Short Protocols in Molecular Biology*. John Wiley and Sons, Inc., New York, USA.

Bansal, O.B., Stokes, A., Bansal, A., Bishop, D. and Roy, P. (1998). Membrane organization of bluetongue virus nonstructural glycoprotein NS3. *J. Virol.* 72, 3362-3369.

Barnard, B.J. (1997). Antibodies against some viruses of domestic animals in southern African wild animals. *Onderstepoort J. Vet. Res.* 64, 95-110.

Barnard, B.J. (1998). Epidemiology of African horse sickness and the role of the zebra in South Africa. *Arch. Virol. Suppl.* 14, 13-19.

Barnard, B.J., Bengis, R., Keet, D. and Dekker, E.H. (1994). Epidemiology of African horse sickness, duration of viraemia in zebra (*Equus burchelli*). *Onderstepoort J. Vet. Res.* 61, 391-393.

Barnard, B.J.H. and Paweska, J.T. (1993). Prevalence of antibodies against equine viruses in zebra (*Zebra burchelli*) in the Kruger National Park, 1991-1992. *Onderstepoort J. Vet. Res.* 60, 175-179.

Basak, A.K., Gouet, P., Grimes, J., Roy, P. and Stuart, D. (1996). Crystal structure of the top domain of African horse sickness virus VP7, comparisons with bluetongue virus VP7. *J. Virol.* 70, 3797-3806.

Basak, A.K., Gouet, P., Grimes, J., Roy, P. and Stuart, D. (1996). Crystal structure of the top domain of African horse sickness virus VP7: comparison with Bluetongue virus VP7. *J. Virol.*70, 3797-3806.

Basak, A.K., Stuart, D.I. and Roy, P. (1992). Preliminary crystallographic study of bluetongue virus capsid protein, VP7. *J. Mol. Biol.* 228, 687-689.

Beaton, A.R., Rodriguez, J., Reddy, Y.K. and Roy, P. (2002). The membrane trafficking protein calpactin forms a complex with bluetongue virus protein NS3 and mediates virus release. *Proc. Natl. Acad. Sci. USA* 99, 13154-13159.

Becker, M.M., Peters, T.R. and Dermody, T.S. (2003). Reovirus σNS and μNS proteins form cytoplasmic inclusion structures in the absence of viral infection. *J. Virol.* 77, 5948-5963.

Belhouchet, M., Mohd Jaafar, F., Firth, A.E., Grimes, J.M., Mertens, P.P. and Attoui, H. (2011). Detection of a fourth orbivirus non-structural protein. *PLoS One* 6, e25697.

Bentley, L., Fehrsen, J., Jordaan, F., Huismans, H. and du Plessis, D.H. (2000). Identification of antigenic regions on VP2 of African horse sickness virus serotype 3 by using phage-displayed epitope libraries. *J. Gen. Virol.* 81, 993-1000.

Bhattacharya, B. and Roy, P. (2008). Bluetongue virus outer capsid protein VP5 interacts with membrane lipid rafts via a SNARE domain. *J. Virol.* 82, 10600-10612.

Bhattacharya, B., Noad, R.J. and Roy P. (2007). Interaction between Bluetongue virus outer capsid protein VP2 and vimentin is necessary for virus egress. *Virol. J.* 4, 7-19.

Blackhall, J., Munoz, M., Fuentes, A. and Magnusson, G. (1998). Analysis of rotavirus nonstructural protein NSP5 phosphorylation. *J. Virol.* 72, 6398-6405.

Blom, N., Sicheritz-Pontén, T., Gupta, R., Gammeltoft, S. and Brunak, S. (2004). Prediction of post-translational glycosylation and phosphorylation of proteins from the amino acid sequence. *Proteomics* 4, 1633-1649.

Boorman, J., Mellor, P.S., Penn, M. and Jennings, M. (1975). The growth of African horse sickness virus in embryonated hen eggs and the transmission of virus by *Culicoides variipennis* Coquillett (diptera: Ceratopogonidae). *Arch. Virol.* 47, 343-349.

Borden, E.C., Shope, R.E. and Murphy, F.A. (1971). Physicochemical and morphological relationships of some arthropod-borne viruses to bluetongue virus - a new taxonomic group. Physiocochemical and serological studies. *J. Gen. Virol.* 13, 261-271.

Boyce, M., Celma, C.P. and Roy, P. (2008). Development of a reverse genetics system for bluetongue virus: recovery of infectious virus from synthetic RNA transcripts. *J. Virol.* 82, 8339-8348.

Boyce, M., Wehrfritz, J., Noad, R. and Roy, P. (2004). Purified recombinant bluetongue virus VP1 exhibits RNA replicase activity. *J. Virol.* 78, 3994-4002.

Breese, S.S., Ozawa, Y. and Dardiri, A.H. (1969). Electron microscopic characterization of African horse-sickness virus. *J. Am. Vet. Med. Assoc.* 155, 391-400.

Bremer, C.W. (1976). A gel electrophoretic study of the protein and nucleic acid components of African horse sickness virus. *Onderstepoort J. Vet. Res.* 43, 193-199.

Bremer, C.W., Huismans, H. and Van Dijk, A.A. (1990). Characterization and cloning of the African horse sickness virus genome. *J. Gen. Virol.* 71, 793-799.

Brookes, S.M., Hyatt, A.D. and Eaton, B.T. (1993). Characterization of virus inclusion bodies in bluetongue virus-infected cells. *J. Gen. Virol.* 74, 525-530.

Brown, M. and Faulkner, P. (1977). A plaque assay for nuclear polyhedrosis viruses using a solid overlay. *J. Gen. Virol.* 36, 361-364.

Burroughs, J.N., O'Hara, R.S., Smale, C.J., Hamblin, C., Walton, A., Armstrong, R. and Mertens, P.P.C. (1994). Purification and properties of virus particles, infectious subviral particles, cores and VP7 crystals of African horse sickness virus serotype 9. *J. Gen. Virol.* 75, 1849-1857.

Butan, C. and Tucker, P. (2010). Insights into the role of the non-structural protein 2 (NS2) in Bluetongue virus morphogenesis. *Virus Res.* 151, 109-117.

Butan, C., Van Der Zandt, H. and Tucker, P.A. (2004). Structure and assembly of the RNA binding domain of bluetongue virus non-structural protein 2. *J. Biol. Chem.* 279, 37613-37621.

Calisher, C.H. and Mertens, P.P.C. (1998). Taxonomy of African horse sickness viruses. *Arch. Virol. Suppl.* 14, 3-11.

Campagna, M., Budini, M., Arnoldi, F., Desselberger, U., Allende, J.E. and Burrone, O.R. (2007). Impaired hyperphosphorylation of rotavirus NSP5 in cells depleted of casein kinase 1a is associated with the formation of viroplasms with altered morphology and a moderate decrease in virus replication. *J. Gen. Virol.* 88, 2800-2810.

Carpano, M. (1931). African horse sickness observed particularly in Egypt and in Eritrea. *Min. Agric. Tech. Sci. Serv. Bull. Cairo* 115, 1-41.

Celma, C.C. and Roy, P. (2009). A viral non-structural protein regulates Bluetongue virus trafficking and release. *J. Virol.* 83, 6806-6816.

Chiam, R., Sharp, E., Maan, S., Rao, S., Mertens, P., Blacklaws, B., Davis-Poynter, N., Wood, J. and Castillo-Olivares, J. (2009). Induction of antibody responses to African horse sickness virus (AHSV) in ponies after vaccination with recombinant modified vaccinia Ankara (MVA). *PLoS One* 4, 1-9.

Chuma, T., Le Blois, H., Sanchez-Vizcaino, J.M., Diaz-Laviada, M. and Roy, P. (1992). Expression of the major core antigen VP7 of African horse sickness virus by a recombinant baculovirus and its use as a group-specific diagnostic reagent. *J. Gen. Virol.* 73, 925-931.

Ciccarone, V.C., Polayes, D. and Luckow, V.A. (1997). Generation of recombinant baculovirus DNA using baculovirus shuttle vector. Reischt, U. (Ed.). Humana Press Inc., New Jersey, pp. 38-96.

Coetzer, J.A.W. and Erasmus, B.J. (1994). African horse sickness. In: *Infectious Diseases of Livestock With Special Reference to Southern Africa.* Coetzer, J.A.W., Thomson, G.R. and Tustin R.C. (Eds.). Oxford University Press S.A., pp. 460-475.

Coetzer, J.A.W. and Guthrie, A. (2004). African horse sickness. In: *Infectious Diseases of Livestock.* Second edition. Coetzer, J.A.W. and Tustin, R.C. (Eds.). Oxford University Press S.A., pp. 1231-1246.

Contin, R., Arnoldi, F., Campagna, M. and Burrone, O.R. (2010). Rotavirus NSP5 orchestrates recruitment of viroplasmic proteins. *J. Gen. Virol.* 91, 1782-1793.

Cowley, J.A. and Gorman, B.M. (1987). Genetic reassortants for identification of the genome segment coding for the bluetongue virus hemagglutinin. *J. Virol.* 61, 2304-2306.

Cutting, J.A. and Roth, T.F. (1973). Staining of phospho-proteins on acrylamide gel electropherograms. *Anal. Biochem.* 54, 386-394.

Dagert, M. and Ehrlich, S.D. (1979). Prolonged incubation in calcium chloride improves the competence of *Escherichia coli* cells. *Gene* 6, 23-28.

De Waal, P.J. and Huismans, H. (2005). Characterization of the nucleic acid binding activity of inner core protein VP6 of African horse sickness virus. *Arch. Virol.* 150, 2037-2050.

Devaney, M.A., Kendall, J. and Grubman, M.J. (1988). Characterization of a non-structural phosphoprotein of two orbiviruses. *Virus Res.* 11, 151-164.

Diprose, J., Burroughs, J.N., Sutton, G., Goldsmith, A., Gouet, P., Malby, R., Overton, I., Ziéntara, S., Mertens, P.P., Stuart, D.I. and Grimes, J.M. (2001). Translocation portals for the substrates and products of a viral transcriptase complex: the Bluetongue virus core. *EMBO J.* 20, 7229-7239.

Drews, M., Paalme, T. and Vilu, R. (1995). The growth and nutrient utilization of the insect cell line *Spodoptera frugiperda* Sf9 in batch and continuous culture. *J. Biotechnol.* 40, 187-198.

Du Toit, R.M. (1944). The transmission of bluetongue and horse sickness by *Culicoides*. *Onderstepoort J. Vet. Sci.* 19, 7-16.

Eaton, B.T., Hyatt, A.D. and Brookes, S.M. (1990). The replication of bluetongue virus. *Curr. Top. Microbiol. Immunol.* 162, 89-118.

Eaton, B.T., Hyatt, A.D. and White, J.R. (1987). Association of bluetongue virus with the cytoskeleton. *Virol.* 157, 107-116.

Eaton, B.T., Hyatt, A.D. and White, J.R. (1988). Localization of the nonstructural protein NS1 in bluetongue virus-infected cells and its presence in virus particles. *Virol.* 163, 527-537.

Eichwald, C., Jacob, G., Muszynski, B., Allende, J.E. and Burrone, O.R. (2004). Uncoupling substrate and activation functions of rotavirus NSP5: phosphorylation of Ser-67 by casein kinase 1 is essential for hyperphosphorylation. *Proc. Natl. Acad. Sci. USA* 101, 16304-16309.

Erasmus, B.J. (1973). The pathogenesis of African horse sickness. In: *Equine Infectious Diseases III: Proceedings of the Third International Conference on Equine Infectious Diseases.* Bryans, J.T. and Gerber, H. (Eds.). Karger, Basel, pp. 1-11.

Erasmus, B.J. (1978). A new approach to polyvalent immunization against African horse sickness. In: *Equine Infectious Diseases: Proceedings of the Fourth International Conference on Equine Infectious Diseases.* Bryans, J.T. and Gerber, H. (Eds.). Veterinary Publications, Inc., New Jersey, pp. 401-403.

Fabbretti, E., Afrikanova, I., Vascotto, F. and Burrone, O.R. (1999). Two non-structural rotavirus proteins, NSP2 and NSP5, form viroplasm-like structures *in vivo*. *J. Gen. Virol.* 80, 333-339.

Fillmore, G.C., Lin, H. and Li, J.K. (2002). Localization of the single-stranded RNA binding domains of bluetongue virus nonstructural protein NS2. *J. Virol.* 76, 499-506.

Firth, A.E. (2008). Bioinformatic analysis suggests that the orbivirus VP6 cistron encodes an overlapping gene. *J. Virol.* 5, 48-58.

Forzan, M., Marsh, M. and Roy, P. (2007). Bluetongue virus entry into cells. *J. Virol.* 81, 4819-4827.

Forzan, M., Wirblich, C. and Roy, P. (2004). A capsid protein of non-enveloped bluetongue virus exhibits membrane fusion activity. *Proc. Natl. Acad. Sci. USA* 101, 2100-2105.

French, T.J., Inumaru, S. and Roy, P. (1989). Expression of two related nonstructural proteins of bluetongue virus (BTV) type 10 in insect cells by a recombinant baculovirus, production of polyclonal ascitic fluid and characterization of the gene product in BTV-infected BHK cells. *J. Virol.* 63, 3270-3278.

Gillian, A.L., Schmechel, S.C., Livny, J., Schiff, L.A. and Nibert, M.L. (2000). Reovirus protein σNS binds in multiple copies to single-stranded RNA and shares properties with single-stranded DNA binding proteins. *J. Virol.* 74, 5939-5948.

Gomatos, P.J., Prakash, O. and Stamatos, N.M. (1981). Small reovirus particle composed solely of σNS with specificity for binding different nucleic acids. *J. Virol.* 39, 115-124.

Gonzalez, S. and Burrone, O. (1991). Rotavirus NS26 is modified by addition of single *O*-linked residues of *N*-acetylglucosamine. *Virol.* 182, 8-16.

Gorman, B.M. (1979). Variation in Orbiviruses. *J. Gen. Virol.* 44, 1-15.

Gouet, P., Diprose, J.M., Grimes, J.M., Malby, R., Burroughs, J.N., Zientara, S., Stuart, D.I. and Mertens, P.P. (1999). The highly ordered double-stranded RNA genome of bluetongue virus revealed by crystallography. *Cell* 97, 481-490.

Grimes, J., Basak, A.K., Roy, P. and Stuart, D.I. (1995). The crystal structure of bluetongue virus VP7. *Nature* 373, 167-170.

Grimes, J.M., Burroughs, J.N., Gouet, P., Diprose, J.M., Malby, R., Zientara, S., Mertens, P.P. and Stuart, D.I. (1998). The atomic structure of the bluetongue virus core. *Nature* 395, 470-478.

Guirakhoo, F., Catalan, J.A. and Monath, T.P. (1995). Adaptation of bluetongue virus in mosquito cells results in overexpression of NS3 proteins and release of virus particles. *Arch. Virol.* 140, 967-974.

Guthrie, A.J. (2007). African horse sickness. In: *Equine Infectious Diseases*. Sellon, D.C. and Long, M.T. (Eds.). Saunders Elsevier, St Louis, pp. 164-171.

Guthrie, A.J., Quana, M., Lourensa, C.W., Audonnet, J., Minkeb, J.M., Yao, J., He, L., Nordgren, R., Gardner, I.A. and MacLachlan, N.J. (2009). Protective immunization of horses with a recombinant canary pox virus vectored vaccine co-expressing genes encoding the outer capsid proteins of African horse sickness virus. *Vaccine* 16, 4434-4438.

Haig, D.A.M., Mcintosh, B.M., Cumming, R.B. and Hempstead, J.F.D. (1956). An outbreak of horse sickness, complicated by distemper in a pack of foxhounds. *J. SA Vet. Med. Assoc.* 27, 245-249.

Hall, T.A. (1999). BioEdit: a user-friendly biological sequence alignment editor and analysis program for Windows 95/98/NT. *Nucl. Acids Symp. Ser.* 41, 95-98.

Hamblin, G., Salt, J.S., Mellor, P.S., Graham, S.D., Smith, P.R. and Wohlsein, P. (1998). Donkeys as reservoirs of African horse sickness virus. *Arch. Virol. Suppl.* 14, 37-47.

Hassan, S.H. and Roy, P. (1999). Expression and functional characterization of bluetongue virus VP2 protein: role in cell entry. *J. Virol.* 73, 7832-7842.

Hassan, S.H., Wirblich, C., Forzan, M. and Roy, P. (2001). Expression and functional characterization of bluetongue virus VP5 protein: role in cellular permeabilization. *J. Virol.* 75, 8356-8367.

Hayama, E. and Li, J.K. (1994). Mapping and characterization of antigenic epitopes and the nucleic acid-binding domains of the VP6 protein of bluetongue viruses. *J. Virol.* 68, 3604-3611.

Henning, M.W. (1956). African horse sickness, perdesiekte, Pestis Equorum. In: *Animal Diseases of South Africa*. Third edition. Pretoria, Central News Agency Ltd., pp. 785-808.

Hess, W.R. (1988). African horse sickness. In: *The Arboviruses: Epidemiology and Ecology Vol II.* Monath, T.P. (Ed.). Boca Raton, Florida: CRC Press Inc., pp. 1-18.

Hewat, E.A., Booth, T.F. and Roy, P. (1992a). Structure of bluetongue virus particles by cryo-electron microscopy. *Virol.* 109, 61-69.

Hewat, E.A., Booth, T.F., Wade, R.H. and Roy, P. (1992b). 3-D reconstruction of bluetongue virus tubules using cryoelectron microscopy. *J. Struct. Biol.* 108, 35-48.

Homan, E.J. and Yunker, C.E. (1988). Growth of bluetongue and epizootic hemorrhagic disease of deer viruses in poikilothermic cell systems. *Vet. Microbiol.* 16, 15-24.

Horscroft, N. and Roy, P. (2000). NTP-binding and phosphohydrolase activity associated with purified bluetongue virus non-structural protein NS2. *J. Gen. Virol.* 81, 1961-1965.

House, J.A. (1998). Future international management of African horse sickness vaccines. *Arch. Virol. Suppl.* 14, 297-304.

Howell, P.G. (1960). The 1960 epizootic in the Middle East and SW Asia. *J. S. Afr. Vet. Med. Assoc.* 31, 329-334.

Howell, P.G. (1962). The isolation and identification of further antigenic types of African horse sickness virus. *Onderstepoort J. Vet. Res.* 29, 139-149.

Howell, P.G. (1963). African horse sickness. In: *Emerging Disease of Animals*. FAO Agricultural Studies, Vol. 2, pp. 71-108.

Huismans, H. (1979). Protein synthesis in bluetongue virus-infected cells. *Virol.* 92, 385-396.

Huismans, H. and Els, H.J. (1979). Characterization of the tubules associated with the replication of three different orbiviruses. *Virol.* 92, 397-406.

Huismans, H. and Erasmus, B.J. (1981). Identification of the serotype-specific and group-specific antigens of bluetongue virus. *Onderstepoort J. Vet. Res.* 48, 51-58.

Huismans, H. and Joklik, W.K. (1976). Reovirus-coded polypeptides in infected cells: isolation of two native monomeric polypeptides with affinity for single-stranded and double-stranded RNA, respectively. *Virol.* 70, 411-424.

Huismans, H. and Van Dijk, A.A. (1990). Bluetongue virus structural components. *Curr. Top. Microbiol. Immunol.* 162, 21-41.

Huismans, H., van der Walt, N.T., Cloete, M. and Erasmus, B.J. (1983). The biochemical and immunological characterization of bluetongue virus outer capsid polypeptides. In: *Double-stranded RNA viruses*. Compans, R.W. and Bishop, D.H.L. (Eds.). New York, Elsevier, pp. 165-172.

Huismans, H., Van Dijk, A.A. and Bauskin, A.R. (1987). *In vitro* phosphorylation and purification of a nonstructural protein of bluetongue virus with affinity for single-stranded RNA. *J. Virol.* 61, 3589-3595.

Hyatt, A.D. and Eaton, B.T. (1988). Ultrastructural distribution of the major capsid proteins within bluetongue virus and infected cells. *J. Gen. Virol.* 69, 805-815.

Hyatt, A.D., Eaton, B.T. and Brookes, S.M. (1989). The release of bluetongue virus from infected cells and their superinfection by progeny virus. *Virol.* 173, 21-34.

Hyatt, A.D., Zhao, Y. and Roy, P. (1993). Release of bluetongue virus-like particles from insect cells is mediated by BTV nonstructural protein NS3/NS3A. *Virol.* 193, 592-603.

Inumaru, S., Ghiasi, H. and Roy, P. (1987). Expression of bluetongue virus group-specific antigen VP3 in insect cells by a baculovirus vector: its use for detection of bluetongue virus antibodies. *J. Gen. Virol.* 68, 1627-1635.

Iwata, H., Yamagawa, M. and Roy, P. (1992). Evolutionary relationships among the gnat-transmitted orbiviruses that cause African horse sickness, bluetongue, and epizootic hemorrhagic disease as evidenced by their capsid protein sequences. *Virol.* 191, 251-261.

Jarvis, D.L. (2009). Baculovirus-insect cell expression systems. *Methods Enzymol.* 463, 191-222.

Johnson, L.N. and Barford, D. (1993). The effects of phosphorylation on the structure and function of proteins. *Annu. Rev. Biophys. Biomol. Struct.* 22, 199-232.

Kar, A.K. and Roy, P. (2003). Defining the structure-function relationship of bluetongue virus helicase protein VP6. *J. Virol.* 77, 11347-11356.

Kar, A.K., Bhattacharya, B. and Roy, P. (2007). Bluetongue virus RNA binding protein NS2 is a modulator of viral replication and assembly. *BMC Mol. Biol.* 8, 4-17.

Kar, A.K., Iwatani, N. and Roy, P. (2005). Assembly and intracellular localization of the bluetongue virus core protein VP3. *J. Virol.* 79, 11487-11495.

Kowalik, T.F. and Li, J.K. (1989). Sequence analyses and structural predictions of double-stranded RNA segment S1 and VP7 from United States prototype bluetongue virus serotypes 13 and 10. *Virol.* 172, 189-195.

Kowalik, T.F., Yang, Y.Y. and Li, J.K. (1990). Molecular cloning and comparative sequence analyses of bluetongue virus S1 segments by selective synthesis of specific full-length DNA copies of dsRNA genes. *Virol.* 177, 820-823.

Kumar, M., Jayaram, H., Vasquez-Del Carpio, R., Jiang, X., Taraporewala, Z.F., Jacobson, R.H., Patton, J.T. and Prasad, B.V. (2007). Crystallographic and biochemical analysis of rotavirus NSP2 with nucleotides reveals a nucleoside diphosphate kinase-like activity. *J. Virol.* 81, 12272-12284.

Laegreid, W.W. (1996). African horse sickness. In: *Virus Infections of Equines*. Studdert, M.J. (Ed). New York, Elsevier, pp. 101-123.

Laemmli, U.K. (1970). Cleavage of structural proteins during the assembly of the head of bacteriophage T4. *Nature* 227, 680-685.

Landt, O., Grunert, H.P. and Hahn, U. (1990). A general method for rapid site-directed mutagenesis using the polymerase chain reaction. *Gene* 96, 125-128.

Le Blois, H., Fayard, B., Urakawa, T. and Roy, P. (1991). Synthesis and characterization of chimeric particles between epizootic haemorrhagic disease virus and bluetongue virus, functional domains are conserved on the VP3 protein. *J. Virol.* 65, 4821-4831.

Le Blois, H., French, T., Mertens, P.P., Burroughs, J.N. and Roy, P. (1992). The expressed VP4 protein of bluetongue virus binds GTP and is the candidate guanylyl transferase of the virus. *Virol.* 189, 757-761.

Levy, J.A., Fraenkel-Conrat, H. and Owens, R.A. (1994). Consequences of virus infection to the cell. In: *Virology*. Fraenkel-Conrat, N.J.H. and Owens, R.A. (Eds.). Prentice-Hall, Englewood Cliffs, pp. 271-316.

Lewellyn, E.B. and Loeb, D.D. (2011). Serine phosphoacceptor sites within the core protein of hepatitis B virus contribute to genome replication pleiotropically. *PLoS One* 6(2), e17202.

Lolli, G., Cozza, G., Mazzorana, M., Cesaro, E.T.L., Donella-Deana, A., Meggio, F., Venerando, A., Franchin, C., Sarno, S., Battistutta, R. and Pinna, L.A. (2012). Inhibition of protein kinase CK2 by flavonoids and tyrphostins. A structural insight. *Biochem.* 51, 6097-6107.

Lord, C.C., Woolhouse, M.E. and Mellor, P.S. (1997). Simulation studies of vaccination strategies in African horse sickness. *Vaccine* 5, 519-524.

Loudon, P.T. and Roy, P. (1992). Interaction of nucleic acids with core-like and subcore-like particles of bluetongue virus. *Virol.* 191, 231-236.

Luckow, V.A., Lee, S.C., Barry, G.F. and Olins, P.O. (1993). Efficient generation of infectious recombinant baculoviruses by site-specific transposon-mediated insertion of foreign genes into a baculovirus genome propagated in *Escherichia coli. J. Virol.* 67, 4566-4579.

Lymperopoulos, K., Noad, R., Tosi, S., Nethisinghe, S., Brierley, I. and Roy, P. (2006). Specific binding of Bluetongue virus NS2 to different viral plus-strand RNAs. *Virol.* 353, 17-26.

Lymperopoulos, K., Wirblich, C., Brierley, I. and Roy, P. (2003). Sequence specificity in the interaction of bluetongue virus non-structural protein 2 (NS2) with viral RNA. *J. Biol. Chem.* 278, 1722-1730.

MacLachlan, N.J. and Guthrie, A.J. (2010). Re-emergence of bluetongue, African horse sickness, and other orbivirus diseases. *Vet. Res.* 41: 35.

MacLachlan, N.J., Balasuriya, U.B., Davis, N.L. and Collier, M. (2007). Experiences with new generation vaccines against equine viral arteritis, West Nile disease and African horse sickness. *Vaccine* 25, 5577-5582.

Manole, V., Laurinmäki, P., Van Wyngaardt, W., Potgieter, C.A., Wright, I.M., Venter, G.J., Van Dijk, A.A., Sewell, B.T. and Butcher, S.J. (2012). Structural insight into African horse sickness virus infection. *J. Virol.* 86, 7858-7866.

Maree, F.F. and Huismans, H. (1997). Characterization of tubular structures composed of nonstructural protein NS1 of African horse sickness virus expressed in insect cells. *J. Gen. Virol.* 78, 1077-1082.

Maree, S. and Paweska, J.T. (2005). Preparation of African horse sickness virus VP7 antigen via a simple method and validation of a VP7-based indirect ELISA for the detection of group-specific IgG antibodies in horse sera. *J. Virol. Methods* 125, 55-65.

Maree, S., Durbach, S. and Huismans, H. (1998). Intracellular production of African horsesickness virus core-like particles by expression of the two major core proteins, VP3 and VP7, in insect cells. *J. Gen. Virol.* 79, 333-337.

Markotter, W., Theron, J. and Nel, L.H. (2004). Segment-specific inverted repeat sequences in bluetongue virus mRNA are required for interaction with the virus non-structural protein NS2. *Virus Res.* 105, 1-9.

Marshall, J.J. and Roy, P. (1990). High-level expression of the two outer capsid proteins of bluetongue virus serotype 10: their relationship with the neutralization of virus infection. *Virus Res.* 15, 189-195.

Martínez-Torrecuadrada, J.L., Diaz-Laviada, M., Roy, P., Sanchez, C., Vela, C., Sánchez-Vizcaíno, J.M. and Casal, J.I. (1996). Full protection against African horse sickness (AHS) in horses induced by baculovirus-derived AHS virus serotype 4 VP2, VP5 and VP7. *J. Gen. Virol.* 77, 1211-1221.

Martínez-Torrecuadrada, J.L., Iwata, H., Venteo, A., Casal, I. and Roy, P. (1994). Expression and characterization of the two outer capsid proteins of African horse sickness virus, the role of VP2 in virus neutralization. *Virol.* 202, 348-359.

Martínez-Torrecuadrada, J.L., Langeveld, J.P.M., Meloen, R.H. and Casal, J.I. (2001). Definition of neutralizing sites on African horse sickness virus serotype 4 VP2 at the level of peptides. *J. Gen. Virol.* 82, 2415-2424.

Martínez-Torrecuadrada, J.L., Langeveld, J.P.M., Venteo, A., Sanz, A., Dalsgaards, K., Hamilton, W.D.O., Meloen, R.H. and Casal, J.I. (1999). Antigenic profile of African horse sickness serotype 4 VP5 and identification of a neutralizing epitope shared with bluetongue virus and epizootic hemorrhagic disease virus. *Virol.* 257, 449-459.

Matsuura, Y., Possee, R.D., Overton, H.A. and Bishop, D.H.L. (1987). Baculovirus expression vectors: the requirement for high level expression of proteins, including glycoproteins. *J. Gen. Virol.* 68, 1233-1250.

McFaydean, J. (1900). African horse sickness. *J. Comp. Path. Ther.* 13, 1-30.

McIntosh, B.M. (1955). Horse sickness antibodies in sera of dogs in enzootic areas. *J. SA Vet. Med. Assoc.* 26, 269-272.

Meggio, F. and Pinna, L.A. (2003). One-thousand-and-one substrates of protein kinase CK2? *FASEB J.* 17, 349-368.

Meiswinkel, R. and Paweska, J.T. (2003). Evidence for a new field *Culicoides* vector of African horse sickness in South Africa. *Prev. Vet. Med.* 60, 243-253.

Meiswinkel, R., Baylis, M. and Labuschagne, K. (2000). Stabling and the protection of horses from *Culicoides bolitinos* (Diptera, *Ceratopogonidae*), a recently identified vector of African horse sickness virus. *Bull. Entomol. Res.* 90, 509-515.

Mellor, P.S. (1993). African horse sickness, transmission and epidemiology. *Vet. Res.* 24, 199-212.

Mellor, P.S. and Hamblin, C. (2004). African horse sickness. *Vet. Res.* 35, 445-466.

Mellor, P.S., Boned, J., Hamblin, C. and Graham, S. (1990). Isolations of African horse sickness virus from vector insects made during the 1988 epizootic in Spain. *Epidemiol. Infect.* 105, 447-454.

Mertens, P.P.C. (2000). Family *Reoviridae*. In: *Virus Taxonomy, Seventh Report of the International Committee on Taxonomy of Viruses.* van Regenmortel, M.H.V., Fauguet, C.M., Bishop, D.H.L., Carstens, E.B., Estes, M.K., Lemon, S.M., Maniloff, J., Mayo, M.A., McGeoch, D.J., Pringle, C.R. and Wickner, R.B. (Eds.). Academic Press, New York, pp. 395-398.

Mertens, P.P.C. and Diprose, J. (2004). The bluetongue virus core: a nano-scale transcription machine. *Virus Res.* 101, 29-43.

Mertens, P.P.C., Burroughs, J.N., Walton, A., Wellby, M.P., Fu, H., O'Hara, R.S., Brookes, S.M. and Mellor, P.S. (1996). Enhanced infectivity of modified bluetongue virus particles for two insect cell lines and for two *Culicoides* vector species. *Virol.* 217, 582-593.

Mertens, P.P.C., Maan, S., Samual, A. and Attoui, A. (2005). The double-stranded RNA viruses: Genus *Orbivirus*. In: *Virus Taxonomy, Eighth Report of the International Committee on Taxonomy of Viruses.* Fauquet, C.M., Mayo, M.A., Maniloff, J., Desselberger, U. and Ball, L.A. (Eds.). Elsevier Academic Press, London, UK, pp. 466-483.

Miller, C.L., Broering, T.J., Parker, J.S., Arnold, M.M. and Nibert, M.L. (2003). Reovirus σNS protein localizes to inclusions through an association requiring the μNS amino terminus. *J. Virol.* 77, 4566-4576.

Mirchamsy, H. and Hazrati, A. (1973). A review of the aetiology and pathology of African horse sickness. *Arch. Inst. Razi.* 25, 23-46.

Modrof, J., Lymperopoulos, K. and Roy, P. (2005). Phosphorylation of bluetongue virus nonstructural protein 2 is essential for formation of viral inclusion bodies. *J. Virol.* 79, 10023-10031.

Mumtsidu, E., Makhov, A.M., Roessle, M., Bathke, A. and Tucker, P.A.J. (2007). Structural features of the Bluetongue virus NS2 protein. *Struct. Biol.* 160, 157-167.

Nason, E., Rothnagel, R., Muknerge, R., Kar, S.K., Forzan, M., Prasad, B.V.V. and Roy, P. (2004). Interactions between the inner and outer capsid proteins of bluetongue virus. *J. Virol.* 78, 8059-8067.

Nieschulz, O. (1932). Over die infectie van muizen met het virus der Zuid-Afrikaansche paardenziekte. *Tydsch. Voor Diergeneesk.* 19, 1433-1445.

Nieschulz, O., Bedford, G.A.H. and du Toit, R.M. (1934). Results of a mosquito survey at Onderstepoort during the summer 1931-1932 in connection with the transmission of horse sickness. *Onderstepoort J. Vet. Sci. Anim. Ind.* 3, 275-335.

O'Reilly, D.R., Miller, L.K. and Luckow, V.A. (1992). An overview of baculoviruses, choosing a transfer plasmid and parent virus, methods for vector construction and gene expression. In: *Baculo-expression Vectors: A Laboratory Manual*. O'Reilly, D.R., Miller, L.K. and Luckow, V.A. (Eds.). W.H. Freeman and Company, New York, pp. 1-36.

Obenauer, J.C., Cantley, L.C. and Yaffe, M.B. (2003). Scansite 2.0: Proteome-wide prediction of cell signalling interactions using short sequence motifs. *Nucl. Acids Res.* 31, 3635-3641.

Oellerman, R.A. (1970). Plaque formation by African horse sickness virus and characterization of its RNA. *Onderstepoort J. Vet. Res.* 37, 137-144.

Oellermann, R.A., Els, H.J. and Erasmus, B.J. (1970). Characterization of African horse sickness virus. *Arch. Gesamte Virusforsch.* 29, 163-174.

Office International des Epizooties (OIE). (2004). Manual of diagnostic tests and vaccines for terrestrial animals, 5th Edition. OIE, Paris, France.

Ong, K.C. and Khoo, H-E. (1997). Biological effects of myricetin. *Gen. Pharmacol.* 29, 121-126.

Owens, R.J., Limn, C. and Roy, P. (2004). Role of arbovirus nonstructural protein in cellular pathogenesis and virus release. *J. Virol.* 78, 6649-6656.

Patel, J.R. and Heldens, J.G.M. (2009). Immunoprophylaxis against important virus disease of horses, farm animals and birds. *Vaccine* 13, 1797-1810.

Piercy, S.E. (1951). Some observations on African horse sickness including an account of an outbreak among dogs. *East African Agric. J.* 17, 62-64.

Possee, R.D. (1997). Baculoviruses as expression vectors. *Curr. Opin. Biotech.* 8, 569-572.

Potgieter, A.C., Cloete, M., Pretorius, P.J. and Van Dijk, A.A. (2003). A first full outer capsid protein sequence data set in the *Orbivirus* genus (family *Reoviridae*). Cloning, sequencing, expression and analysis of a complete set of full-length outer capsid VP2 genes of the nine African horse sickness virus serotypes. *J. Gen. Virol.* 84, 1317-1326.

Prasad, B.V., Yamaguchi, S. and Roy, P. (1992). Three-dimensional structure of single-shelled bluetongue virus. *J. Virol.* 66, 2135-2142.

Purse, B.V., Brown, H.E., Harrup, L., Mertens, P.P.C. and Rogers, D.J. (2008). Invasion of bluetongue and other orbivirus infections into Europe: the role of biological and climatic processes. *Rev. Sci. Tech.* 27, 427-442.

Ramadevi, N. and Roy, P. (1998). Bluetongue virus core protein VP4 has nucleoside triphosphate phosphohydrolase activity. *J. Gen. Virol.* 79, 2475-2480.

Ramadevi, N., Burroughs, N.J., Mertens, P.P., Jones, I.M. and Roy, P. (1998). Capping and methylation of mRNA by purified recombinant VP4 protein of bluetongue virus. *Proc. Natl. Acad. Sci. USA* 95, 13537-13542.

Rao, C.D., Kiuchi, A. and Roy, P. (1983). Homologous terminal sequences of the genome double-stranded RNAs of bluetongue virus. *J. Virol.* 46, 378-383.

Ratinier, M., Caporale, M., Golder, M., Franzoni, G., Allan, K., Nunes, S.F., Armezzani, A., Bayoumy, A., Rixon, F., Shaw, A. and Palmarini, M. (2011). Identification and characterization of a novel non-structural protein of bluetongue virus. *PLoS Pathog.* 7, e1002477.

Rawlings, P., Meiswinkel, R., Labuschange, K., Welton, N., Baylis, M. and Mellor, P.S. (2003). The distribution and species characteristics of the *Culicoides* biting midge fauna of South Africa. *Ecol. Entomol.* 28, 559-566.

Reddy, Y.V., Ding, Q., Lees-Miller, S.P., Meek, K. and Ramsden, D.A. (2004). Non-homologous end joining requires that the DNA-PK complex undergo an autophosphorylation-dependent rearrangement at DNA ends. *J. Biol. Chem.* 279, 39408-39413.

Rodriguez, M., Hooghuis, H. and Casta, M. (1992). African horse sickness in Spain. *Vet. Microbiol.* 33, 129-142.

Roy, P. (1992). Bluetongue virus proteins. *J. Gen. Virol.* 73, 3051-3064.

Roy, P. (2008). Functional mapping of bluetongue virus proteins and their interactions with host proteins during replication. *Cell. Biochem. Biophys.* 50, 143-157.

Roy, P., Adachi, A., Urakawa, T., Booth, T.F. and Thomas, C.P. (1990). Identification of bluetongue virus VP6 protein as a nucleic acid-binding protein and the localization of VP6 in virus-infected vertebrate cells. *J. Virol.* 64, 1-8.

Roy, P., Fukusho, A., Ritter, G.D. and Lyon, D. (1988). Evidence for genetic relationship between RNA and DNA viruses from the sequence homology of a putative polymerase gene of bluetongue virus with that of vaccinia virus, conservation of RNA polymerase genes from diverse species. *Nucl. Acids Res.* 16, 11759-11767.

Roy, P., Mertens, P.P. and Casal, I. (1994). African horse sickness virus structure. *Comp. Immunol. Microbiol. Infect. Dis.* 17, 243-273.

Rozen, S. and Skaletsky, H.J. (2000). Primer3 on the WWW for general users and for biologist programmers. In: *Bioinformatics Methods and Protocols*. Krawetsz, S. and Misener, S. (Eds.). Humana Press Inc., Totawa, NJ, USA, pp. 365-386.

Salama, S.A., Dardiri, A.H., Awad, F.I., Soliman, A.M. and Amin, M.M. (1981). Isolation and identification of African horse sickness virus from naturally infected dogs in upper Egypt. *Canadian J. Comp. Med. Vet. Sci.* 45, 392-396.

Sambrook, J. and Russell, D.W. (2001). *Molecular Cloning, A Laboratory Manual*. Cold Spring Harbour Laboratory Press, Cold Spring Harbour.

Sanchez-Vizcaino, J.M. (2004). Control and eradication of African horse sickness with vaccine. *Dev. Biol.* 119, 255-258.

Sarcevic, B., Mawson, A., Baker, R.T. and Sutherland, R.L. (2002). Regulation of the ubiquitin-conjugating enzyme hHR6A by CDK-mediated phosphorylation. *EMBO J.* 21, 2009-2018.

Scanlen, M., Paweska, J.T., Verschoor, J.A. and Van Dijk, A.A. (2002). The protective efficacy of a recombinant VP2-based African horse sickness vaccine candidate is determined by adjuvant. *Vaccine* 20, 1079-1088.

Silvestri, L.S., Taraporewala, Z.F. and Patton, J.T. (2004). Rotavirus replication: plus-sense templates for double-stranded RNA synthesis are made in viroplasms. *J. Virol.* 78, 7763-7774.

Smith, G.E., Summers, M.D. and Fraser, M.J. (1983). Production of human beta interferon in insect cells infected with a baculovirus expression vector. *Mol. Cell. Biol.* 12, 2156-2165.

Sobell, H. (1985). Actinomycin and DNA transcription. *Proc. Natl. Acad. Sci. USA* 82, 5328-5331.

Sotelo, P.H., Schümann, M., Krause, E. and Chnaiderman, J. (2010). Analysis of rotavirus non-structural protein NSP5 by mass spectrometry reveals a complex phosphorylation pattern. *Virus Res.* 149, 104-108.

Stassen, L., Huismans, H. and Theron, J. (2011). Membrane permeabilization of the African horse sickness virus VP5 protein is mediated by two N-terminal amphipathic α-helices. *Arch. Virol.* 156, 711-715.

Stassen, L., Huismans, H. and Theron, J. (2012). African horse sickness virus induces apoptosis in cultured mammalian cells. *Virus Res.* 163, 385-389.

Stäuber, N., Martínez-Costas, J., Sutton, G., Monastyrskaya, K. and Roy, P. (1997). Bluetongue virus VP6 protein binds ATP and exhibits an RNA-dependent ATPase function and a helicase activity that catalyse the unwinding of double-stranded RNA substrates. *J. Virol.* 71, 7220-7226.

Stoltz, M.A., van der Merwe, C.F., Coetzee, J. and Huismans, H. (1996). Subcellular localization of the non-structural protein NS3 of African horse sickness virus. *Onderstepoort J. Vet. Res.* 63, 57-61.

Stone-Marschat, M.A., Moss, S.R., Burrage, T.G., Barber, M.L., Roy, P. and Laegreid, W.W. (1996). Immunization with VP2 is sufficient for protection against lethal challenge with African horse sickness virus Type 4. *Virol.* 220, 219-222.

Stuart, D.I. and Grimes, J.M. (2006). Structural studies of orbivirus proteins and particles. *Curr. Top. Microbiol. Immunol.* 309, 221-244.

Sutton, G., Grimes, J.M., Stuart, D.I. and Roy, P. (2007). Bluetongue virus VP4 is an RNA-capping assembly line. *Nature Struct. Mol. Biol.* 14, 449-451.

Tan, B.H., Nason, R., Stäuber, N., Jiang, W., Monastyrskaya, K. and Roy, P. (2001). RGD tripeptide of bluetongue virus VP7 protein is responsible for core attachment to *Culicoides* cells. *J. Virol.* 75, 3937-3947.

Taraporewala, Z., Chen, D. and Patton, J. (2001). Multimers of the bluetongue virus nonstructural protein, NS2, possess nucleotidyl phosphatase activity: similarities between NS2 and rotavirus NSP2. *Virol.* 280, 21-31.

Taraporewala, Z., Chen, D. and Patton, J.T. (1999). Multimers formed by the rotavirus nonstructural protein NSP2 bind to RNA and have nucleoside triphosphatase activity. *J. Virol.* 73, 9934-9943.

Taraporewala, Z.F., Jiang, X., Vasquez-Del Carpio, R., Jayaram, H., Prasad, B.V. and Patton, J.T. (2006). Structure-function analysis of rotavirus NSP2 octamer by using a novel complementation system. *J. Virol.* 80, 7984-7994.

Taraporewala, Z.F., Schuck, P., Ramig, R.F., Silvestri, L. and Patton, J.T. (2002). Analysis of a temperature-sensitive mutant rotavirus indicates that NSP2 octamers are the functional form of the protein. *J. Virol.* 76, 7082-7093.

Theiler, A. (1921). African horse sickness (pestis equorum). *SA Dept. Agri. Sci. Bull.* 19, 1-29.

Theron, J. and Nel, L.H. (1997). Stable protein-RNA interaction involves the terminal domains of bluetongue virus mRNA, but not the terminally conserved sequences. *Virol.* 229, 134-142.

Theron, J., Huismans, H. and Nel, L.H. (1996). Identification of a short domain within the non-structural protein NS2 of epizootic haemorrhagic disease virus that is important for single strand RNA-binding activity. *J. Gen. Virol.* 77, 129-137.

Theron, J., Uitenweerde, J.M., Huismans, H. and Nel, L.H. (1994). Comparison of the expression and phosphorylation of the non-structural protein NS2 of three different orbiviruses, evidence for the involvement of an ubiquitous cellular kinase. *J. Gen. Virol.* 75, 3401-3411.

Thomas, C.P., Booth, T.F. and Roy, P. (1990). Synthesis of bluetongue virus-encoded phosphoprotein and formation of inclusion bodies by recombinant baculovirus in insect cells, it binds the single-stranded RNA species. *J. Gen. Virol.* 71, 2073-2083.

Thompson, G.M., Jess, S. and Murchie, A.K. (2012). A review of African horse sickness and its implications for Ireland. *Irish Vet. J.* 65, 9.

Turnbull, P.J., Cormack, S.B. and Huismans, H. (1996). Characterization of the gene encoding core protein VP6 of two African horse sickness virus serotypes. *J. Gen. Virol.* 77, 1421-1423.

Uitenweerde, J.M., Theron, J., Stoltz, M.A. and Huismans, H. (1995). The multimeric nonstructural NS2 proteins of bluetongue virus, African horse sickness virus, and epizootic hemorrhagic disease virus differ in their single-stranded RNA-binding ability. *Virol.* 209, 624-632.

Urakawa, T., Ritter, D.G. and Roy, P. (1989). Expression of largest RNA segment and synthesis of VP1 protein of bluetongue virus in insect cells by recombinant baculovirus, association of VP1 protein with RNA polymerase activity. *Nucl. Acids Res.* 17, 7395-73401.

Van Dijk, A.A. (1998). African horse sickness vaccine development. In: *Proceedings of the Eighth International Conference of Equine Infectious Diseases*. Wade, J.F. (Ed). R and W Publications, Newmarket, UK, pp. 261-265.

Van Dijk, A.A. and Huismans, H. (1980). The *in vitro* activation and further characterization of the bluetongue virus-associated transcriptase. *Virol.* 104, 347-356.

Van Dijk, A.A. and Huismans, H. (1988). *In vitro* transcription and translation of bluetongue virus mRNA. *J. Gen. Virol.* 69, 573-581.

Van Niekerk, M., Smit, C.C., Fick, W.C., Van Staden, V. and Huismans, H. (2001). Membrane association of African horse sickness virus nonstructural protein NS3 determines its cytotoxicity. *Virol.* 279, 499-508.

Van Oers, M.M. (2011). Opportunities and challenges for the baculovirus expression system. *J. Invertebr. Pathol.* 107, Suppl. S3-15.

Van Staden, V. and Huismans, H. (1991). A comparison of the genes which encode nonstructural protein NS3 of different orbiviruses. *J. Gen. Virol.* 72, 1073-1079.

Van Staden, V., Stoltz, M.A. and Huismans, H. (1995). Expression of nonstructural protein NS3 of African horse sickness virus (AHSV): evidence for a cytotoxic effect of NS3 in insect cells, and characterization of the gene products in AHSV-infected Vero cells. *Arch. Virol.* 140, 289-306.

Van Staden, V., Theron, J., Greyling, B.J., Huismans, H. and Nel, L.H. (1991). A comparison of the nucleotide sequences of cognate NS2 genes of three different orbiviruses. *Virol.* 185, 500-504.

Vasquez-Del Carpio, R., Gonzalez-Nilo, F.D., Riadi, G., Taraporewala, Z.F. and Patton, J.T. (2006). Histidine triad-like motif of the rotavirus NSP2 octamer mediates both RTPase and NTPase activities. *J. Mol. Biol.* 362, 539-554.

Vende, P., Taraporewala, Z.F. and Patton, J.T. (2002). RNA-binding activity of the rotavirus phosphoprotein NSP5 includes affinity for double-stranded RNA. *J. Virol.* 76, 5291-5299.

Venter, G.J. and Meiswinkel, R. (1994). The virtual absence of *Culicoides imicola* (Diptera: Ceratopogonidae) in a light-trap survey of the colder, high-lying area of the eastern Orange Free State, South Africa, and implications for the transmission of arboviruses. *Onderstepoort J. Vet. Res.* 61, 327-340.

Venter, G.J. and Paweska, J.T. (2007). Virus recovery rates for wild-type and live-attenuated vaccine strains of African horse sickness virus serotype 7 in orally infected South African *Culicoides* species. *Med. Vet. Entomol.* 21, 377-383.

Venter, G.J., Graham, S.D. and Hamblin, C. (2000). African horse sickness epidemiology. Vector competence of South African *Culicoides* species for virus serotypes 3, 5 and 8. *Med. Vet. Entomol.* 14, 245-250.

Verwoerd, D.W. and Huismans, H. (1969). On the relationship between bluetongue, African horse sickness and reoviruses: hybridization studies. *Onderstepoort J. Vet. Res.* 36, 175-179.

Verwoerd, D.W. and Huismans, H. (1972). Studies on the *in vitro* and the *in vivo* transcription of the bluetongue virus genome. *Onderstepoort J. Vet. Res.* 39, 185-191.

von Teichman, B.F., Dungu, B. and Smit, T.K. (2010). *In vivo* cross-protection to African horse sickness serotypes 5 and 9 after vaccination with serotypes 8 and 6. *Vaccine* 28, 6505-6517.

Vreede, F.T. and Huismans, H. (1998). Sequence analysis of the RNA polymerase gene of African horse sickness virus. *Arch. Virol.* 143, 413-419.

Wade-Evans, A.M., Pullen, L., Hamblin, C., O'Hara, R.S., Burroughs, J.N. and Mertens, P.P. (1997). African horse sickness virus VP7 sub-unit vaccine protects mice against a lethal, heterologous serotype challenge. *J. Gen. Virol.* 78, 1611-1616.

Wechsler, S.J. and McHolland, L.E. (1988). Susceptibilities of 14 cell lines to Bluetongue virus infection. *J. Clin. Microbiol.* 26, 2324-2327.

Wetzel, H., Nevill, E.M. and Erasmus, B.J. (1970). Studies on the transmission of African horse sickness. *Onderstepoort J. Vet. Res.* 37,165-168.

White, D.M., Wilson, W.C., Blair, C.D. and Beaty, B.J. (2005). Studies on overwintering of bluetongue viruses in insects. *J. Gen. Virol.* 86, 453-462.

Wilson, A., Mellor, P.S., Szmaragd, C. and Mertens, P.P. (2009). Adaptive strategies of African horse sickness virus to facilitate vector transmission. *Vet. Res.* 40, 16.

Wirblich, C., Bhattacharya, B. and Roy, P. (2006). Nonstructural protein 3 of bluetongue virus assists virus release by recruiting ESCRT-I protein Tsg101. *J. Virol.* 80, 460-473.

Wu, X., Chen, S.Y., Iwata, H., Compans, R.W. and Roy, P. (1992). Multiple glycoproteins synthesized by the smallest RNA segment (S10) of bluetongue virus. *J. Virol.* 66, 7104-7112.

Xu, G., Wilson, W., Mecham, J., Murphy, K., Zhou, E-M. and Tabachnick, W. (1997). VP7: an attachment protein of bluetongue virus for cellular receptors in *Culicoides variipennis*. *J. Gen. Virol.* 78, 1617-1623.

Xue, Y., Ren, J., Gao, X., Jin, C., Wen, L. and Yao, X. (2008). GPS 2.0: Prediction of kinase-specific phosphorylation sites in hierarchy. *Mol. Cell. Proteomics* 7, 1598-1608.

Yin, J., Li, G., Ren, X. and Herrler, G. (2007). Select what you need: a comparative evaluation of the advantages and limitations of frequently used expression systems for foreign genes. *J. Biotechnol.* 127, 335-347.

Zhang, X., Boyce, M., Bhattacharya, B., Schien, S., Roy, P. and Zhou, Z.H. (2010). Bluetongue virus coat protein VP2 contains sialic acid-binding domains, and VP5 resembles enveloped virus fusion proteins. *Proc. Natl. Acad. Sci. USA* 107, 6292-6297.

Zhao, Y., Thomas, C., Bremer, C. and Roy, P. (1994). Deletion and mutational analyses of bluetongue virus NS2 protein indicate that the amino but not the carboxy terminus of the protein is critical for RNA-protein interactions. *J. Virol.* 68, 2179-2185.

Appendix

Nucleotide sequence alignment of the wild-type NS2 gene and mutant NS2 genes of AHSV-9 generated during the course of this study (sequence differences are highlighted)

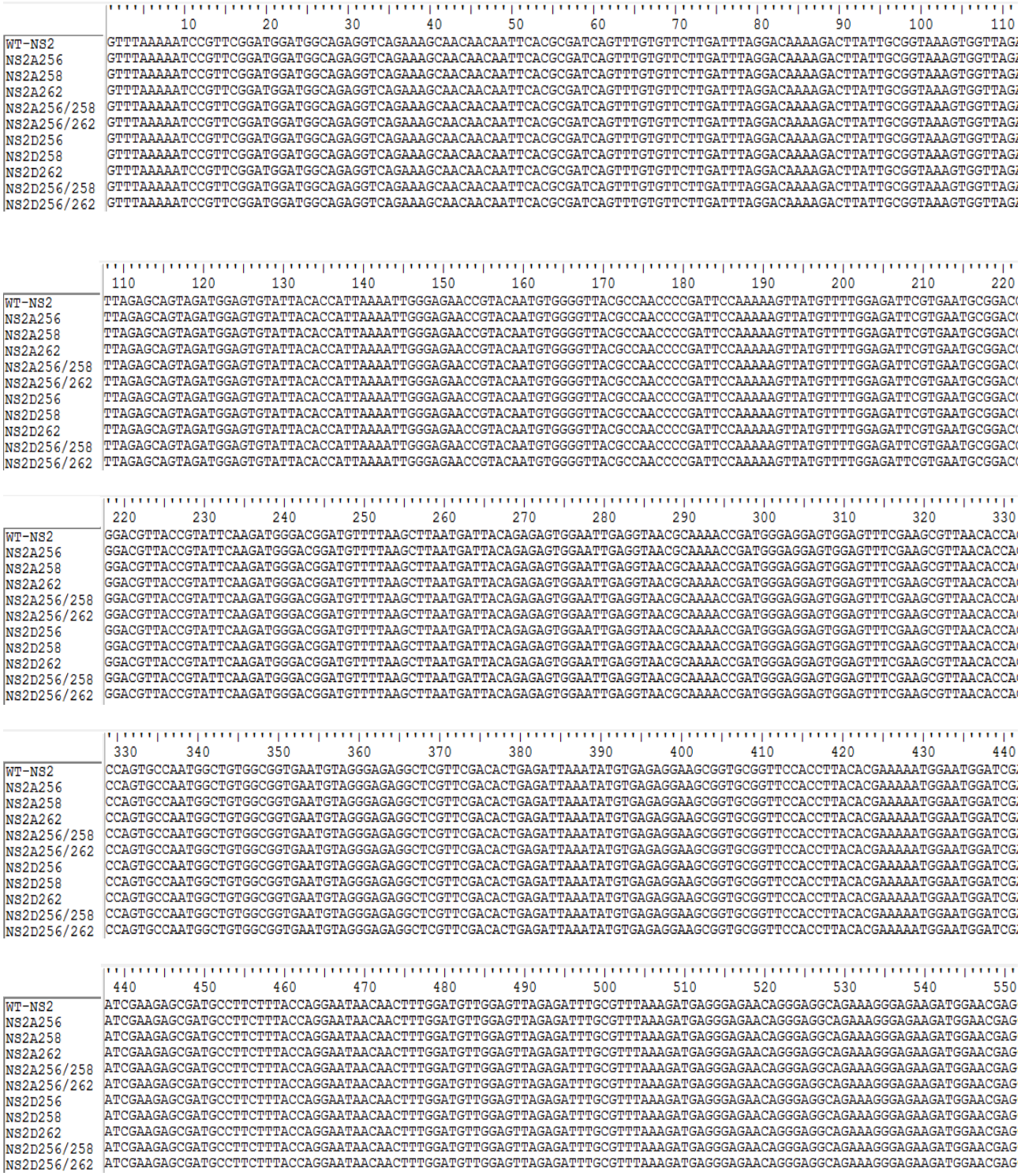

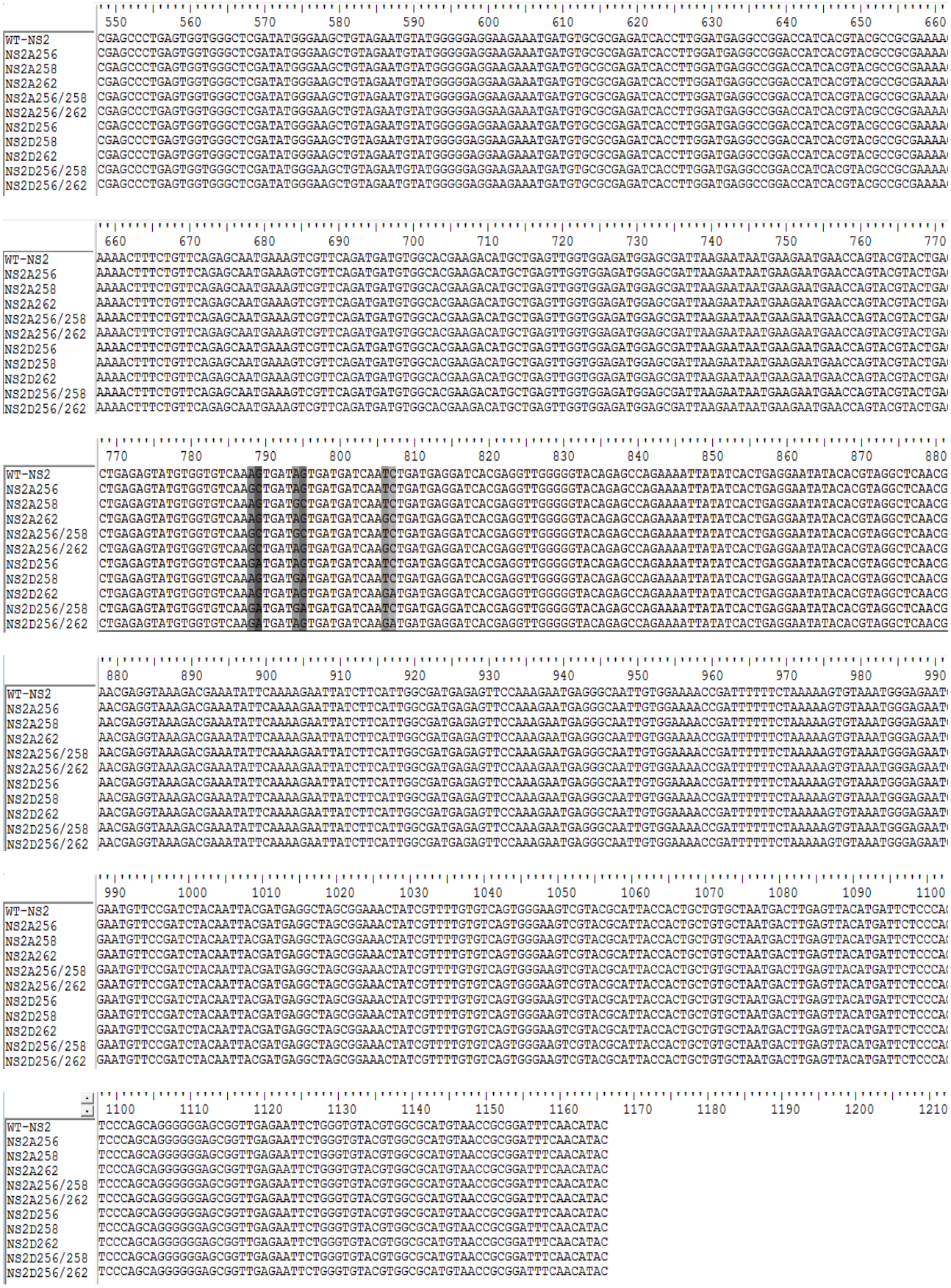

Amino acid sequence alignment of the wild-type NS2 protein and mutant NS2 proteins of AHSV-9 generated during the course of this study (sequence differences are highlighted)